2015

Production of activated carbon from fast pyrolysis biochar and the detoxification of pyrolytic sugars for ethanol fermentation

Bernardo Gusman del Campo
Iowa State University

Production of activated carbon from fast pyrolysis biochar and the detoxification of pyrolytic sugars for ethanol fermentation

by

Bernardo G. del Campo

A dissertation submitted to the graduate faculty
in partial fulfillment of the requirements for the degree of

DOCTOR OF PHILOSOPHY

Major: Mechanical Engineer

Program of Study Committee:
Robert C. Brown, Major Professor
Xianglan Bai
David A. Laird
Mark Mba-Wright
Max D. Morris
Huaiqing Wu

Iowa State University

Ames, Iowa

2015

DEDICATION

To my family and friends spread all over the world, and to those enthusiastic, creative and rational thinkers….

TABLE OF CONTENTS

NOMENCLATURE

AC	Activated Carbon
AB	Activated Biochar
BC	Biochar
BET	Brunauer, Emmett, and Teller
CO_2	Carbon Dioxide
DCFROR	Discounted cash flow rate of return
EIA	Energy Information Administration
GHG	Greenhouse gases
IPCC	Intergovernmental Panel on Climate Change
Mg	Mega gram, equivalent to a metric ton
min	minutes
NCG	Non-Condensable Gases
ppm	parts per million
RSM	Response Surface Methodology
SA	Surface Area
STP	Standard Temperature and Pressure
ton	unit weight equivalent to 1000 Kg or 2204 lb.
Vol	volatiles, Thermogravimetric analysis.

ACKNOWLEDGEMENTS

I would like to thank all the students, professors, and colleagues who have helped me with my research, classes, projects, articles, and dissertation. I thank Dr. Robert C. Brown especially, for his long term support and mentoring throughout my PhD program; Dr. David Laird for his continuous assistance with biochar topics and chemical analysis; my friends Matt Kieffer, Juan Proano, Edson Vendrusculo, and Dan Wilson, who have assisted me numerous times with laboratory analysis, reviews, intense discussions, and critical thinking, and certainly—Drs. Max Morris, Xianglan Bai, and Mark Wright —for their help and input on various topics of my research.

Finally, I would like to thank my family for their encouragement and my fiancée for her hours of patience and constant support.

ABSTRACT

The objective of this study was to valorize two prominent products from the fast pyrolysis of lignocellulosic biomass. Biochar was converted to activated carbon and pyrolytic sugar was purified to improve their fermentability. After investigating the technical feasibility of producing ethanol from pyrolytic sugars a techno-economic analysis was performed to understand the economic impacts of the newly proposed pathway in a commercial scale thermochemical biorefinery.

Typical fast pyrolysis biochar has a very low porosity (<0.05 cc/g) and surface area (<10 m2/g). However, with one-step physical activation (steam or carbon dioxide), the surface area can be dramatically improved. Specific operating conditions resulted in red oak activated biochars with more than 800 m^2/g and corn stover activated biochar with more than 500 m^2/g. Various studies have shown that activated carbon and biochar can effectively adsorb numerous inorganic and organic compounds, potentially making them an integral component of a biorefinery.

In the second part of this study, various biochar and activated biochars were made and used to detoxify the water-soluble fraction of bio-oil to produce ethanol. It was shown that biochars, activated biochars, and commercially activated carbon were effective in removing fermentation inhibitors. Removing these inhibitors can lead to increased bacterial growth and ethanol production during the fermentation of pyrolytic sugar. All three materials showed that pyrolytic sugars can be detoxified and fermented to produce ethanol. Microplate studies showed that BET surface area, quantity of micropores, and external surface area were positively correlated with bacterial growth, but had weak or no correlation with ethanol production. The DFT pore mode and pH of the adsorbent material correlated with ethanol production.

A techno-economic analysis was performed to demonstrate the economic benefits of producing activated carbon. Activated carbon can be utilized within the biorefinery or sold externally as an alternative revenue stream. The newly proposed thermochemical biorefinery

with ethanol fermentation of pyrolytic sugars, activated carbon manufacturing, and the use of lower-cost, sustainably harvested biomass presented fairly high internal rate of returns but with significantly higher capital costs compared to previous models. This model resulted in an internal rate of return of up to 16% with the commercialization of 31 million gallons of transportation fuels and various co-products. The gross revenue on an annual base was $154 million from a total project investment of $414 million. As demonstrated in our model, it is profitable to build a biorefinery under these conditions, particularly in the Midwest with an abundant corn stover supply.

CHAPTER 1 GENERAL INTRODUCTION

Rationale and Overview

Since the Industrial Revolution, petroleum-based fuels have played a vital role in our high energy-dependent societies, leveraging the growth and progress of nations. Nevertheless, petroleum-based fuels have several disadvantages that have become increasingly evident[1]. Global warming, loss of biodiversity, water and air pollution, and health problems are just few of the many problems associated with the combustion of petroleum, natural gas, and coal[1-3]. Conversely, a promising area of research is developing fuels, chemicals, and materials in an environmental and sustainable way. The bioeconomy, a bio-based platform, has a long way to develop before achieving its goal of replacing petroleum products and non-renewable energy sources. However, in order to replace petroleum products with biobased products, economic benefits must be eminent in order to compete with the well-established petrochemical industry, which has nearly two centuries of research, development, and employment. There are many challenges to transform biomass crops into valuable cost effective products. To better understand and overcome the challenges associated with biomass, it is necessary to re-evaluate the entire realm of renewable energy systems from the production to the processing and utilization.

Biomass is defined as organic matter of recent biological origin. Although biomass includes a wide variety of materials derived from plants, animals, and microorganisms, it is most frequently associated with plant fibers obtained from woody or herbaceous biomass in the context of bioenergy. Through photosynthesis, plants and certain microorganisms store energy from sunlight in chemical bonds by absorbing and transforming carbon dioxide (CO_2) from the air and water (H_2O) into carbohydrates. These carbohydrates are converted into various organic molecules that constitute the different vegetable tissues and organs. During fast pyrolysis, these vegetable components produce hundreds of chemicals that devolatilize into bio-oil and gases, and leave behind a solid carbonaceous charcoal like material. Depending on its chemical composition, biomass reacts differently in specific processing conditions and produces varying yields of the three main pyrolysis products[4,5]. For example, biomass that contains higher alkali

and earth alkali metals (nutrients that are accounted in the ash fraction) fragments and catalyzes the production of light oxygenates (such as organic acids), lowering the yield of anhydrosugars in the bio-oil while increasing the biochar yield[6].

The main challenge biomass-based products face is finding an economical and efficient application of every link in the production process to compete with petro-base products that are currently being utilized. Several factors associated with biomass production have to be addressed to make the system economically attractive and technically feasible. Some important factors that researchers have been addressing are; improving the harvest and biomass processing procedures, addressing the low energy density, high moisture and ash content of biomass, addressing the need to recycle the nutrients, and the competition for land and inputs with food, and more[7]. These all pose great challenges to the growth and development of a sustainable economy. At the forefront, finding the appropriate technologies to transform different types of biomass into valuable products is the first challenge of fast pyrolysis. For example, bio-oil can account for 70% w.t. of the initial biomass[8], but it is composed of hundreds of compounds in very small concentrations. However with specific treatments, the sugar fraction in the bio-oil can be increased from a small percentage to up to 30% of the bio-oil, making it practical to purify and convert into valuable products[6].

On the other hand, the environmental problems are urgent and need for the deployment of "green" technologies is more eminent than ever. The economic problems associated with environmental causes is one of the greatest challenges that humanity has yet to face[3]. The anthropocentric increase of carbon dioxide is the main contributor to the problem, increasing by a rate of roughly 2 ppm annually. The carbon dioxide concentration in the earth's atmosphere pre-Industrial Revolution was 280 ppm. After the development of fossil fuels, carbon dioxide concentration has steadily risen to the current value of +400 ppm[3]. In fact, with the present adoption of technologies and lifestyle changes, the world is expected to rise to 450 ppm of CO2 in the atmosphere by 2050, which is set as the threshold of irreversible damage to ecosystems and the environment[3]. If CO_2 levels continue to rise in the next coming decades, humankind might bear witness to melting glaciers and perennial ice regions, abrupt changes in seasonal

patterns, pronounced droughts and floods, and rising sea levels[2,3]. The scale of this problem will require radical strategies, such as substitutions for petroleum-based fuels, reduction of overall greenhouse gas emissions, achieving carbon negative technologies, and most importantly, embracing conservation. Technologies like biochar, and carbon capture and sequestration can result in the effective removal of CO_2 from the atmosphere[9].

Activated carbon from biochar may very well be a leading technology to catalyze the development of a bioeconomy. In order for that to happen, a few topics need to be addressed and improved. First of all, the current value of biochar in large scale application for carbon sequestration, combustion or soil amendment is low; ranging from $100 to 500 per ton in bulk scale[10]. However, the main problem for implementation of biochar as a soil amendment in cash crops is the large application rate and high capital expenditure that is needed to produce the biochar[11]. On the other hand, activated carbon derived from biochar for industrial uses in filtration and purification applications present a better opportunity for higher value added products in a market that already has an established infrastructure. By supplying inexpensive charcoal feedstock from the thermochemical process with effective activation techniques[12-14], biochar can be turned into a cost competitive renewable alternative to traditional activated carbon[15], thus creating a significant revenue stream for a biorefinery[16,17].

Activated carbon is a highly porous carbonaceous material engineered for different applications. This internal porosity created is manifested by the extensive area generated on the surface of the material. Typical commercial activated carbon has 500 to 2000 m^2 per gram. The most common feedstock that is used to produce AC is coal[18], due to its high carbon content, high abundance, and low cost. Other traditional sources include petroleum coke, wood and coconut shells[19,20]. Common applications of activated carbon include the removal of organic and inorganic contaminants from liquid and gas streams, the separation of gases, and the support for heterogeneous catalysts, etc[21]. One of the most widely known applications is the purification of water and beverages, due to its particular affinity to organic compounds[22]. Liquid applications include the removal of dissolved organics from waste water, along with color, odor and undesired flavors from drinking water[23]. The filtration of specific compounds from gas effluents,

such as mercury, is another main application of activated carbon. It is often used in mercury scrubbing by impregnating the carbon material with chloride[24]. Mercury scrubbing is utilized in many coal power stations and incinerators and natural gas wellheads. Food product decolorizing, such as sugars and molasses, is another frequent use of activated carbon. The raw concentrated liquor is percolated through powder or granular AC and colored bodies and some mineral ash is removed from the solution[18]. Molasses number is a typical test performed to compare the amount of colored bodies removed from the solution of different adsorbents, and are compared to a standard carbon. The good de-colorization materials have high surface area but most importantly, favorable relation of micro and macro pore which are vital for the removing of polydisperse colorants[25]. The macropores is thought to serve as channels for rapid diffusion and the small pores being the adsorption sites[25,26]. Activation process with higher burn off rates can lead to pore enlargements, which is seek when removing large molecular weight compounds[25]. However, adsorption efficiency is quite more complicated than surface area and pore structure of the activated carbon. Other important properties include; functional groups, oxygen surface group, biomass precursor, nature of the adsorbate, binder, molecular weight of the absorbate, size and solution conditions (pH, temperature, ionic strength, adsorbate concentration), etc[27].

Contaminants adhere to the surface of the carbon can be remove from the solution when filtered through this solid adsorbant. Once the material is saturated it can be disposed or in some cases regenerated. The regeneration of the surface can be achieved by desorbing the adsorbate by changing the temperature or pH of the solution. Alternatively, it could be reactivated in similar fashion to the original activation process regenerating the pore structures and its adsorption capacity.

In order to manufacture activated carbon from biomass, it has to be first carbonized and later activated in a more severe thermochemical process[28]. The carbonization of the material is typically achieve with 250 to 400 °C under low oxygen content for long times (various hours to days), until a high fixed carbon charcoal is obtained[29]. Later the charcoal is activated. Activation of biochar can be done in multiple ways, including physical and chemical methods or a combination of both[30]. Chemical activation is performed by either using solid or liquid chemicals

such as inorganic acids, bases, carbonates, and salts. The charcoal and chemical mix is thermally treated during various hours in a kiln between 300 to 500°C[15]. Alternatively, various gases can be utilized to activate the charcoal. Gaseous oxidizing agents, such as steam, carbon dioxide, oxygen, or ozone at high temperature (500 to 1000°C) react with the carbon breaking the aromatic rings of the amorphous and crystalline carbon structures. For example steam and CO_2 are frequently used as they are inexpensive and easier to handle. At lower temperatures steam is preferred as it is more reactive than CO_2 at a given temperature, and the molecule is smaller which leads to better diffusion, reaction rate and micro porous formation[25]. As the carbonized material is "activated", the porosity and surface area of the particles is severely increased. Due to the activation process, various gases evolve from the charcoal decomposition (mainly CO, CO_2 and water vapor) decreasing the AC yield which in turn modify the surface's physical and chemical properties. As previously mentioned, activation reduces the mass, increase the surface and alters the surface chemistry through the formation and destruction of various organic functional groups[31].

In order to understand the properties that make activated carbon a good adsorbent for filtering, removing chemicals and detoxifying, it is important to understand the adsorption process, surface properties and the relation with the adsorbate (gas or liquid) that is being removed. Adsorption involves two substances; the adsorbate (in this case the impurity dissolved in the solution) and adsorbent (activated carbon). Adsorption is the attraction of atoms, ions, gas, liquid molecules or dissolved solids onto the surface of a material. Adsorption is different to absorption, which the solute diffuses and permeates through the solid absorbent. Adsorption occurs on the exterior of the solid particles in the micropores or external surface area (comprising the meso and macropores)[25]. Due to this, creating more surface area on the material is one of the properties used to determine the material's capability to adsorb unwanted compounds from liquid or gas streams.

The physical nature of adsorption is governed by surface interaction, Van der Waals forces, and is referred as physisorption. Along with the physical adsorption process, activated carbons can also remove certain compounds through chemical attraction or chemisorption. On a

microscopical level the adsorbate (ions, molecules or gases) diffuses through the media to the external surface of the particle, travel through the channels and is retained in the pores (physisorption), or reacts with different functional groups present on the surface (chemisorption). The type of pores produced in the activation is a key parameter that will determine the size of molecules that could physically travel and be retained. The pores are typically characterized by the diameter, being micropores (less than 2nm of diameter), mesopores (2 to 50 nm) and macropores (more than 50 nm). For example, the levoglucosan molecule has roughly 0.4 nm (4 Å) of cross sectional area[32] and smaller pores than the size of the adsorbate will not be an effective adsorption site.

Physical and chemical adsorption differs not only on the forces or activation energy and the change of level of electronic state, but also in the reversibility of the process. Since physisorption is governed by Van der Waals forces existing between adsorbent and adsorbate, which are very weak, it can be easily reversed by heating or by decreasing pressure. Then the adsorbate desorbs from the surface and the AC can be reused. However in chemisorption processes, the attraction between adsorbate and adsorbent is very strong, similar to those of chemical reactions, and in many cases cannot be reversed or is just partially achieved.

Adsorption process is usually modeled using isotherms. The isotherms relate the amount of adsorbate adsorbed by the adsorbent at a constant temperature, and is typically characterize through its pressure, if it is gas, or concentration if the adsorbate is a liquid[33]. These empirical relations are used to predict the adsorption capacity and equilibrium concentrations. The empirical data obtained through isotherms are fitted by different equations; Freundlich, Langmuir, linear, BET, NLDFT, etc. and the parameters are defined for specific temperatures, pressures, pH, concentrations and competing ions.

Based on the isotherms data and kinetics studies, various properties of the activated carbon can be obtained to determine the correct utilization. For example, the capacity of an adsorbent to remove chemicals, the retention time or bed length necessary for efficient removal, the media exhaustion time, the efficacy of removal and the relationship of equilibrium concentration and temperature, etc. Depending on its application, activated carbon formulations

are powder (most commonly used), granular and specialty forms. Their pricing depends on the purity, application, formulation and performance.

Objectives

The ultimate goal of this project was to valorize two prominent products from the fast pyrolysis of lignocellulosic biomass. Specific objectives include: (1) convert biochars into activated carbon with high surface area and porosity, (2) evaluate the technical feasibility of activated carbons for removing toxic agents from the water soluble bio-oil fraction to increase production of ethanol from pyrolytic sugars, and (3) conduct a techno-economic analysis to determine the economic impacts of the newly proposed thermochemical biorefinery producing value-added activated carbons from biochar.

Dissertation Organization

This dissertation contains a general introduction, followed by three papers for publication. The first paper discusses the production of activated carbon from fast pyrolysis biochar through the use of steam at various conditions and a methodology for optimizing this process. The second paper focuses on the utilization of biochar as a detoxification agent to ferment the pyrolytic sugars separated from bio-oil, which also contain fermentation inhibitors. The third paper considers the economic feasibility of pyrolysis-based biorefinery that produces sugars and activated carbon among its products.

CHAPTER 2 OPTIMIZING THE PRODUCTION OF ACTIVATED CARBON FROM FAST PYROLYSIS CHAR

B.G. del-Campo[1,2], M.D. Morris[1], D.A. Laird[1] , M.M. Kieffer[1] & R. C. Brown[1]

Abstract

Fast pyrolysis of red oak wood yields approximately 10-30 wt% biochar, considered a low value co-product. Production of high value activated carbon using steam was investigated at different activation conditions. The relationship between activation parameters, surface area, and revenue was evaluated using response surface methodology. A second-degree model showed a maximum economic benefit at 800°C with 5 minutes of steam activation, yielding $907 of net revenue per metric ton of biochar.

Innovation

Fast pyrolysis, a thermochemical process that yields bio-oil as its primary product, is developing rapidly as a mean of producing advanced biofuels and other bio-based products. Co-products include non-condensable gases and a carbon-rich solid residue known as char (or biochar when incorporated into the soil). Biochar, representing 10-30 wt% of the products, is currently a relatively low value agricultural soil amendment with an estimated wholesale value around $100 per ton[10]. Thus, it is priced no higher than its precursor biomass. Developing additional, value-added applications for the biochar produced during fast pyrolysis would enhance the overall economic viability of fast pyrolysis technologies. One approach to developing such biochar products is upgrading the biochar to high value activated carbon (AC) with high surface area and porosity.

Introduction

Activated carbon (AC) has been historically used as an adsorbent. More recently, it has found additional applications, such as catalysts, electrodes, super capacitors, membranes, carbon

fibers, and nanoparticles.[34-37] Research has focused on understanding surface characteristics and adsorption mechanisms,[38,39] selectivity and capacity for removal of various contaminants[14,40], and the use of AC for novel chemical applications[39,40]. In addition, the production of activated carbon from alternative feedstock, such as olive stones, waste plastics, municipal waste sludge, coke, rice husk, palm oil sludge, etc.[14,38,41-44] has been an important topic in recent years. The benefits of leveraging the economics of the pyrolysis platform through production of inexpensive activated carbon could significantly impact the industrial and agricultural sectors of the economy[21,42].

Activated carbon is generally classified as a specialty chemical valued according to its composition, performance, formulation, precursor material, grade, and other properties. Its price is highly variable depending upon purity, applications, and quantities required. Table 1 illustrates the variation in current prices of roughly 60 different activated carbon products sold in bulk quantities (pallet size or larger) in the US as quoted by the manufacturers or distributors.

Table 1: Comparison of various activated carbons*

Feedstock	Products	Bulk price ($/ton)	Price range ($/ton)	Surface area (m^2/g)	Ratio 10^{-6} ($/$m^2$)
Coal	18	5753	1190-16343	846	6.8
Coconut	19	5834	1870-18267	1121	5.2
Wood	8	7393	2200-16016	1583	4.7
Unknown	11	8517	2100-15541	1050	8.1
Other**	3	14097	11520-18100	533	26.4
Total/Ave.	59	6970	1190-18267	1040	10.2

*Bulk price and surface area represent averages for each feedstock.
**Includes feedstocks, such as bamboo and bones.

Activated carbon (AC) has a large internal porosity and surface area as well as a high degree of surface reactivity. One gram of a commercially produced activated carbon has a surface area typically ranging from 500 to 2000 m^2. Feedstocks currently used to produce activated carbon include wood, nutshells, peat, coke, coal, and petroleum-pitch. Numerous

industries use AC for removing both organic and inorganic contaminants from process streams[33,45,46], for uses including filtering effluent from municipal sewage plants, recycling industrial water, scrubbing mercury from coal-fired power plants, and removing odors and hydrocarbons from industrial exhaust gases[47-50].

The price of commercial activated carbon ranges from hundreds to thousands of dollars per metric Ton, depending upon formulation, specificity, and performance (Figure 1). The global market for 2002 was estimated to be 750,000 metric Tons with increasing growth of ~5% annually [51]. The acquisition of raw material is a major cost in the production of activated carbon[52], especially with high quality biomass precursors. Fast pyrolysis biochars are potentially an abundant, inexpensive and renewable carbonaceous material that can be engineered for different applications[53], such as carbon sequestration and soil amendment[54], as well as activated carbon[28].

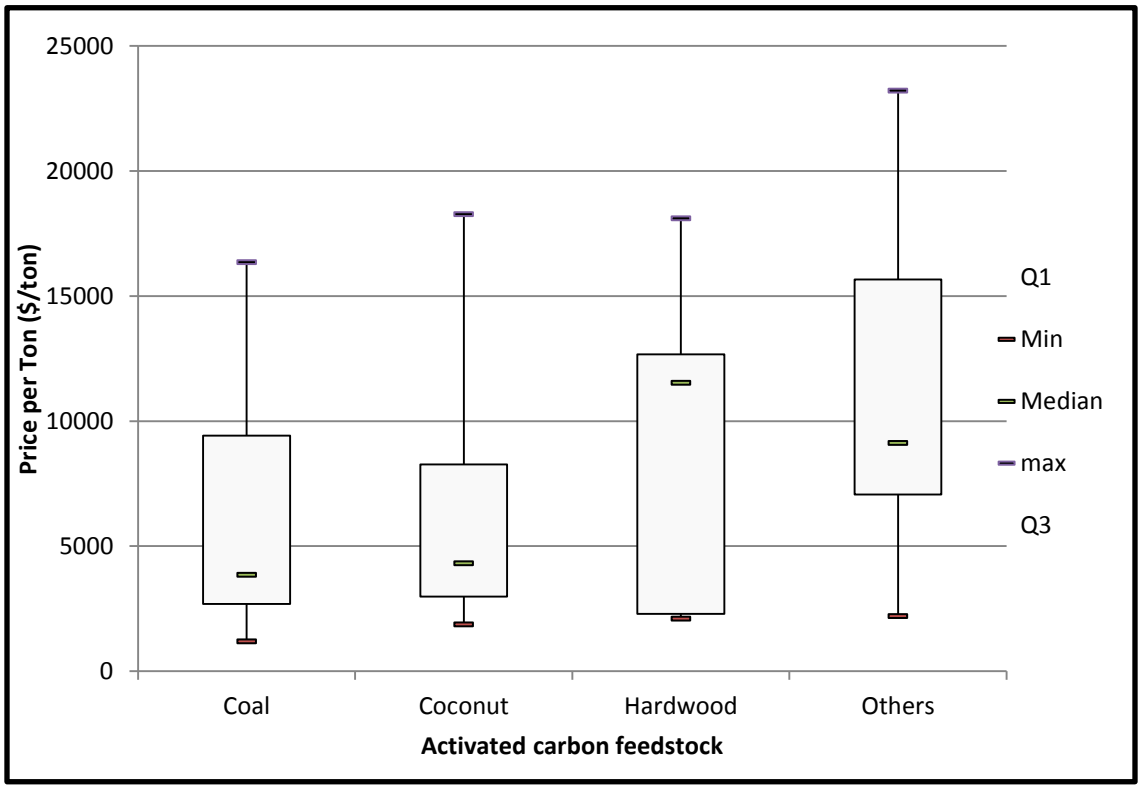

Figure 1. Box plot diagram with price distribution, min, max and average of activated carbons produced from various feedstocks

The manufacture of AC from biomaterials involves both carbonization and a further activation step with more stringent thermochemical conditions. Carbonized material can be activated either chemically or physically. In chemical activation, the carbonized material is exposed to strong acids, bases, carbonates, and numerous inorganic salts at temperatures ranging from 300 to 500°C. Physical activation is the treatment of the carbonized material with gaseous oxidizing agents, such as steam, carbon dioxide, oxygen, or ozone at temperatures ranging from 500 to 1000°C. As the carbonized material is activated, the internal porosity and surface area are increased through differential oxidation of labile components. During the activation procedure, various gases, primarily CO and CO_2, are evolved, decreasing the yield of the AC product relative to the starting carbonized material and increasing the microcrystalline graphitic structures[28,31,55]. Activation also alters the surface chemistry of AC through both the formation and destruction of various organic functional groups[31]. Organic functional groups on AC surfaces are responsible for the adsorption of molecules involving chemical reactions, also referred as chemisorption. However, physisorption is an adsorption process governed by van der Waals forces not involving activation energy, neither perturbation of the electronic state of the adsorbate, which is closely related to the degree of activation and the pore structure of the adsorbate.

The final physicochemical characteristics and potential uses of activated carbon are greatly influenced by the biomass feedstock, feedstock pretreatments, carbonization method, and activating conditions, such as temperature, pressure, gas type and flow rates, heating rates, holding times, and quenching conditions[51]. The adsorption efficiency of AC for a target chemical species is related to the final surface area, internal pore structure, and functional groups present on AC surfaces. The adsorption efficiency is also influenced by properties of the target molecule and the media being filtered (gas or liquid). Adsorption efficiency is a key parameter in setting the economic value of an AC for an intended application. This determines the removal rates and the capacity or amount of adsorbant that can be removed by the filtering media.

Due to the complexity of the interaction between AC and target molecules, no one AC property fully describes the AC quality for a particular application. In general, the surface area

and porosity are important characteristics that correlate with the reactivity, catalytic behavior, and adsorption capabilities of various substrates[21,56-59]. Thus, surface area is a first tier parameter for screening the degree of activation and the quality of an adsorbent[21,38,60]. For instance, based upon a survey performed on different ACs for this study, it was found the correlation of price and surface area for 16 coconut shell ACs was 0.57, highlighting the relative importance of this parameter in determining product quality.

Therefore, maximization of the Brunauer-Emmett-Teller surface area (BET) and porosity were the primary goals of this study. These parameters were measured through nitrogen adsorption, a technique that uses the physical multilayer adsorption of gas molecules on a solid surface to estimate the specific surface area of the material. To determine the best activation conditions, Response Surface Methodology (RSM) was used with fitted polynomial models to better understand the interaction effects among multiple variables and optimize surface area and resulting economic value[61-64].

Materials and Methods

Raw material and sample preparation

Red oak biomass (*Quercus spp.*) was used as feedstock for this study. Size reduction of the biomass was performed with a 60 HP Artsway hammer mill equipped with a 1/8" screen. The biomass was pyrolyzed using a fluidized bed process development unit capable of processing 8 kg/hr of biomass located at the Iowa State University BioCentury Research Farm (Boone Co., Iowa, United States). The pyrolysis reactor was operated at 500°C and used nitrogen gas at 183 slpm to fluidize the reactor. Solid biochar particles were collected in two high efficiency cyclonic filters designed to catch particles up to 1 µm. Both cyclones were heat traced to 400°C to prevent premature condensation of bio-oil. Further details on this reactor are found in Pollard et al.[65]

Some sand used in the fluidized bed reactor elutriated from the reactor and was removed by gas cyclones along with the char. Since the presence of sand in the biochar was an artifact of

the production method, it was later removed by flotation of the char in water followed by filtration to separate the char from the water. The biochar was oven dried followed by screening to remove fine particles smaller than 212 µm (sieve #70). The recovered biochar was washed in methanol (8:1 v/v ratio of methanol to biochar) to remove organic compounds that might have been adsorbed in the biochar during pyrolysis and char cooling. Finally, the sample was washed in an acidic solution for 20 min to reduce the ash fraction using 10:1 v/v 0.1 M of H_2SO_4 to biochar and dried at 105°C for 48 hrs. The surface area of the biochar before and after acid washing was 1.2±0.5 m^2/g and 9.3±3.2 m^2/g, respectively.

Reactor design and activation

The bench scale fixed bed biochar activation reactor consisted of a 40 cm vertical chamber and a steam generator (Figure 2). Both modules were powered by electric heaters operated by Watlow programmable temperature controllers with type K thermocouples placed at the steam port and the center of the reactor. Evaporating distilled water in a heated copper coil generated steam with a flow controlled by a peristaltic pump. Nitrogen gas continuously flushed the sample in the activation chamber at 1mL min^{-1} gr^{-1} of char.

Biochar was activated in special mesh baskets containing 1.2±0.15g of material. Steam continuously flushed the sample at a rate of 1mL min^{-1} gr^{-1} at the desired temperature and residence time. After activation, samples were rapidly quenched by flushing with nitrogen gas until the temperature was less than 50°C. After reaching room temperature, the sample was weighed to calculate material loss during activation (burn off):

$$\text{Bo} = \frac{W_b - W_{ac}}{W_b} x\ 100 \quad (1)$$

where:
Bo = burn off (%),
W_b = initial biochar weight d.b. (g), and
W_{ac} = activated char weight d.b. (g).

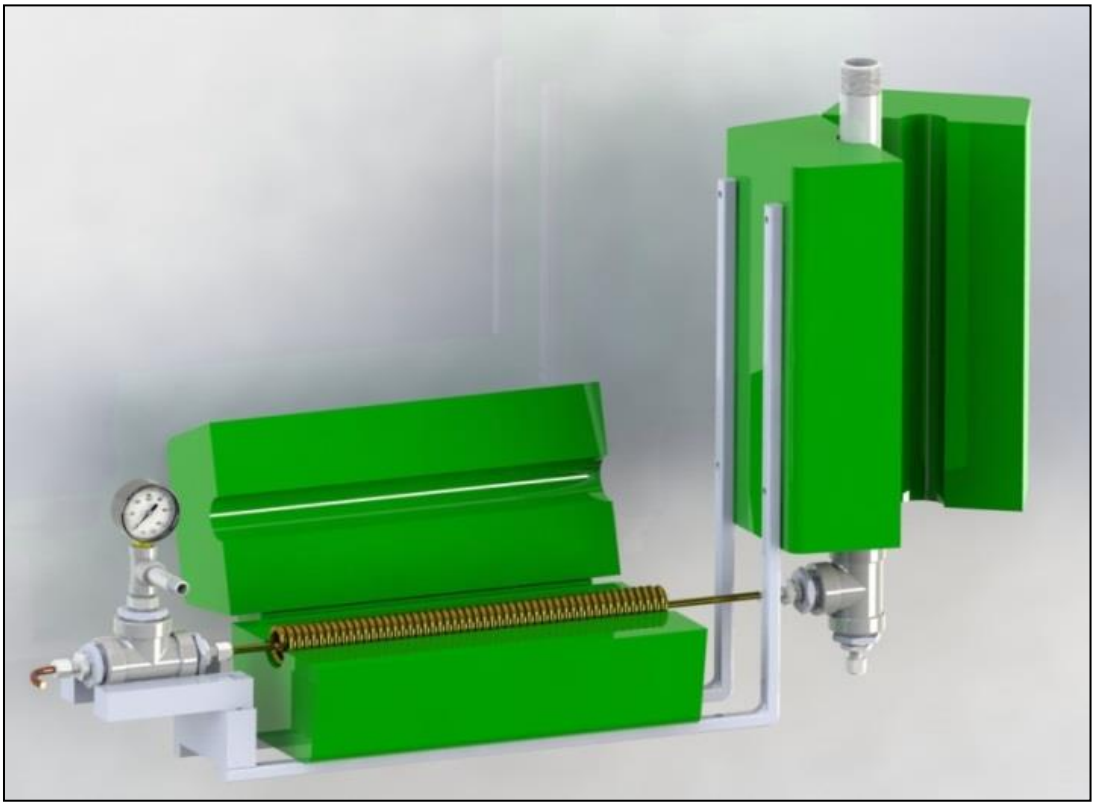

Figure 2. Reactor assembly for steam activation of biochar

Physisorption analysis was performed with 0.1g samples degassed for 4 hrs at 300°C under vacuum at absolute pressure of less than or equal to 100 Pa. BET surface area measurements were performed using N_2 with a Quantachrome NOVA 4200e Gas Sorption Analyzer. Seven adsorption points were measured in the range of 0.01 to 0.3 P/P_o. The pressure range for calculating BET was adjusted by the presence of a micropore using the Nova-win 11.02 software. Activated and non-activated biochars exhibited Type I & II isotherms as described by the Brunauer, Emmett, and Teller theory[66].

Statistical analysis, optimization and economic results

This study utilized a full three level factorial design with three replications for a total of 27 experimental runs. Response surface methodology was used to understand the contribution of each variable and to optimize the two most important variables defining activation (temperature and residence time). The design matrix was previously established with preliminary testing to set

a reasonable center point and range for each variable tested. For activation, the temperature range was between 400 and 800°C (maximum recommended temperature for the heaters) and the biochar holding time was between 5 and 60 mins. Runs were performed in randomized orders to avoid systematic errors. Two dependent variables, burn-off (%) and BET surface area were recorded for every run.

Another dependent variable studied was gross revenue. This variable was the result of combining the output of the process (activated carbon yield expressed as a mass percentage remaining to the initial feedstock), surface area per unit mass obtained by different activation treatments, and a theoretical price per unit surface area (Eq. 2). This new dependent (gross revenue) was optimized with RSM:

$$\mathrm{GR} = (1 - \mathrm{Bo}) \times \mathrm{S}_A \times P_B \quad (2)$$

where:
GR = Gross Revenue produced per Ton of biochar ($/ton),
Bo = burn off (%),
S_A = BET surface area (m^2/g), and
P_B = bulk price to surface area ratio 10^{-6}($/m).

The bulk price to surface area ratio used for the calculations was of $\$4 \times 10^{-6}$ m^{-2}. This parameter was set to reflect the variation in price for the different adsorbent qualities as measured by the surface area. Note, the bulk price to surface area ratio for commercial wood base activated carbon was in the order of 4.7×10^{-6} $\$m^{-2}$ as shown in Table 1. Net revenue is given by:

$$\mathrm{NR} = \mathrm{GR} - \mathrm{Cc} - \mathrm{Oc} \quad (3)$$

where:
NR= net revenue per ton of biochar ($/ton),
GR = gross revenue produced per ton of biochar ($/ton),
Cc= capital cost per ton of biochar ($/ton), and
Oc= operational cost per ton of biochar ($/ton).

Next, Eq. 3 was calculated for every processing condition, where the gross revenue is the result of Eq. 2. The capital cost was calculated by scaling equipment costs and capital

investments from previous research in activated carbon economics[16,44] and operational costs calculated from each process input and the associated expenses of every treatment combination.

The surface area and revenue data were fit to a second-degree polynomial model to plot their surface response:

$$Y = a_o + a_1X_1 + a_2X_2 + a_{11}X_1^2 + a_{22}X_2^2 + a_{12}X_1 X_2 + \in \quad (4)$$

Where X_1 and X_2 are the independent variables that defines the response variable (Y). The variable Y is a function of both independent variables and the experimental error term, denoted as ϵ. If it is present and the term is statistically significant, the curvature in the response surface is represented by the quadratic terms X^2_1 and X^2_2. The interaction effect is denoted by X_1X_2 term.

Equation 4 models the previous production parameters (temperature and residence time) with surface area, yield of activation (1-Bo), and quality of adsorbent (bulk price to surface area ratio). In this fashion, the optimum product value was obtained for different activation conditions.

Response surface methodology was utilized to optimize the dependent variables and to determine maximum process conditions for BET surface area and gross revenue. These results were later compared with production and capital costs to optimize the economics, Eq. 4.

The use of RSM methodology helped to identify interaction effects among variables, which independent experiments could not determine. The experiment design and the replications were important considerations to strengthen the prediction model, minimize the experimental errors (Type I and II) and deal with different sources of variability inherent to biomass heterogeneity, equipment performance and different operators. Experimental design and statistical analysis were achieved with JMP 10.0.

Results and Discussion

As shown in Figure 3, five different feedstocks pyrolyzed in ISU labs resulted in biochars with surface areas of less than 20 m^2/g and most commonly less than 10 m^2/g. These results are one order of magnitude less than traditional slow pyrolysis chars at similar reaction conditions and two to three orders of magnitude less than most commercial activated carbons. Biochar's properties greatly depend on the feedstock used, pyrolysis conditions, and post-treatments. Some processing conditions resulted in biochars with high surface areas and porosities, and in some cases, similar to commercial activated carbons[28,67,68]. However, other researchers have also noted poor microporosity on fast pyrolysis chars, which makes them relatively poor sorbents[51,69,70]. Surface areas for these biochars are typically less than 10 m^2/g (Figure 3).

In research conducted by El-Hendawy et al. (2001), non-activated biochar had the lowest adsorption capacity compared to physically and chemically activated biochar. For example, the differences for methylene blue adsorption were closely related to the degree of activation and porosity characteristics of the activated material. We hypothesize the operating conditions for fast pyrolysis reactions might be responsible for the small porosity developed in biochars. Fast pyrolysis is typically performed at high heating rates (on the order of 100° C/s or higher), short residence times (few seconds), and relatively low temperatures (400-550°C) to maximize the production of bio-oil. Slow pyrolysis biochars are typically produced at very low heating rates (typically less than 1° C/s), long residence times (hours), but with similar low temperatures as fast pyrolysis conditions. Conversely, typical physical activation requires several hours of reaction time and temperatures of at least 700°C to produce highly porous materials. Bio-oil and non-condensable gases evolved during the process reduce the available solid carbon for activation. For similar temperature regimes, fast pyrolysis will have lower biochar yields and higher ash content, which potentially compromise the development of porosity and surface area that can be achieved during activation. Thus, slow pyrolysis biochar could be a better precursor for production of activated carbon.

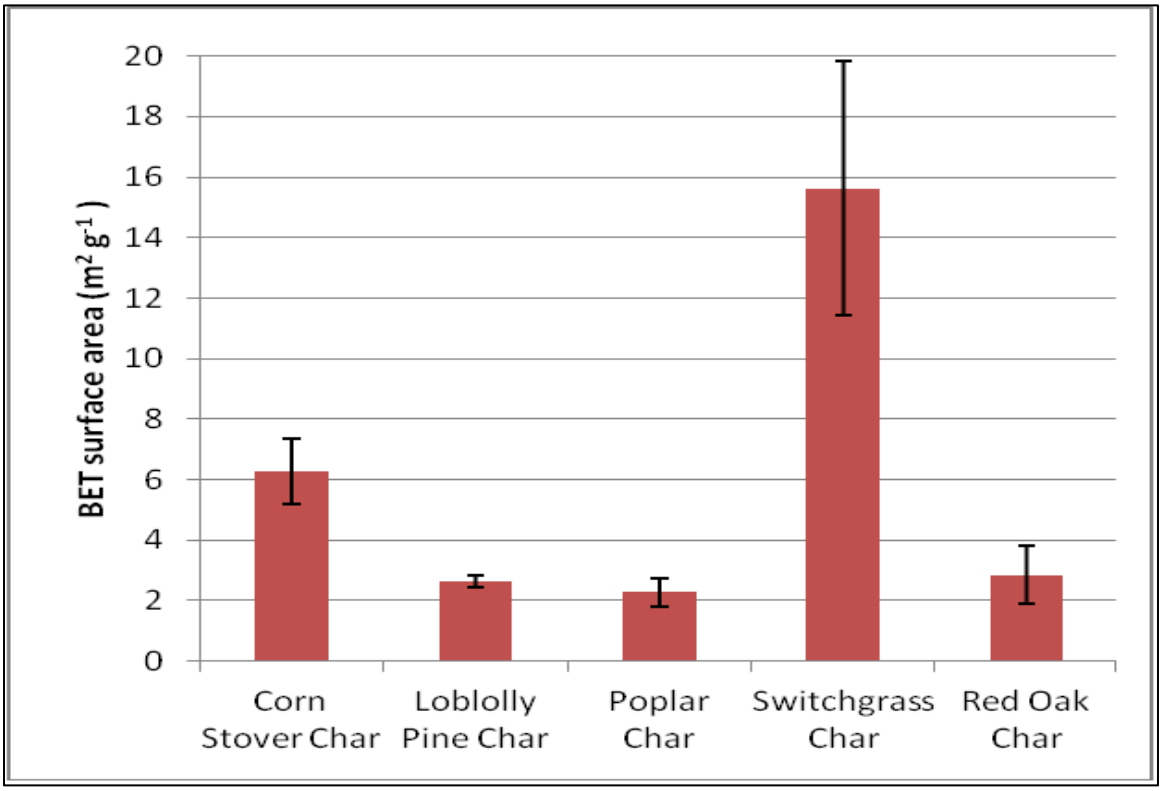

Figure 3. Average BET surface area of five fast pyrolysis biochar (non-activated materials).

The low surface area is also the result of condensation of bio-oil on biochar surfaces during pyrolysis. This phenomenon could be especially important in continuous production systems when the biochar is being quenched in contact with pyrolysis vapors. These volatile compounds can be seen in the vials from the degasser station of the surface area analyzer. In some cases, desorbed compounds on fast pyrolysis biochar shown in Figure A1 accounted for up to 5 wt%. These volatiles have been more clearly observed after washing biochar samples with methanol or other solvents (Figure A2). These volatiles are adsorbed onto the active site of the carbon, reducing specific surface area, as seen when comparing BET surface area for as received biochar and solvent washed biochar. Another limiting factor previously mentioned is many biochars have high ash content, even after acid wash, which does not contribute to the adsorption capacity of the biochar.

Steam activation of fast pyrolysis biochars can substantially increase BET surface areas. For example, the initial red oak biochar sample, pyrolyzed at 500˚C, had a surface area of 1.2

m^2/g. Steam activation at 400°C for 5 minutes, increased surface area by fifty folds or 52.7 m^2/g (Table 2). In general, the specific surface area of ACs made from fast pyrolysis biochar increased with increasing activation temperature within the temperature range for this study (between 400 and 800°C). In a similar study, Ioannidou and Zabaniotou (2007) reported the maximum temperature achieved during activation is the single most important parameter determining the surface area of the product. However, there is a residence time that determines the optimum degree of activation for a certain temperature. For activation at 400 and 600°C, the optimal residence time was longer than one hour. However, for activation at 800°C, the optimal time was only 5 minutes. The maximum surface area achievable in activated carbon is a function of both temperature and residence time. Prolonged exposure during activation results in thin pore walls that collapse, forming a smaller number of large pores and decreasing overall surface area[38,71]. Chemically, as the activation continues, more carbon is devolatilized as CO and CO_2[71] and ash content increases. Excessive oxidation of the sample (Table 2) is especially important during prolonged activation treatments at high temperatures, which results in a rate of mass loss of gases greater than the rate of pore formation and ultimately the surface area achieved[17]. It appears that the process is inherently unstable at more stringent conditions, which is reflected in the variability of the results for conditions that result in higher surface areas.

Table 2: BET surface area and standard deviation m^2/g for all treatment combinations of red oak char

Temp/Time	**5 min**	**32.5 min**	**60 min**	*Average group*
400°C	52.7 ±37.5	127.6 ±13.7	145.4 ±74.5	*108.6 ±60.0*
600°C	350.7 ±72.8	355.3 ±105.7	635.8 ±141.1	*447.2 ±170.6*
800°C	656.6 ±185.3	526.9 ±129.4	401.8 ±67.0	*528.4 ±161.4*
Average group	*353.3 ±280.4*	*336.6 ±192.6*	*394.3 ±229.4*	*361.4 ±228.9*

The influence of residence time and temperature on surface area is presented in Figure 4. Dots represent the experimental results and the gradient mesh indicates the fitted surface response model.

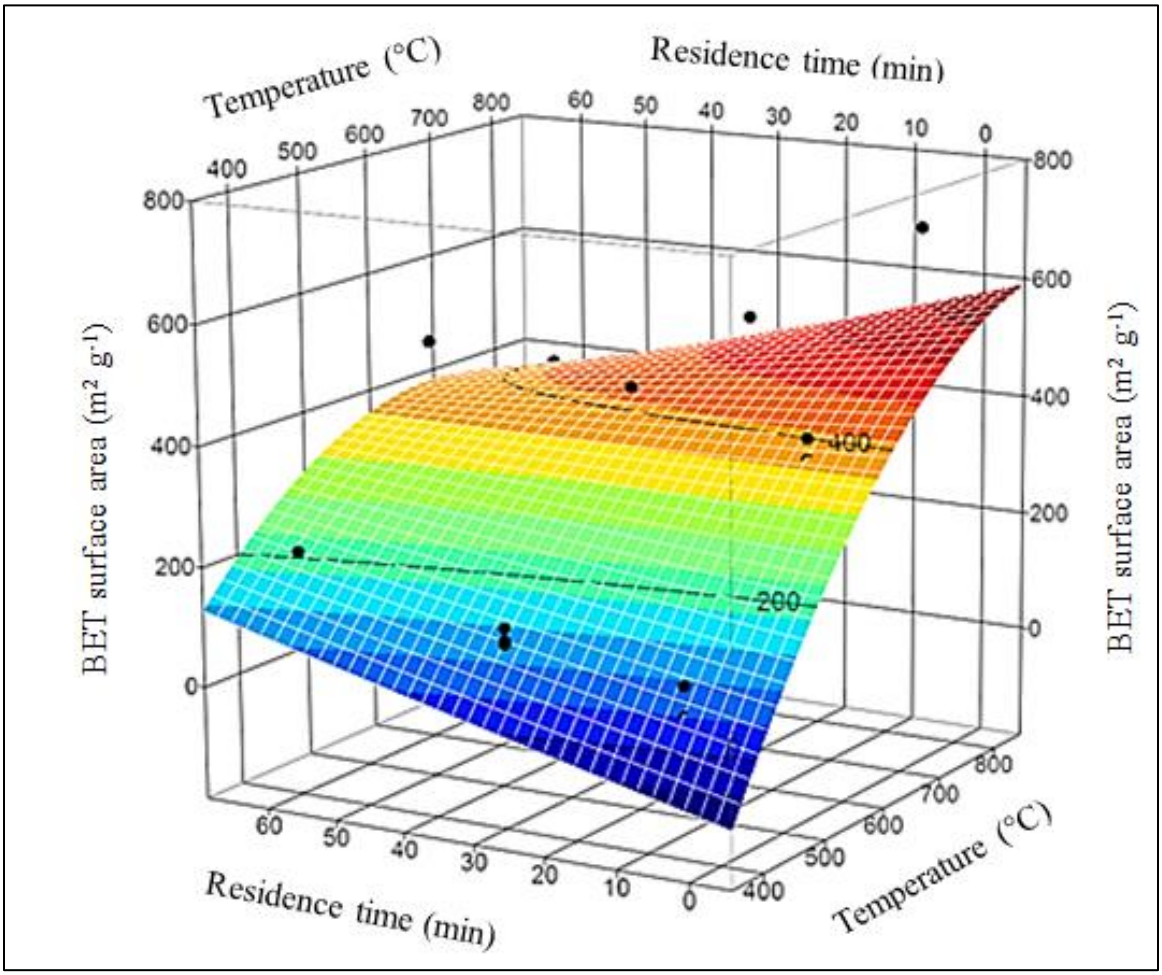
Temperature (°C)
400
500
600
700
800
Residence time (min)
60
50
40
30
20
10
0
BET surface area (m² g⁻¹)
800
600
400
200
0
400
200
Residence time (min)
60
50
40
30
20
10
0
Temperature (°C)
400
500
600
700
800
BET surface area (m² g⁻¹)
800
600
400
200
0

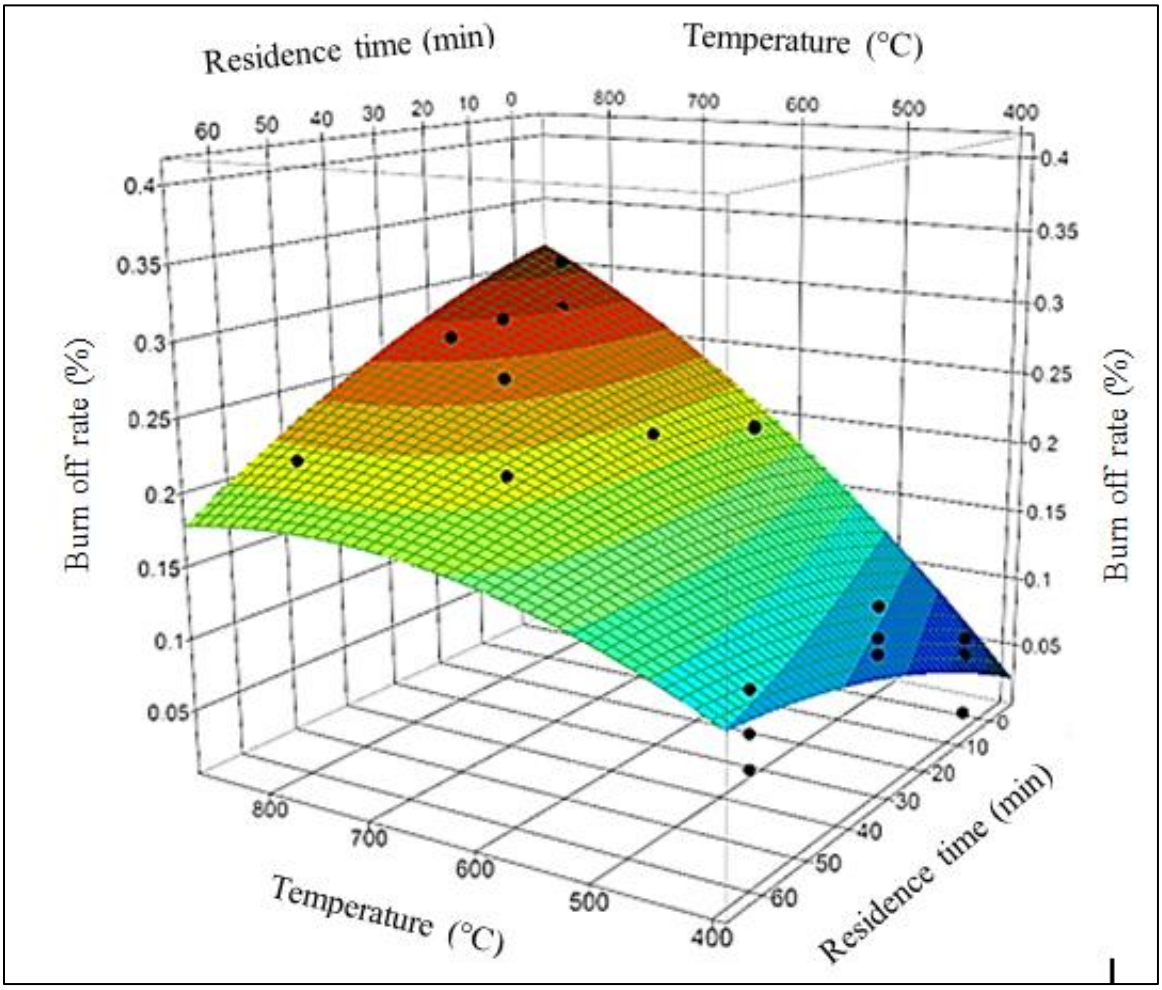

Figure 4. RSM plot shows the influence of pyrolysis temperature, residence time, and surface area (top) and burn off (bottom) on red oak activated carbon. Only data points (black dots) above the model surface are shown to avoid confusion to their location (the R^2 for the surface area model was 84.4% and burn off 82.5%).

For the conditions investigated, this model indicates higher temperatures and short residence times produced overall larger surface areas and burn off . The model predicts a maximum surface area is produced at conditions outside the range of temperature and residence time tested, which could not be validated because of constraints on the reactor's operating range. The activated carbons produced in this study have specific surface areas falling in the lower end of commercial adsorbent materials, typically ranging from 500 to 2000 m^2/g.

Large standard deviations (Table 2) among replications indicated surface area measurements were influenced by unaccounted parameters or other sources of errors within the experiment. Several factors that may have contributed to the observed variability include heterogeneity within the biochar feedstock, such as the presence of foreign materials and errors associated with specific runs, including the precision of sensors and heating elements, mass flow meters, tightness to air or gas leaks, differences in mixing, gas diffusion and human error. A second order polynomial model represented the relationship between surface area, pyrolysis temperature, and residence time (Table A-2).

As activation temperatures increased and/or residence times increased, the overall burn off rate of the activated carbon increased (Figure 4). However, the best fitted model for burn off was a first order. Compared to BET response, where the quadratic term for temperature was significant, the burn off (%) quadratic term did not meet the significance level, while other first order parameters, such as temperature, intercept, and interaction between temperature and residence time did. This result is likely due to the large noise in this measurement and the relatively larger mean squared error to the model for this parameter. The ANOVA for this model was significant with $p<0.001$. The lack of fit test was not significant and the residual versus predicted plot showed a fairly random distribution without a clear pattern.

In general, as activation temperature increased both mass burn off during activation and specific surface area of the ACs increased. This trend has also been seen in previous studies[17,30,72]. For example, this relationship of surface area and burn off (%) has been reported by Tam and Antal (1999), where the surface area is correlated with the yield of AC in the range of 15 to 60% of burn off. Within this region, the surface area per gram of activated carbon can be represented by an inverse function of the yield for burn off, reaching more than 1000 m^2/g. From a practical standpoint, maximizing the activation process based on the burn off can be a simple, effective method to optimize the process. Materials with high surface areas can be achieved by more severe activation conditions at the expense of mass loss and overall throughput (Figure 5).

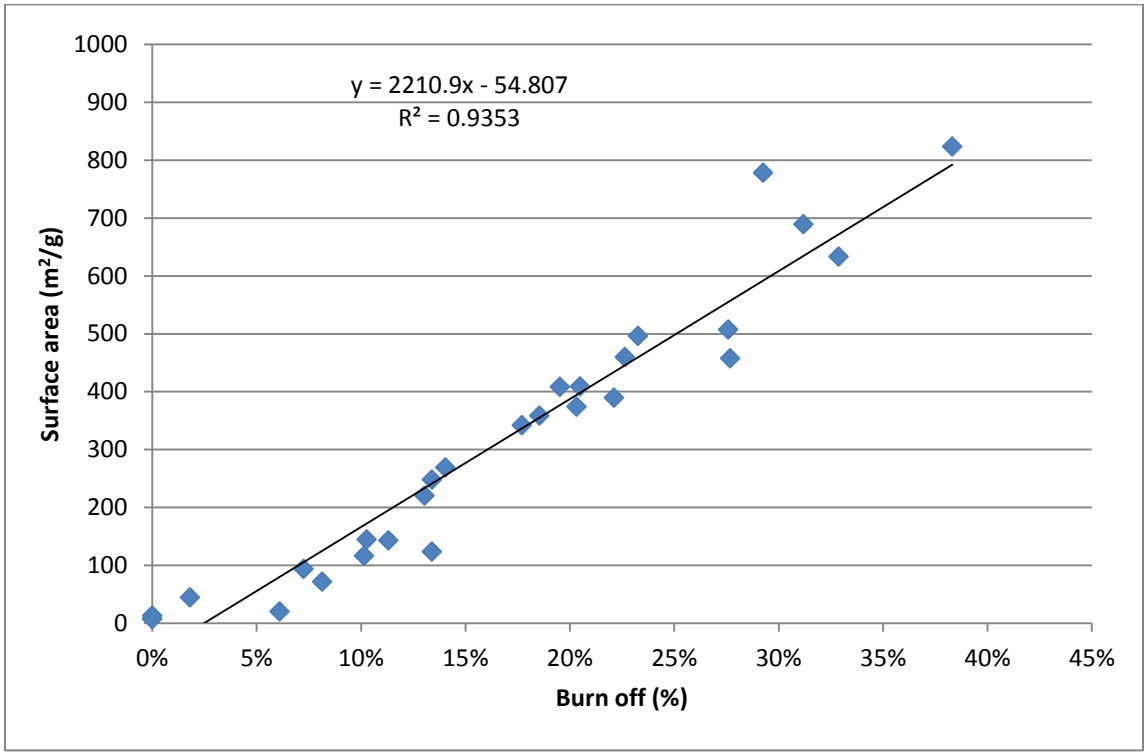

Figure 5. Surface area vs. extent of burn off for all temperatures and residence time treatments.

Using a prediction profiler can maximize the total surface area of the activated carbon produced from a given amount of feedstock. The maximum ratio of surface area to mass loss achieved was 365 m^2/g and 18% burn off. This result is achieved for an activation temperature of 600°C and 60 min of residence time (Figure 6).

An economic evaluation was performed by defining a new variable called gross value, defined as the amount of activated carbon yield, multiplied by the surface area and the bulk price to surface area index (to reflect sorbent quality) for each activation treatment (Figure 7).

Based on a theoretical value of $4x10^{-6}(\$/m^2)$ for commercially available activated carbon, a gross value optimum can be found, which differs from optimizing the activation reaction towards the highest surface area to burn off conditions. The excessive burn off lessens the overall AC yield and lowers the economic gross value from the process. The highest gross value for activating the biochar was attained around 800°C and 5 min of residence time. At this condition,

approximately $1540 can be obtained for every metric Tons of raw biochar, which will result in 720 kg of activated carbon (burn off of 28%) with 543 m^2/g (Figure 7).

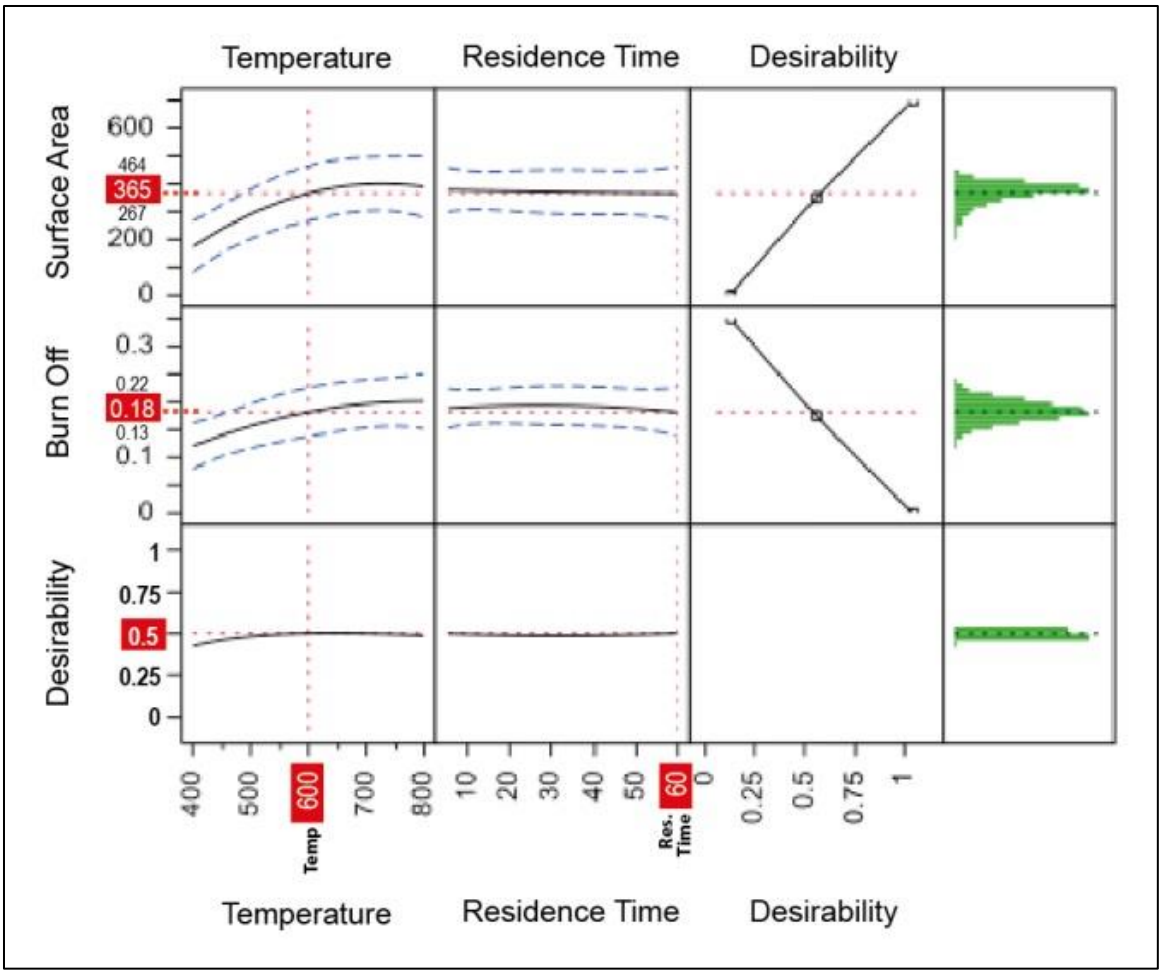

Figure 6. Predictor profiler, desirability functions and frequency distribution graph for surface area and burn off.

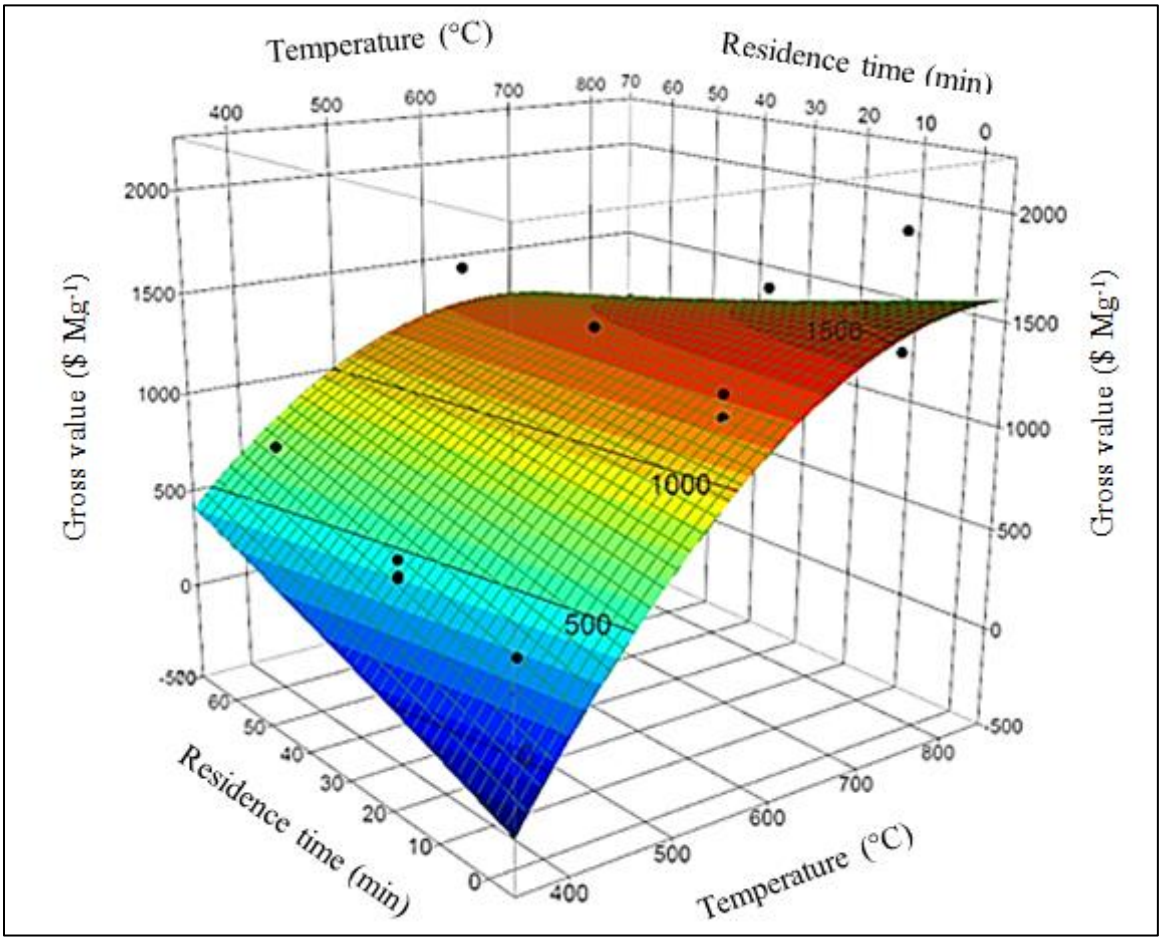
Temperature (°C)
Residence time (min)
Gross value ($ Mg-1)
Gross value ($ Mg-1)
Residence time (min)
Temperature (°C)
1500
1000
500

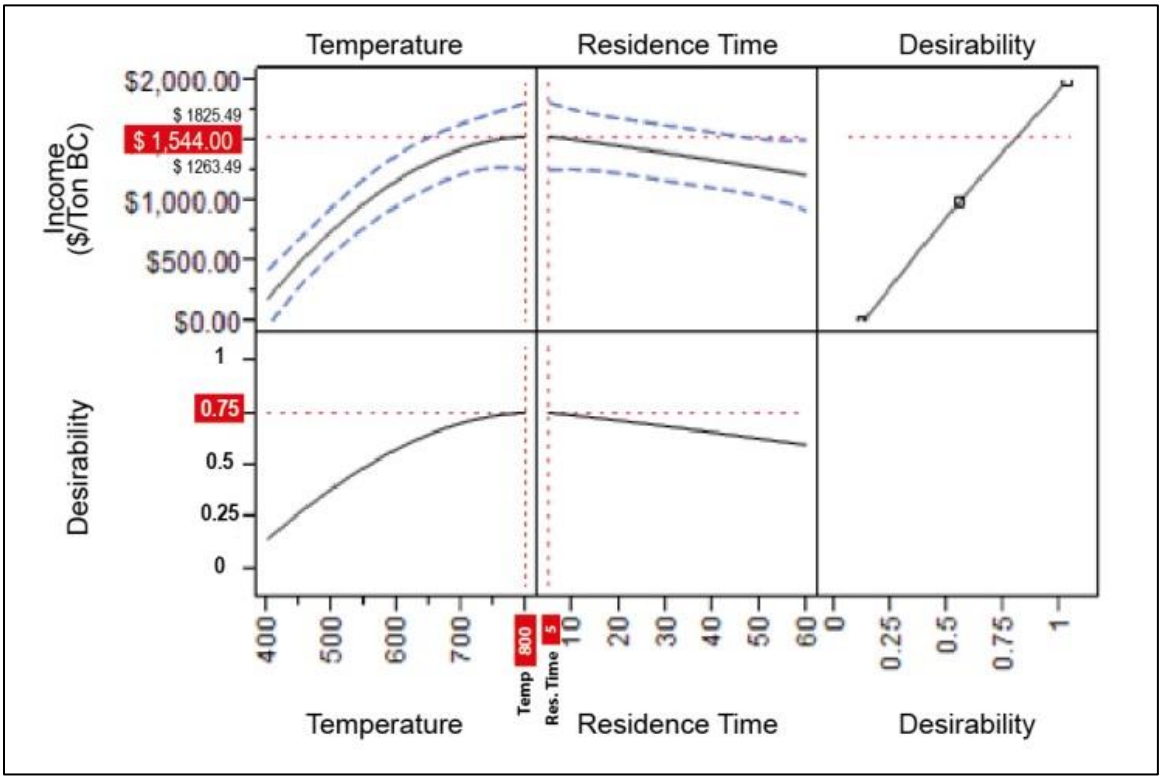

Figure 7. RSM plot for gross value $/ton of biochar for the different treatment combinations (top) and predictor profiler (bottom). Only data points above the model surface are shown to avoid confusion as to their location (the R^2 for this model was 86.6%).

An economic feasibility study for producing activated carbon under these conditions was studied. Assumptions for capital and operational costs were scaled from Lima et al. (2008) and Torrik et al. (2013). However, the proposed plant was downsized to a processing capacity of 3200 Tons of biochar per year using a scaling factor of 0.7. The fixed capital investment varied between 2.0 and 3.8 million dollars depending on the reactor, nitrogen generator, and steam boiler size for different conditions. Depreciation was calculated over a 10-year period, based upon the double declining balance depreciation method.

For operational costs, the price of biochar feedstock was set to 100 $/ton and other inputs, such as natural gas, fuel, and electricity, were based on historical 10-year averages (International Energy Agency Annual Energy Outlook 2012), and other materials were based on current commodity prices.

For the purpose of this study, both capital costs and operational costs vary greatly with different operating conditions to manufacture activated carbon. Regarding operational costs, the amount of natural gas required to increase the temperature of steam from 400 to 800˚C is $20 per Ton (Table 3). However, a change in residence time from 5 min to 60 min increases the overall energy usage and operating costs by more than $500 per Ton (Table 3). For equipment cost, the residence time defines the throughput and ultimately, the scale of the equipment. For example, the reactor capacity, nitrogen generator, and boiler size, depend upon the throughput of the process. A continuous reactor that processes 10 Ton of biochar daily with a residence time of 60 min (0.41 Ton/ hr) is 12 times larger than the same throughput with a 5 min residence time, and similarly with other associated equipment (Table A4 details the capital and operational costs of the process).

The operational costs associated with activating the biochar for 60 min is much higher than with 5 min of activation (Table 3). For this study, generating high temperature steam for 60 minutes, as used in the laboratory trials (1 mL/g min^{-1}), accounted for 44-50% of the total costs, resulting in negative net revenues. On the other hand, activation with 5 minutes and temperatures of 800˚C instead of 400˚C produced a 1.6% increase in overall costs, but with a significantly higher surface area. Under 800°C and 5 minutes, the estimated net revenue would result in approximately $907 per Ton (Figure 8). While there are higher capital costs associated with increasing residence time to 60 min, the operational costs contribute the largest cost.

Table 3: Predicted gross value, operational and capital costs, and estimated net revenue per metric Ton of biochar activated for all combinations of reaction conditions

Predicted gross value $ per Ton (surface response model)			
	Time (min)		
Temp °C	5	30	60
400	197.81	383.42	584.78
600	1,183.58	1,207.49	1,214.81
800	1,544.43	1,406.64	1,219.93

Operational costs $ per Ton			
	Time (min)		
Temp °C	5	30	60
400	564.26	792.13	1,028.43
600	569.60	826.29	1,092.49
800	574.94	860.46	1,156.55

Capital cost $ per Ton			
	Time (min)		
Temp °C	5	30	60
400	62.67	93.96	117.74
600	62.67	93.96	117.74
800	62.67	93.96	117.74

Net revenue $ per Ton			
	Time (min)		
Temp °C	5	30	60
400	(429.13)	(502.67)	(561.39)
600	551.30	287.24	4.58
800	906.82	452.22	(54.36)

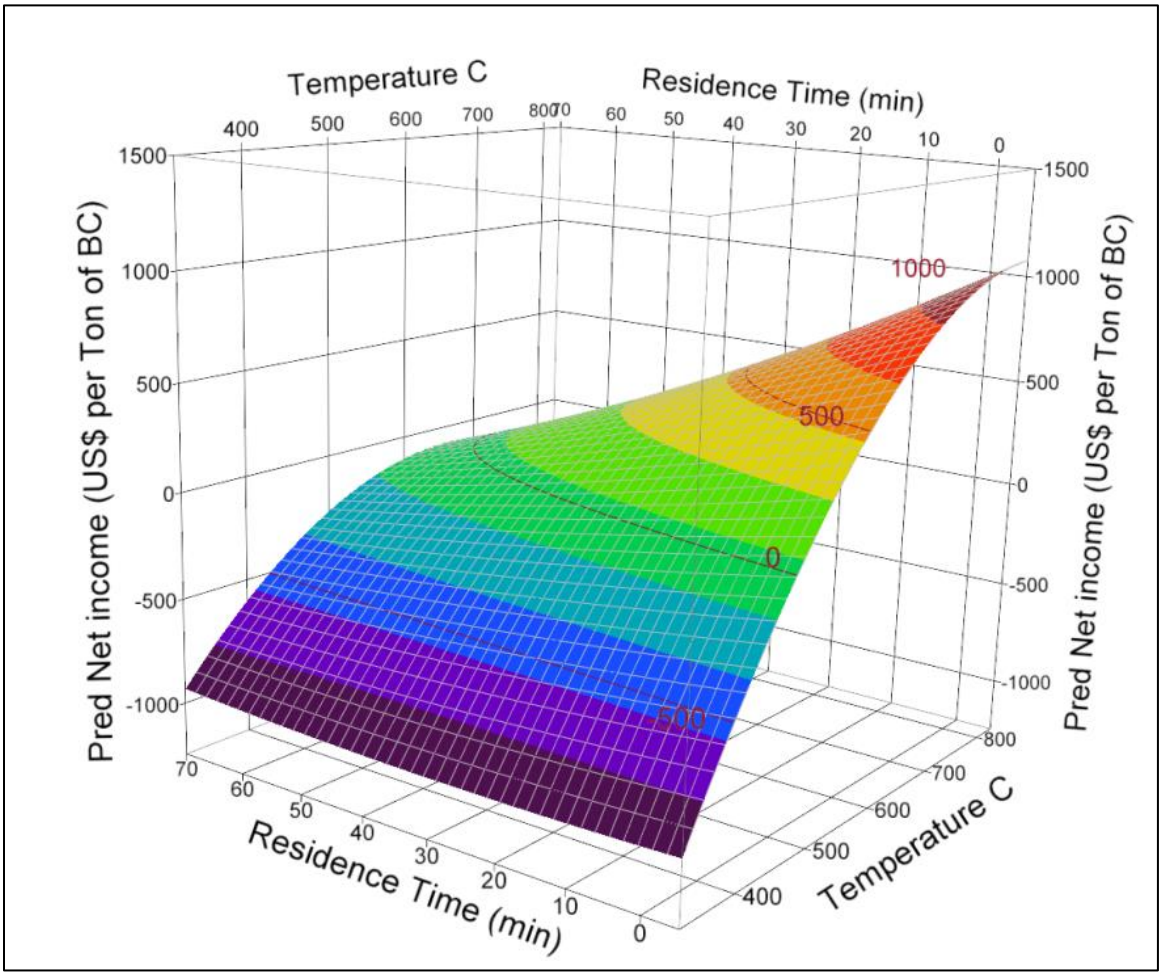

Figure 8. RSM plot for net revenue (gross revenue minus capital and operational costs) per every Ton of biochar activated.

At 800°C and 5 min of activation, an activated carbon facility operating 320 days per year would be able to produce 2500 Tons of activated carbon. The total estimated cost for production ranges from 0.62 to 1.27 $/Kg and for the best economic scenario, the production cost was 0.63 $/Kg with a predicted gross value of 1.5 $/Kg.

RSM provided an effective and simple approach for optimizing a combination of factors, especially when a response fits a higher degree order model. RSM proved an effective tool when significant interaction effects of independent variables are present and when dealing with important variability, such as materials or production methods**.**

Conclusions

This study found that activated carbon can be produced by steam activation of fast pyrolysis char. Fast pyrolysis biochar initially had very low porosity and surface area (1.2 ± 0.5 m^2/g), and was converted to activated carbon of more than 500 m^2/g using a one-step physical activation.

RSM helped to optimize the activation process to yield the highest surface area material or highest economic benefits from the process. In addition, RSM facilitated experimental work, and understanding the relationship between surface area achieved and operating conditions. The best economic scenario was found at 800°C and a residence time of 5 minutes resulting in 543 m^2/g of BET surface area with a burn off of 28% and $907 net revenue.

This same methodology can be utilized to determine and produce specific activated carbons targeted toward specific applications. Surface area is commonly used for characterizing and screening adsorbents. However, it does not necessarily best correlate with specific chemical adsorption. With this approach, different processes and materials can be optimized to meet various industrial applications with a similar, simple practical approach to this study.

Acknowledgements

Financial support from the Iowa Energy Center is gratefully acknowledged. In addition, we would like to thank Bojun Song and Thaddeus Steinberg for their assistance in performing experiments.

Appendix

Table A1: Experimental set up and results for every combination of temperature and residence time

Temperature	Residence Time	Run	Surface Area	Burn off
400	5	1	44.4	1.8%
400	32.5	1	116.5	10.2%
400	60	1	71.3	8.1%
400	5	2	20.1	6.1%
400	32.5	2	123.4	13.4%
400	60	2	144.7	10.3%
400	5	3	93.7	7.3%
400	32.5	3	142.9	11.3%
400	60	3	220.3	13.0%
600	5	1	408.8	20.5%
600	32.5	1	248.0	13.4%
600	60	1	778.2	29.3%
600	5	2	374.2	20.3%
600	32.5	2	358.4	18.5%
600	60	2	633.2	32.9%
600	5	3	269.0	14.0%
600	32.5	3	459.4	22.6%
600	60	3	495.9	23.3%
800	5	1	689.0	31.2%
800	32.5	1	664.9	77.5%
800	60	1	341.6	17.7%
800	5	2	457.2	27.7%
800	60	2	389.6	Holder Broke
800	32.5	2	408.3	19.5%
800	5	3	823.5	38.3%
800	32.5	3	507.4	27.6%
800	60	3	474.1	Holder Broke

The variability of the results is something to further investigate. The surface area results could be due to processing parameters that might vary within different batches. For example; differences in mixing that enhanced heat transfer or the effective contact and diffusion of the oxidizing agents through the biochar material (and not just through the surface) within certain

batches. Also, another variable that needs to be carefully looked into is the procedure for quenching the char after activation, which can lead to continuing activation.

An ANOVA indicated the intercept, temperature, residence time, and temperature squared are all significant terms. A lack of fit test, which tests whether the fitted model provides inadequate approximation of the "true surface," was not significant (p=0.28). Therefore, the second degree model described the response surface fairly well. A plot of residuals relative to predicted surface area (not shown) yielded randomly scattered data points with no evidence the surface area could be better approximated using a higher order polynomial.

Table A2: Estimated parameters for the surface area model and significance level.

Term	Estimate	Standard Error	t Ratio	p-value|
Intercept	370.6	37.5	9.89	<.0001
Temp	178.5	21.5	8.29	<.0001
R. Time	-6.3	22.8	-0.28	0.7846
Temp*R.Time	-70.5	26.2	-2.68	0.0163
$Temp^2$	-84.6	38.4	-2.2	0.0428
R. $Time^2$	1.6	36.6	0.04	0.9656

Figure A1. Bio-oil desorbed and condensed on the glass vials from the degassing stage of the surface area analyzer.

Figure A2. Water (left), methanol (middle), and acid (left) wash of fast pyrolysis chars previous activation**.**

Table A3: Techno-economic assumptions for capital and operational cost

DCFROR Worksheet

Assumptions	**Value**
Fixed Capital Investment (U$S)	38000
Equity	100%
Loan Interest	8%
Loan Term, years	10
Working Capital (% of FCI)	15%
Salvage Value	
General Plant	0
Type of Depreciation	DDB
General Plant	200
Depreciation Period (Years)	
General Plant	10
Income Tax Rate	39%
Cost Year for Analysis	2011

Example for best case scenario 800°C & 5 min	
Percent AC Yield	0.8
Annual Operating Days	320
Annual Operating Hours	7680
Feedstock Biochar (kg/day)	10000
Feedstock (kg/yr)	3200000
Feedstock (Ton/yr)	3200
Activated Char Yield (kg/day)	8000
Activated Char Yield (kg/year)	2560000
Activated Char Yield (Ton/year)	2560
Men per Shift	2
Shifts per Day	3
Hours per Day	24
$/hr	18

Capital Costs

Equipment	**Scale (kg/day)**	**Cost**	**Scaling fact.**	**Scale Mult.**	**Scaled cost**
Ball mill	10000	50000	0.7	1	50000
Boiler steam producer	4695	62685	0.7	978	20905
Nitrogen Generator	6000	1500000	0.7	600	299289
Rotary kiln (one)	10000	410000	0.7		410000
Rotary cooler	10000	65000	0.7	10000	65000
Sieve	10000	50000	0.7		50000
Total equipment cost	10000	2137685	0.7	8000	2137685
Equipment installation	10000	175000	0.7		175000
Instrumentation	10000	136000	0.7		136000
Piping & material transport	10000	155000	0.7		155000
Electrical installation	10000	97000	0.7		97000
Buildings	10000	97000	0.7		97000
Yard improvements	10000	38000	0.7		38000
Service facilities	10000	292000	0.7		292000
Land	10000	19000	0.7		19000
Engineering& supervision	10000	195000	0.7		195000
Construction expense	10000	233000	0.7		233000
Contractor's fee	10000	38000	0.7		38000
Contingency	10000	155000	0.7		155000
Total capital					3767685

Table A3 Continued

Operating costs annual estimates without steam and nitrogen gas production

Item	Scale (kg/day)	Annual Cost	$/day	$/ton of char cost	Scaled Annual Cost
Biochar Cost	10000		10000	100	320000
Steam	10000				
Chem. pretreatment	10000				169408
Water	10000	1000	3.125	0.390625	1000
Natural gas	10000	10000	31.25	3.90625	10000
Electricity	10000	38000	118.75	14.84375	38000
Operating labor	10000	316000	987.5	123.4375	316000
Maintenance labor	10000	42000	131.25	16.40625	42000
Supervision	10000	47000	146.875	18.359375	47000
Fringe benefits	10000	126000	393.75	49.21875	126000
Operating supplies	10000	32000	100	12.5	32000
Maintenance supplies	10000	21000	65.625	8.203125	21000
General & admin.	10000	319000	996.875	124.609375	319000
Property ins. & tax	10000	17000	53.125	6.640625	17000
Depreciation (10 year)	10000	212000	662.5	82.8125	212000
Total	10000	1181000	3690.625	461.328125	1670617

CHAPTER 3 IMPROVING PYROLYTIC SUGAR FERMENTABILITY THROUGH TREATMENT WITH BIOCHAR AND ACTIVATED BIOCHAR

Bernardo G. Del Campo[a], Jieni Lian[b], Xuefei Zhao[d], Laura R. Jarboe[e], Zhiyou Wen[d] and Robert C. Brown[a*]

To be submitted to Biomass & Bioenergy
[a] Mechanical Engineering, Iowa State University, United States
[c] Bioeconomy Institute, Iowa State University, United States
[d] Food Science, Iowa State University, United States
[e] Chemical and Biological Engineering, Iowa State University, United States

Abstract

Bio-oil from the fast pyrolysis of biomass is composed of hundreds of compounds. Depending on processing conditions it can contain 7-30 wt% of fermentable anhydrosugars. After these pyrolytic sugars are separated from the bio-oil, some compounds that are inhibitory towards fermentation remain, dramatically reducing the production of ethanol by engineered *Escherichia coli KO11+ lgk*. This study evaluated the efficacy of biochars, activated biochar and activated carbon for removing toxic agents, increasing bacterial growth and ethanol production. The detoxification of 20 g/L of pyrolytic sugars with non-activated red oak biochar resulted in a 5-fold increase of ethanol production and bacterial growth compared to untreated pyrolytic sugars. Pyrolytic sugar detoxified with commercial activated carbon and activated biochar showed 9% and 18% of the theoretical ethanol yield in preliminary fermenters trials, respectively, while untreated pyrolytic sugars showed no cell growth or ethanol production. This is the first demonstration that biochar can detoxify pyrolytic sugars for fermentation.

Highlights

- Activated and non-activated biochars of different formulations and feedstocks were produced.
- Commercial AC and activated and non-activated biochars detoxified pyrolytic sugars and improved fermentability.

- Commercial AC and red oak biochar showed higher ethanol yields than other adsorbents.
- Inhibitor removal with pure compounds showed different removal efficiencies for different adsorbents.
- BET and DFT surface area correlated best with bacterial growth but poorly with ethanol production.

Keywords

Pyrolytic sugar, detoxification, biochar, ethanol, levoglucosan.

1. Introduction

The thermochemical processing of biomass via fast pyrolysis is a rapidly developing technology that produces bio-oil, biochar and non-condensable gases for the production of renewable fuels, chemicals, and energy. Fast pyrolysis of biomass is achieved through high heating rates (~100 °C/s), low residence times (<20 seconds), high temperatures (~500°C), and most importantly, in the absence of oxygen or starved air conditions. From the process (Figure 1), approximately 50-70 wt% of the biomass is turned into bio-oil, 15-30 wt% into non-condensable gases and 15-30 wt% into biochar [65,73-75]. Various studies have reported that bio-oil components can be converted into chemicals and fuels [8,74,76]. Kuzhiyil et al. (2012), found that bio-oil solutions containing as much as 20-40 wt% sugars can be produced from fast pyrolysis, if acid is used to passivate alkali metals present in the biomass.

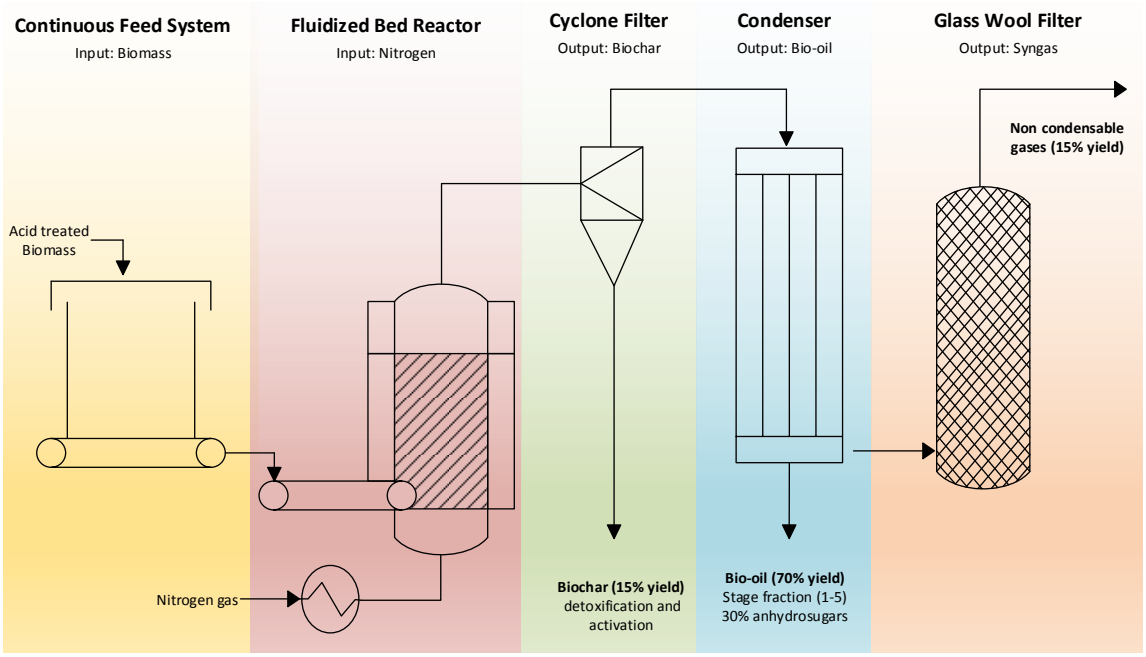

Figure 1. Fast pyrolysis process and typical bio-oil, biochar and non-condensable gases mass distribution adapted from [65]

The first two stages from the bio-oil is often grouped into two distinctive fractions: water soluble sugars and water insoluble phenolic oligomers fraction. The soluble fraction includes pyrolytic anhydrosugars, especially levoglucosan and cellobiosan. This fraction is an attractive source of carbon and energy for biological fermentation [8,77]. However, biocatalysts used to ferment the water soluble fractions are vulnerable to poisoning by contaminants co-produced in the pyrolysis process.

There are hundreds of compounds in pyrolysis oils (furans, phenols, ketones, aldehydes, anhydrosugars, carboxylic acids, etc.). These compounds can be partially segregated by different condensers and electrostatic precipitators into distinct stage fractions based on their dew points and vapor pressures during bio-oil recovery [65]. Stage fractions 1 and 2 collect the "heavy ends" operating at highest temperatures, between 345 and 102 °C, collecting large molecular weight water insoluble phenolic oligomers and water soluble sugars. Stage fractions 3 and 4 recover compounds with dew points close to phenol. The temperature of the condensers are kept between 129 and 77 °C and condenser 4 is assisted with and electrostatic precipitator to enhance recovery.

Stage fraction 5 is designed to remove the remaining condensable vapors, being mostly water and light oxygenates compounds, such as acetic, formic acids using the lowest temperature condenser of 18 °C. Further details on the fractionating bio-oil recovery system can be found in Ref.[65] and production and characterization of clean pyrolytic sugars can be found in Ref. [78]

The water soluble sugars are mostly derived from cellulose and hemicellulose biomass fractions [73]. Water can be used for rinse out these anhydrosugars to effectively separate the phenolic oligomers extracting a concentrated sugar fraction [75,78].

Water insoluble phenolic oil, which is derived from lignin, are thus concentrated and can be thermochemically processed via hydroprocessing to produce chemicals or combusted to produce heat and power [79]. The resulting sugar solution is mostly anhydrosugars, but also contains roughly 3-6 wt% of soluble constituents other than carbohydrates (Rover et al., 2014a). These impurities are mostly organic acids, furans and phenolic compounds, which are biocatalyst inhibitors' in small concentrations [77,78]. The sugar solution, referred to as pyrolytic sugar, contains approximately 40 wt% levoglucosan and other fermentable substrates such as cellobiosan, xylose, galactose and mannose [74,78]. Although this study targets the production of ethanol, there are numerous other fermentable products that could possibly be produced from anhydrosugars, including; butanol, fatty acids, and citric acid which can be turned into multiple commodity chemicals [8].

Depending on the feedstock, operating conditions and pretreatments, 7 to 30 % of the original biomass weight can be recovered as levoglucosan [8,78-83]. Organisms that encode levoglucosan kinase can convert levoglucosan to glucose-6-phosphate in an ATP-dependent reaction (Layton et al., 2011) and thus utilize levoglucosan with the same redox and ATP demand as glucose. With the theoretical yield of 2 mol ethanol produced per mol of hexose sugar, this corresponds to a theoretical ethanol yield of 57% by weight. However, inhibitors formed in the pyrolysis reactions including phenols, furfural, formic acid, valeric acid, 5-methyl-furfural and butyric acid [80,84] can dramatically reduce the fermentability of sugar solution and consequently, the yield and concentration of the final product. For example, 5-HMF (furan group) and guaicol, reported in the pyrolytic sugars at concentrations of 0.32% and 0.1%

respectively [78], are three times higher than the concentrations reported by Zaldivar et al (2000) to completely inhibit *Escherichia coli* growth. Therefore, it is expected that pyrolytic sugars that have been thoroughly cleaned with water and detoxified with adsorbent materials can increase sugar utilization and ethanol yields.

Several methods have been proposed for removing compounds that are toxic to microorganisms, including but not limited to overliming, acid hydrolysis, extraction with solvents, charcoal treatment, and ionic resins [75,78,85]. Activated carbon is a traditional adsorbent that has been used for decades to remove various kinds of organic and inorganic contaminants in liquid media [19,21,77,86-91]. In an effort to remove inhibitors in bio-oil, researchers have used activated carbon as an adsorptive media, which results in substantial improvements of fermentation output [85].

As previously mentioned, fast pyrolysis also produces a carbonaceous solid, biochar, a relatively low-value co-product. This carbon rich material can be burned for energy production, or incorporated into agricultural lands as soil amendment. Numerous studies have shown that biochar can readily be upgraded through chemical or physical treatments to make "activated carbon" [28,40], which is effective at removing contaminants from air, water, and soil.

The goal of this study was to evaluate the usefulness of biochars and activated biochars for detoxifying pyrolytic sugar solutions for fermentation to ethanol. These results are compared to the performance of commercial activated carbon.

2. Materials and Methods

2.1. Preparation of pyrolytic sugar syrup

Bio-oil used in this study was produced from red oak biomass (*Quercus rubra*). The production and fractionation of bio-oil (Pollard et al., 2012) and the recovery of pyrolytic sugar syrup were described previously (Rover et al., 2014a). The woody biomass was processed in a

fluidized-bed fast pyrolyzer at 500°C. Bio-oil was recovered in 5 distinct stage fractions (SF), with the heaviest fractions (SF1 and SF2) containing most of the anhydrosugars. A sugar phase was obtained with a simple separation by rinsing with de-ionized water at room temperature at a weight ratio of 1:1 water to bio-oil. The pyrolytic syrup was dried with a rotary evaporator at 40°C until no more condensation was observed on the round bottom flask. For further details in the separation of the pyrolytic sugars from the heavy ends of bio-oil, see Rover et al (2014).

2.2. Production of activated and non-activated biochars

The biomass feedstocks (red oak, corncob, switchgrass and corn stover) were collected from the Biocentury Research Farm (ISU). Biochars were produced through fast pyrolysis of biomass at 500°C in a fluidized bed reactor under nitrogen gas at 4 L/min STP. Further details on the fast pyrolysis system can be found in Ref. [65]

A portion of the biochar from each feedstock was activated using a e continuous high temperature auger reactor (Figure 2). The reactor auger length was 50 cm, with a 2.54 cm diameter and 1.25 cm pitch flighting constructed from 316 stainless steel. Both steam and carbon dioxide ports were located at the final section of the auger reactor, and the temperature is typically kept at 800°C. The residence time or activation intensity is varied (Table 1) adjusting the speed of the auger. Steam or carbon dioxide were heated to 800°C before they were injected at the end of the reactor in a counter flow direction with the char being activated. The steam was produced by evaporating distilled water through a heated stainless steel coil metered by a peristaltic pump.

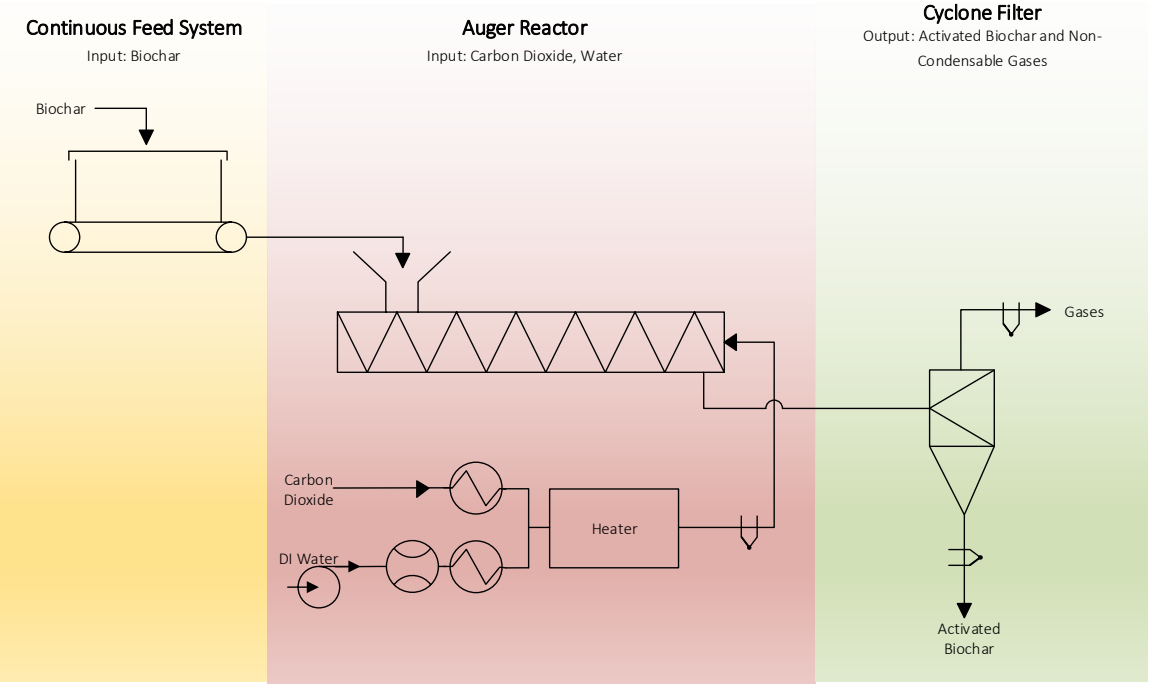

Figure 2. Design of a high temperature reactor for physical activation of biochar

Various crop residues were pyrolyzed and activated in both powder and pellet forms. The pellets were obtained from ISU Biocentury research farm. The pelletized biomass feedstock was pyrolyzed in the auger reactor at 500 °C with approximately 20 seconds of residence time. Powder materials were obtained by sieving the fines and ball milling the larger particles to less than 47 µm (US sieve #400). The resulting materials used for detoxification included; corn cob activated and non-activated biochar, corn stover activated pellets and corn stover biochar powder, switchgrass biochar powder and activated pellets, and red oak biochar and activated biochar powder. All the adsorptive materials were tested against commercial activated carbon (G60 Darco®) and pure levoglucosan fermentation (no pyrolytic sugar).

Various activated biochars from different feedstocks were assessed on their physical parameters for evaluating its detoxification effect. Physical activation was done with various temperatures and conditions (Table 1) in order to have a broad spectrum of materials with different surface area (0-1000 m^2/g) and pore distributions (0.01 to 0.37 mL/g). These physical surface properties were evaluated to see if there was any correlation with fermentability. Biochar

and activated biochar pH was measured by mixing biochar and distilled water at a ratio of 1:10 w/w.

2.3. Physi-sorption analysis

Analysis was performed with 0.1 g samples degassed for 4 hours at 300 °C with a vacuum reaching at least 100 Pa of absolute pressure. BET surface area, NLDFT, t-plot and full isotherm measurements were made using N_2 adsorption with a Quantachrome NOVA 4200e Gas Sorption Analyzer. Seven adsorption points ranged from 0.01 to 0.3 P/P_o were measured and the data was corrected for micro pore volume using the Nova win 11.02 software for establishing the optimum range. Full isotherm consisted of 30 adsorption and 20 desorption points evenly distributed.

2.4. Detoxification of pyrolytic sugars and inhibitors removal

Pyrolytic sugar syrup was weighed and diluted with E-pure ™ water to concentrations of 5, 10, 20 and 40 g/L. The ultrapure water purification system, E-pure ™, consists of 4 cartridges with various adsorbants and final micro filter to remove sediments impurities and microbial contaminants. . The sugar syrups were then held at 4 °C for 24 hours to precipitate lignin oligomers, followed by extraction of the liquid solution with a syringe. The resulting sugar syrup was either used directly for fermentations (non-detoxified) or detoxified with biochar. The general procedure for pyrolytic sugar detoxification was: 1) adding 1 g of detoxifying media (e.g. activated biochars) to 100 mL of sugar solution, 2) manually stirring the mixture for a few seconds, 3) leaving the mixture to sit for one hour at 4^oC to allow for adsorption of organic compounds, and 4) centrifuging at 8000 G for 3 min and filtering with a 0.45 µm syringe filter. The 10X stock LB growth media was added to make the pyrolytic sugar syrup plus 1X LB and the pH was adjusted to 7.0 with H_2SO_4 or NaOH 1.0 M. The use of this media for fermentation is described below. Commercial G60 Darco® activated carbon was used as a control for all biochars.

2.5. Analysis with FT-IR

Biochar samples were characterized before and after use with pyrolytic sugars. Biochars that were used for detoxification were dried with a vacuum evaporator for 48 hours at 60 °C. The samples were ball-milled with Retsch PM 100 in order to pass through a #100 mesh sieve. A Fourier transform infrared spectroscopy (Nicolet FT-IR 6700, Thermo Electron Corporation, Madison, WI, USA) was used to measure the surface functional groups of bio-chars by measuring absorbance with an attenuated total reflectance (ATR) accessory. The crystal used on the ATR accessory was diamond. Compared with the traditional infrared techniques, the ART-FTIR technique not only shortens the analysis time, but also improves the quality of biochar spectra. The 256 scans of spectra of a sample were obtained at 8 cm^{-1} resolution from 650 to 4000 cm^{-1}. The spectral absorbance peaks of the functional group by FTIR were analyzed by comparing the peak position with known peaks via reference.

2.6. Analysis with GC-FID

Ethanol and inhibitors in sugar syrup were analyzed by gas-chromatography with flame ionization detector (GC-FID). The following compounds were used for calibration: methylcyclopentenolone, m-tolualdehyde, 1,2,3-trimethoxybenzene, 2,6-dimethoxyphenol, 4-methyl-2,6-dimethoxyphenol, hydroquinone, 1,2-benzenedimethanol, 2,5-dimethoxybenzylalcohol, 4-hydroxy-3-methoxyacetophenone, 2,4-dimethoxyacetophenone, Levoglucosan, and 3,5-dimethoxy-4-hydroxyacetophenone. Samples of fermentation broth were centrifuged at 8000 G for 3 min and separated from the precipitates. The supernatant was filtered after two-fold dilution with E-pure water and put in 2 mL GC-vials for ethanol analysis. A one microliter sample (split ratio of 25:1) was injected into a Varian 450-GC (Palo Alto, CA) and dispersed by 30 m x 0.25 mm x 0.25 mm Zebron ZB-WAXplus column (Torrance, CA) with helium gas as carrier at a constant flow rate of 1.4 mL/min. The running method was set up with an injection temperature at 200 °C and an column temperature at 35 °C for 5 min, subsequently increased to 130 °C at 10 °C/min, and further raised to 210 °C at 30 °C/min. Pure chemicals (Sigma, USA) were used for standard curves ranged from 0.1 to 1 g/L.

2.7. Analysis with IEC

Samples containing pyrolytic sugar were diluted by E-pure water to concentration of levoglucosan between 0.1-10 ppm. The diluted samples were then passed through 0.22 µm PTFE filter and transferred into 2 ml glass IEC vials. Ten µL of the sample was fully injected into a Dionex ion electronic chromatography (IEC) ICS 5000 system (Sunnyvale, CA) equipped with a CarboPacTM PA 20 (4 x 50 mm) analytical column and a CarboPacTM PA 20 (3 x 30 mm) guard column. The elution solvent is 0.01 M NaOH at a flow rate of 0.5 mL/min, and a conduction detector was used for peak analysis. Pure levoglucosan was used as a calibration standard, and all the analysis concentrations were in the range of calibration.

2.8. Overliming and neutralization

In stirred fermentation trials (200 mL automatic biofermenter), $Ca(OH)_2$ powder was added to the sugar solution to adjust the pH to 8.0 to precipitate contaminants [92]. Sulfuric acid 50% (w/v) was used to neutralize the solution to a pH of 7.0 at room temperature. The samples were centrifuged at 8000 G for 3 min and passed through a 0.45 µm filter.

2.9. Strains and medium

E. coli KO11 previously engineered to express the levoglucosan kinase gene (*lgk*) codon optimized for *E. coli* was used for ethanol fermentation (Layton et al., 2011). Luria Broth (LB) medium was used for seed cultures. Pyrolytic sugar syrup diluted to 0.5 - 5 % w/v was added to the LB medium. The pyrolytic sugar syrup contained about 40% (w/w) sugars[92].

2.10. Ethanol fermentation

Fermentation trials were performed in 15 mL vials using 1 mL of sample to prescreen different biochar materials, and a 200 mL automated bioreactor for closely monitoring the conditions and assessing fermentation capabilities.

E. coli was pre-cultured overnight in 50 mL of LB medium in a 250 mL flask at 37 °C in a shaker at 200 rpm with 34μg/ml chloramphenicol. For the screening test of biochar detoxification ability, 200 μL of pre-cultured cell suspension was added to 4 mL medium in a 15 mL tube. The tube was then sealed with a rubber stopper and incubated at 37 °C, 150 rpm. At 48 hours of cultivation, 1 mL of sample was taken for measuring cell growth and ethanol production. All the fermentation tests were performed in triplicate. Analytical grade levoglucosan 99.6% purity (Carbosynth Limited, UK) in water was used as a control for every fermentation test.

For the fermentation trials performed with the 200 mL bioreactor, 10% v/v seed broth was inoculated into 150 mL of LB medium with 2% w/v pyrolytic sugars (detoxified and non-detoxified) was used. The fermentation was performed at 37 °C stirred at 150 rpm with pH maintained at 6.5 an automated metering system supplying KOH 1M. The bacteria growth was observed with UV-vis spectroscopy at the optical density 550nm (OD_{550nm})

3. Results and Discussion

3.1 Activation results and adsorbent characterization

Biochars and activated biochar from various thermochemical treatments (Table 1) resulting in a wide range physisorption characteristics such as surface area and pore volumes (Table 2). These parameters are typically maximized in high adsorptive media, which typically means higher adsorption efficiency, or in this case detoxification. In addition to these physical adsorption parameters, different particle sizes ranging from less than 150 µm (activated carbon #100 mesh sieves) to 5-8 mm length (pellets and granular forms) were investigated.

Table 1: Different media used for detoxification

Feedstock	Thermal Process	Formulation	Pyrolysis / Activation	pH	S.A.*
Corn Cob	Biochar	Grits	Pyrolysis 500°C N_2 gas	8.2	4
Corn Stover	Biochar	Powder	Pyrolysis 500°C N_2 gas	8.7	6
Red Oak	Biochar	Powder	Pyrolysis 500°C N_2 gas	5.7	2
Switchgrass	Biochar	Powder	Pyrolysis 500°C N_2 gas	8.8	6
Darco ®	Commercial AC	Fine Powder	Steam Activated	6.0	917
Corn Cob	Activated biochar	Grits	Steam Activated 400°C 5 min	9.1	66
Corn Stover	Activated biochar	Pellets	CO_2 Activated 800°C 5 min	9.8	303
Red Oak	Activated biochar	Powder	Steam Activated 400°C 5 min	7.7	97
Switchgrass	Activated biochar	Pellets	CO_2 Activated 800°C 5 min	9.6	411

* Surface Area measured by BET method m^2/g

Physical activation with steam or carbon dioxide increased the pH of all samples by at least one unit while the surface area and total pore volume increased more than ten times to the initial charcoal feedstock,[34]). For example, red oak biochar BET surface area increased from 2 to 97 m^2/g and its pore volume from 0.01 to 0.09 mL/g when the biochar is activated with steam at 400°C for 5 min. Different activation procedures and intensity resulted in a range of various physical surface properties.

All of the activated biochars had high pH due to alkali and alkaline earth metals in the ash. Activation increased the pH of these materials, which is also thought to be the result of removing heteroatoms with acidic functional groups [31,34]. Corn cob, corn stover and switchgrass

biochars were alkaline in the pH range of 8 to 9, and red oak biochar was slightly acidic (pH 5.7). Commercial activated carbon was slightly more acidic than red oak biochar with pH of 6.0. The different pH's for different biochars shows that there is a large variability in chemical composition. These differences in composition could possibly lead to important differences in detoxification.

Adsorption isotherms are typically used to classify the behaviors between adsorbent and adsorbate. There are 6 main types of adsorption isotherms defined by IUPAC, and the first three types (Figure 3) are typically seen from these carbonaceous materials [46,72,89], and were also seen from this study. The type I isotherm is commonly present in highly microporous structures where pores are filled with relatively low pressures, approximately 0.1 P/Po. The type II isotherm shows that both micro and meso porosity are followed by a monolayer adsorption at lower partial pressures and a multilayer formation at relatively high partial pressures [93]. The type III isotherm, with a typical convex shape, is characteristic of weak adsorbate interactions common of nonporous adsorbants (such as the selected fast pyrolysis biochars). This behavior can be strengthened once the multilayer has been formed at higher pressures. In summary types I and II isotherms were observed for activated materials and types II and III isotherms were observed for the biochars physical adsorption of nitrogen at 77 K on the particle surfaces and pores.

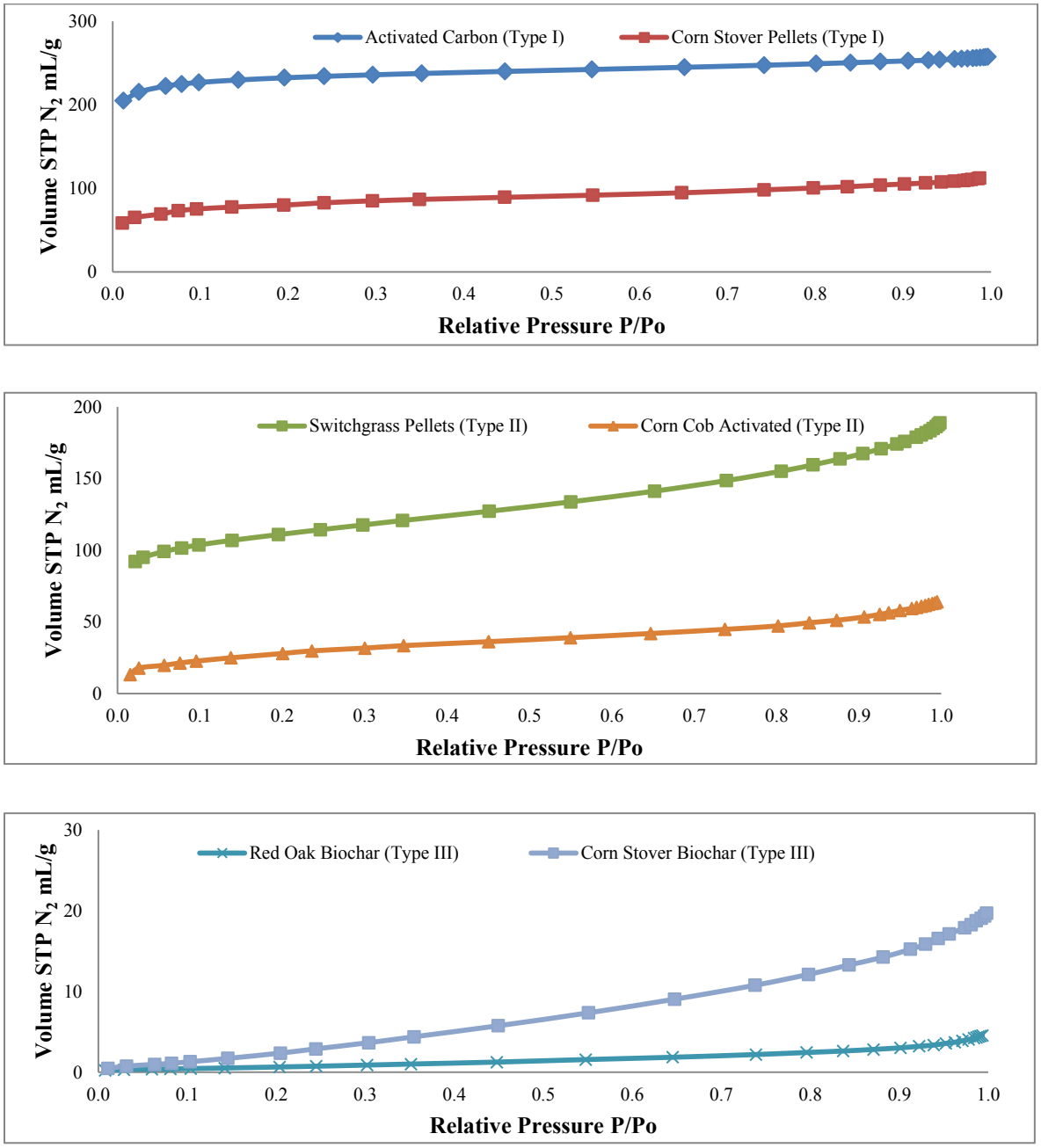

Figure 3. Examples of nitrogen adsorption isotherm Types I, II and III for various biochars, activated biochars and commercial activated carbon.

Six physisorption parameters were measured in order to investigate their relationship with detoxification capacities of the materials. Two methodologies were used to assess the total

surface area of the samples, BET and DFT. The contribution of the micropores and external (non-porous) surface areas were measured with T-plot methods. DFT was also used for estimating the pore diameter mode of the materials.

Table 2: Physisorption characteristics of biochar and activated biochar

Method	BET S.A.	Micropore S.A.	External S.A.	Cumulative S.A	Cumulative pore volume	Pore diam. (mode)
	BET (m^2/g)	T-plot (m^2/g)	T-plot (m^2/g)	DFT (m^2/g)	DFT mL/g	DFT nm
Corn Stover BC	6	0	6	13	0.03	5.2
Red Oak BC	2	0	2	3	0.01	4.7
Corn Cob BC	4	0	4	4	0.01	4.8
Darco Com. AC	917	848	69	1100	0.37	1.7
Corn cob AB	66	15	51	54	0.06	2.1
Corn stover pellets AB	303	221	82	331	0.16	1.7
Red oak AB	97	23	74	82	0.09	1.9
Switchgras pellets AB	411	265	145	501	0.26	1.9

Note: “AC.” refers to Activated Carbon; “AB” Activated Biochar, “BC” Biochar (non activated) “S.A.” to Surface area; “BET” to Brunauer, Emmett and Teller, “DFT” to density functional theory.

In all cases following activation, the BET, micro-pore, external surface areas and pore volume increased, leading to the mode pore diameter decreasing to less than half of its original width. The formation of micro-pores (less than 2 nm width) is a typical result of the activation process, and consequently the relative contribution of surface area from mesopores is significantly decreased (p-value< 0.05). Therefore the pore diameter measured by DFT for biochars doubles with respect to activated biochars (Table 2). Orthogonal contrast analysis (in appendix) showed in higher surface area (statistically different with $p<0.05$) for the activated carbon, activated biochar pellets, activated biochars (powders) than all the non-activated biochar medias. Orthogonal contrast analysis for the DFT pore mode of the adsorbents also showed statistical differences between biochars (with larger pores) and the rest of the activated materials, but did not result in differences between activated carbon and activated biochars.

3.2 Bacterial growth and ethanol production from pyrolytic sugars

A preliminary trial with a 200 mL batch fermenter was performed with commercial activated carbon (AC), red oak activated biochar (ROAB) and non-detoxified pyrolytic sugars (Figure 4). This trial was meant to prove the validity of using different adsorbants to detoxify and subsequently ferment anhydrosugars in closely monitored conditions. After the fermentation of pyrolytic sugars is proven to be feasible, optimization of the detoxification media and processing conditions could be further investigated. The detoxification efficiency was evaluated through the comparison of ethanol production and optical density 550 nm (OD_{550nm}) through sampling every 12 hours for 3 days.

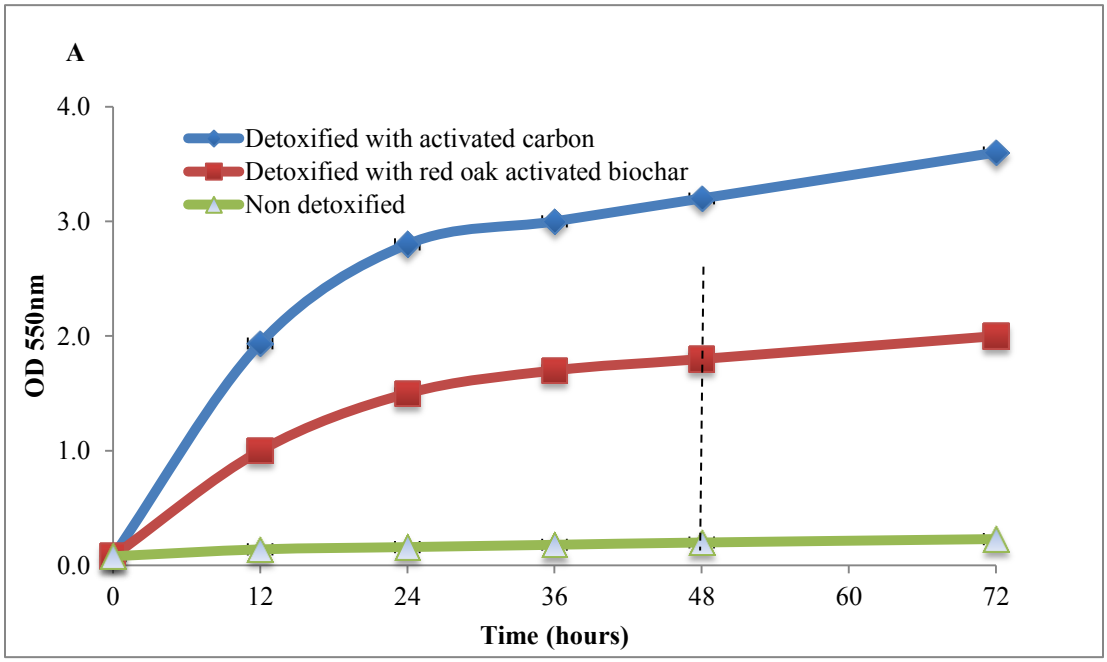

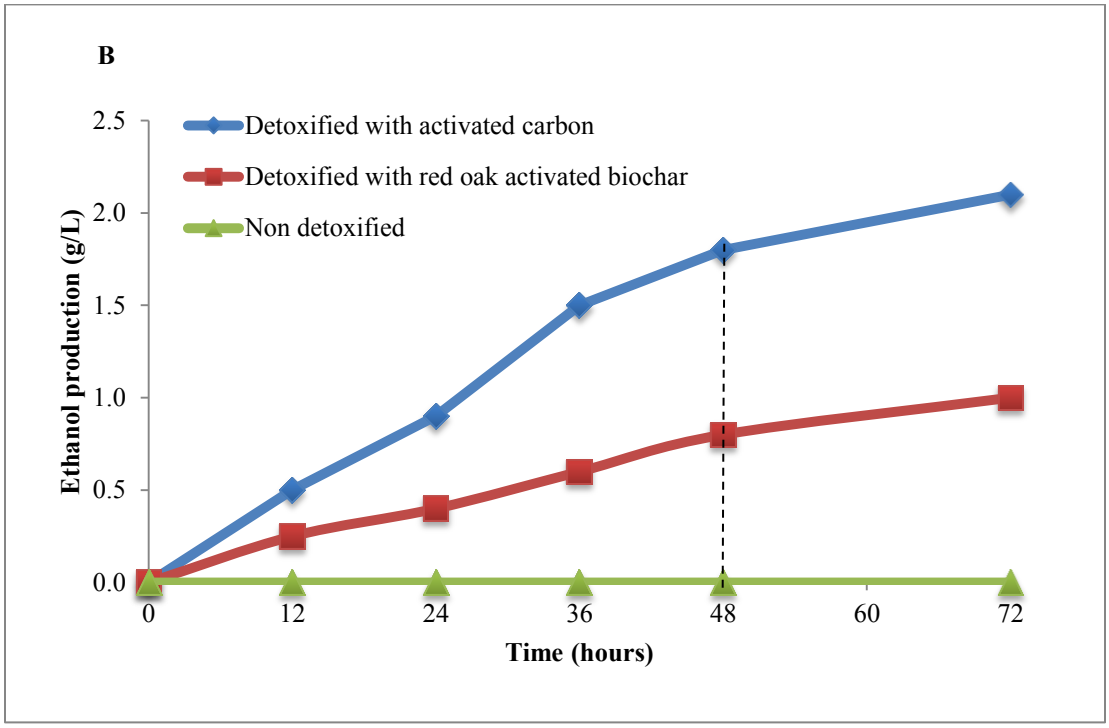

Figure 4. E. coli growth and ethanol production from non-detoxified and detoxified pyrolytic sugars. (A) E. coli growth with 20 g/L of pyrolytic sugars, (B) Ethanol production with 20 g/L of pyrolytic sugars. The fermentation was performed at 37 °C, 150 rpm and pH at 6.5 for 72 hours.

Based on this preliminary 72 hour fermentation, untreated pyrolytic sugars showed a very small bacterial biomass development (OD_{550nm}) of 0.23, and no detectable ethanol production resulting from the inhibitor compounds present with the pyrolytic sugars. Commercial activated carbon, however, showed good detoxification performance, with the highest ethanol production at approximately 2.1 g/L and OD_{550nm} of 3.6. ROAB produced 1.0 g/L of ethanol and a bacterial growth of almost 2 ($OD_{550\ nm}$). The OD_{550nm} for both AC and AROB resulted in similar correlation of ethanol production and bacterial growth of 0.92. In addition, it appears that the increase of ethanol for both treatments would have been improved with longer fermentation, as the curves for OD_{550nm} and ethanol production, did not reach the plateau region with 72 hours of fermentation.

Fermentation of pyrolytic sugar was greatly improved with both detoxification treatments compared with the raw sugars. The AROB treatment shows significant improvement over non-

detoxified bio-oil. The ethanol production of AROB treated sugar however, is 50% of that of commercial AC treated pyrolytic sugars. This is the first time activated biochar has been used for detoxification of fermentation products, and our experiment shows that it can effectively be used to enhance the production of ethanol from pyrolytic sugars. As many researchers have mentioned [94,95], pyrolytic sugars contain numerous inhibitor compounds, such as phenolics, and furanics. Commercial AC has been used as an absorbent for detoxification of cellulose pyrolysate for ethanol fermentation [86,96]. However, the pretreatment method with biochar has not been previously characterized. Using biochar instead of AC can be a promising alternative pretreatment.

These fermentation results led us to further explore the potential utilization of non-activated biochar and activated biochar for detoxification.

3.3 Levoglucosan, phenol and furan adsorption test with GC-FID

In order to assess whether pyrolytic sugars are adsorbed and removed with the detoxification agents; biochar, activated biochar, and activated carbon with levoglucosan were analyzed for its concentration before and after the detoxification step. Distilled water containing 50 g/L of analytical grade levoglucosan and 1 wt% of the detoxifying agent was shaken overnight and concentration measured after removing the adsorbent (Figure 5).

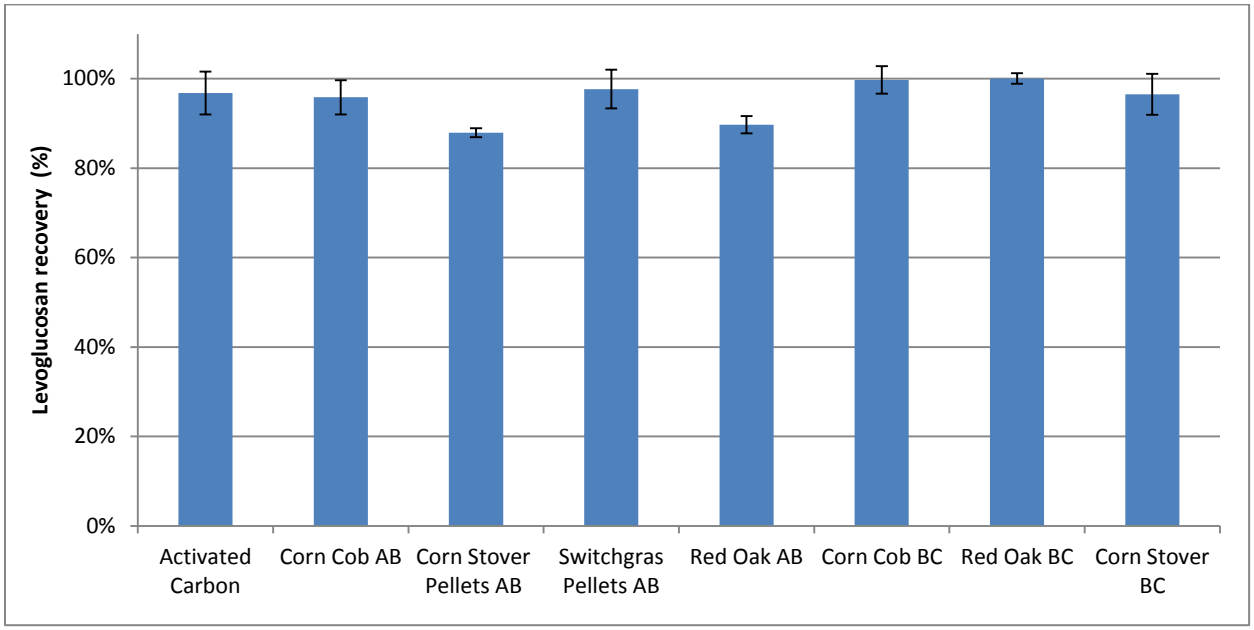

Figure 5. Lack of levoglucosan removal after detoxification with various biochars and activated biochars treatments.

There was no statistical significance of levoglucosan removal between different detoxification treatments. Activated carbon, activated biochar, and biochar containing 50 g/L of analytical grade levoglucosan had small or non-removal of levoglucosan during the detoxifying step, which was done at room temperature and shacked overnight.

Solutions with 1% w.t. with analytical grade furan (Sigma-Aldrich CAS# 98-01-1) and phenol (Sigma-Aldrich CAS# 108-95-2) were prepared. Detoxification with 1 % w.t. biochar and activated biochar was used to evaluate the detoxification potential of different materials using a similar procedure to the detoxification of pyrolytic sugars (Figure 6).

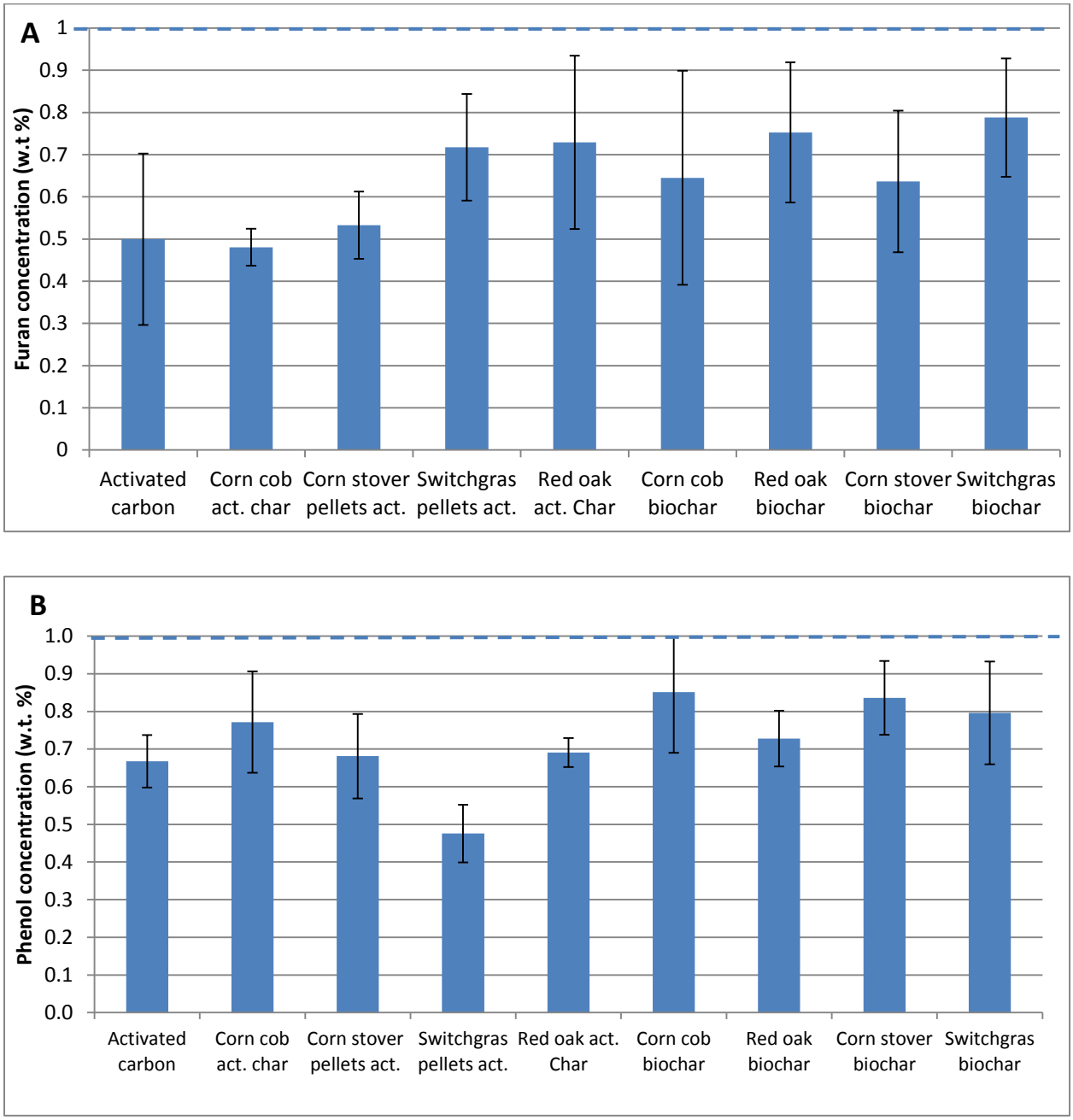

Figure 6: Furan (A) and phenol (B) concentration after detoxification with various biochar and activated char adsorbents.

From the detoxification step some materials showed adsorption capacities similar to the commercial activated carbon control. Activated corn cob char showed a reduction of furan concentration from 10 to 4.8 g/L and switchgrass activated char had a similar reduction with

phenol concentration. However, if these were the final concentration present in the detoxified pyrolytic sugars, then the bacteria growth will still be affected and the ethanol production compromised as the concentration is higher than the inhibitory levels[97].

3.4 Detoxification evaluation of biochars and activated biochars via bacterial growth and ethanol fermentation

In order to assess the detoxification performance, various solutions of pyrolytic sugars were tested for both bacterial growth and ethanol production using 15 mL vials measured in 24 well-microplates. Trials were made using 1 mL of sugar solution detoxified with 1 wt% of activated or non-activated biochar and evaluated after 48 hours of fermentation (Figure 7 and 8).

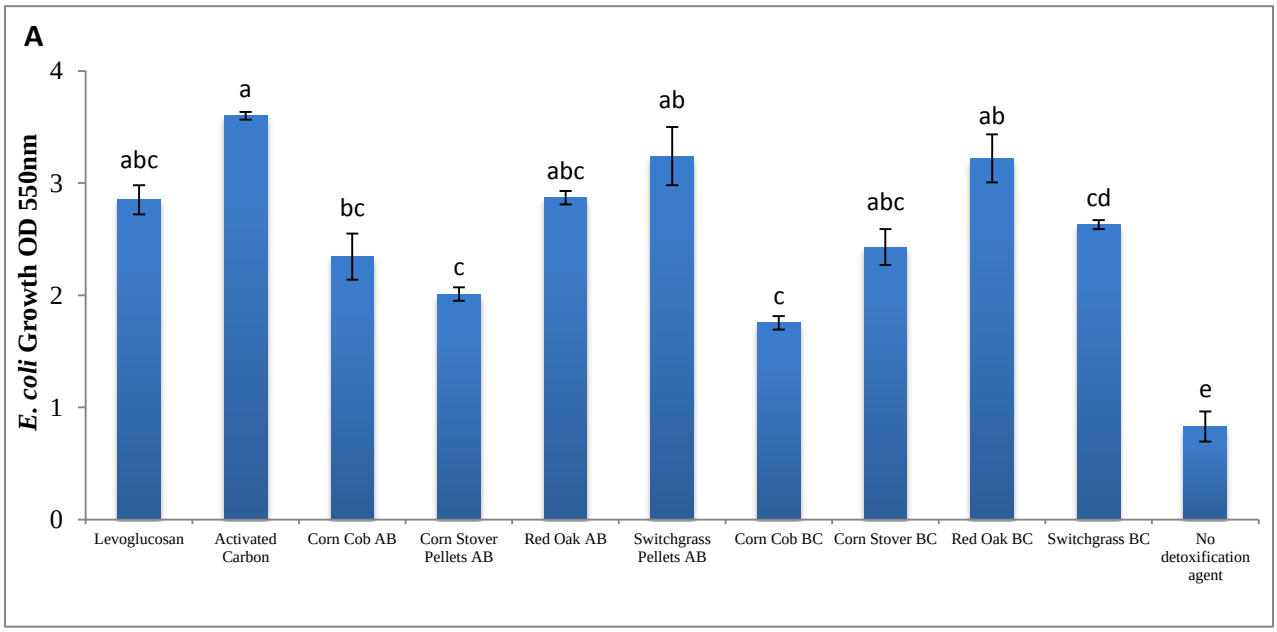

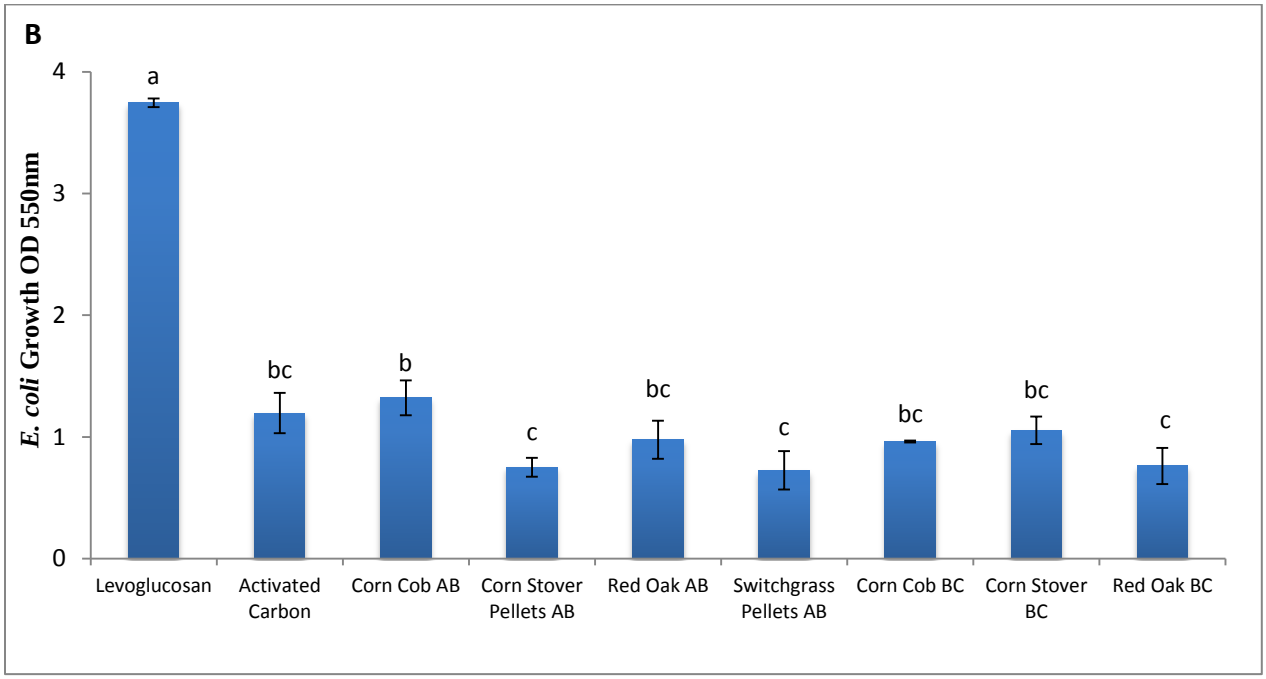

Figure 7. Bacterial growth with 20 and 40 g/L of pyrolytic levoglucosan detoxified with various carbon adsorbants. (A). 20 g/L of pyrolytic sugars (particles size<150 um), (B) 40 g/L of pyrolytic sugars. The culture was used 37 °C for 48 hours. Values are the average of three measurements with error bars indicating the standard error.

The data presented is the mean and error bars display the standard deviation. The letters show the Tukey's Honestly Significant Difference (HSD) test result. Growth OD550nm with the same letter are belonging to same group and are not significantly different. Letters alphabetically rank the groups with Growth OD550nm value from the largest to the lowest.

At 20 g/L, sugars detoxified with the commercial activated carbon supported a similar amount of growth as the pure levoglucosan control. The fact that the commercial activated carbon can detoxify the pyrolytic sugars and improve fermentability is consistent with the previous reports that motivated this study [85]. However, at 40 g/L even the commercial activated carbon was unable to sufficiently detoxify the sugars, and the resulting growth was much less than that observed with the pure levoglucosan control.

In the presence of 20 g/L pyrolytic sugars, a variety of biochars were comparable to the commercial activated carbon in terms of enabling bacterial growth. Specifically biochars

produced from red oak and corn stover and activated biochar produced from red oak and switchgrass resulted in comparable OD_{550nm} to AC and to the levoglucosan control. Furthermore, all biochars and activated biochars were able to significantly increase fermentability relative to the non-detoxified sugars.

The particle size and time for adsorption to reach equilibrium could have been one of the causes of low detoxification and poor bacterial growth as the concentration increases. Decreasing particle size of the activated carbon has been shown to significantly improve contaminants uptake and decrease retention time [98]. For our first assessment of fermentation and detoxification with was performed during one hour with no shaking. For low concentration of pyrolytic sugars, and associated contaminants, materials formulation with larger particle size (pelletized materials) had very similar bacterial growth than the powder formulations such as activated carbon and red oak biochar (figures in appendix). However, once the concentration was increased to 40 g/L both types of pellets, those made from corn stover and those from switchgrass, supported the lowest bacterial growth of all treatments.

The ethanol production test of pyrolytic levoglucosan shows in Figure 7. At 5 g/L there was no significant difference in any of the detoxifying media, among them and against the analytical grade levoglucosan control. The concentration of ethanol was roughly 0.15 g/L for all of the treatments. At 10 g/L of levoglucosan and pyrolytic sugars ethanol production with the pure levoglucosan was higher than any of the detoxified pyrolytic treatments, 32-39% greater. Within the pyrolytic sugar fermentations, there were no major differences due to the type of detoxifying media used. Also, there were no differences among the detoxified pyrolytic treatments between 5 and 10 g/L of pyrolytic sugars, with approximately 0.15 g/L of ethanol production respectively. Pure levoglucosan fermentation of 5 and 10 g/L resulted in a significantly higher concentration of ethanol, 0.16 and 0.24 g/L respectively, clearly marking the concentration at which inhibition was first observed.

At 20 g/L concentration and with the detoxified materials grinded to less than 150 um, the ethanol concentration of all treatments resulted in 22 to 60% higher than those previously observed at 10g/L. Red oak biochar followed by commercial activated carbon returned the

highest ethanol yields from all fermentation treatments of pyrolytic sugars at 20 g/L. The pure levoglucosan control in all cases returned higher fermentation output than the pyrolytic sugars. The ethanol concentration with red oak biochar is almost 6 times higher than with pyrolytic sugars with no detoxifying agent. When comparing overall activated biochars and non-activated biochar, there were no significant differences in terms of ethanol production and bacterial growth for activated vs. non-activated. At 40 g/L there was no ethanol production due to the inhibitors present in the sugar fraction or the high levels of sugars that could have been detrimental to the bacterial growth (results not shown).

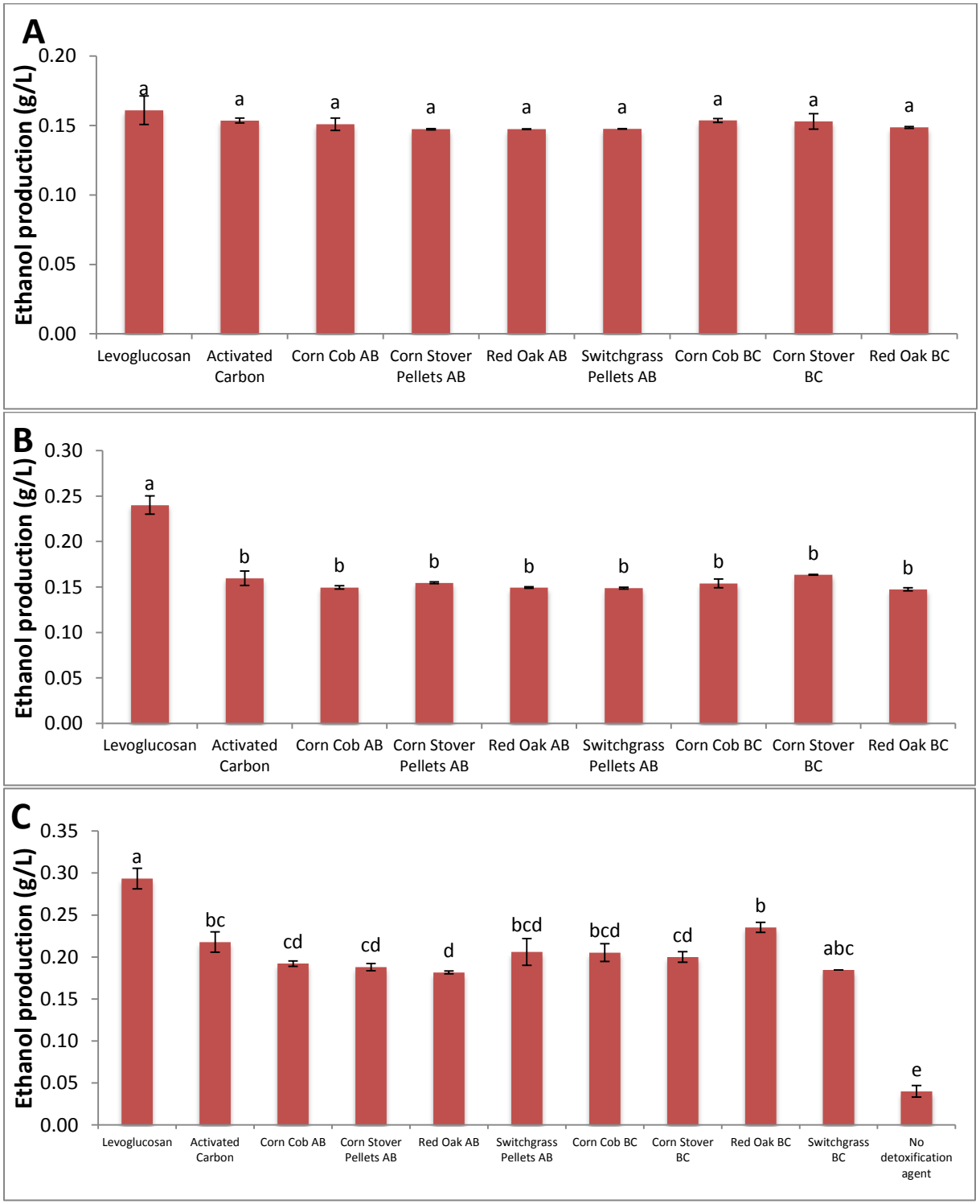

Figure 8. Ethanol production in microplates from (A) 5 g/L, (B) 10 g/L and (C) 20 g/L of pyrolytic levoglucosan concentration detoxified with various carbon adsorbants.

The data presented is the mean and error bars display the standard deviation. The letters show the Tukey's Honestly Significant Difference (HSD) Test result. Same letter are belonging to same group and are not significantly different of ethanol concentration among the treatments. Letters alphabetically rank the groups from the largest to the lowest production.

Besides temperature, all the other parameters (such as pH, stirring, oxygen concentration, etc.) could not be optimized in the small vials setting. Nevertheless, the results gathered could be used as proxy for screening the most promising materials for larger scale fermentation trials where each variable could be closely monitored.

Comparing with the small-scale fermentation and the bioreactor at 20 g/L, the ethanol concentration obtained in the bioreactor was much higher due to the ability to precisely control the parameters. For example, for the optical density for the activated carbon was 3.6 in the small trials and 3.2 on the large fermenter, but the ethanol yield was 0.22 in the small vials versus 1.8 in the bioreactor. Red oak activated biochar had a similar trend were the bacterial growth was 1.8 on the biofermenter and 2.87 on the small vials but the ethanol concentration was 0.80 and 0.18 g/L, respectively.

In addition, the bioreactor and the small vials also differ in the correlation of bacterial growth and ethanol production. Generally it will be expected that as higher bacterial growth will result in higher ethanol production, but the results were weakly correlated with the microplate tests. However, when comparing the correlation within AC and AROB (for OD_{550nm} and ethanol production) over time the correlations of these two parameters were 0.93 and 0.92. Showing a much stronger association of both parameters within treatments over time, but was not the case when comparing the OD_{550nm} and ethanol in microplates for the same treatment with different concentrations or within different treatments.

With the fermentation results obtained from microplates, various physisorption properties were compared to bacterial growth and ethanol production in order to assess whether there is a correlation exists between them (Table 3 and Figure 18).

Table 3: Correlation coefficients of physisoption parameters with ethanol production and optical density 550 nm with 20 g/L of levoglucosan

Correlation coefficient	$OD_{550\ nm}$	Ethanol yield
BET S.A.	0.59	0.18
Micropore S.A.	0.58	0.25
External S.A.	0.36	-0.32
DFT Cum. S.A.	0.60	0.22
DFT Cum. Pore volume	0.58	0.08
DFT Pore Diam. Mode	-0.32	0.47
pH	-0.71	-0.36

The correlation between biomass bacterial growth (optical density) and ethanol production for each treatment was relatively low for any of the fermentation test in microplates (0.49 for 5 g/L, 0.36 for 10 g/L and 0.33 for 20 g/L). It was hypothesized that optical density could explain the ethanol production within treatments and therefore be used as a simple proxy for fermentability assessment [99]. However for these fermentation conditions and substrates used, bacterial growth was not closely correlated with ethanol production when using microplates. Likely the production of ethanol was self-inhibited near 0.15-0.20 g/L, but the bacterial biomass was inhibited for some treatments only, resulting in a weak dependence between these two variables. Also, for 48 hours with no optimization of fermentation parameters besides temperature, different treatments could have different bacterial growth rates (lag, exponential or stationary phase) and could have needed more time to ferment the sugars.

Another reason why the optical density and ethanol production were not closely related, could be the differences in bio-oil inhibitory chemicals remaining in the solutions (which are different for the detoxification treatments), and can alter the optical density reading for some materials. If this was the case, another methodology that accounts for these colored bodies and better differentiates from the bacterial cells might be needed, such as a count of colony forming units (CFU) on a count plate.

Although activated biochars presented higher surface area, micropore volume, and total pore volume with higher OD_{550nm} or bacterial growth, none of these physisorption characteristics largely explained ethanol yields from these microplates' results. On the other hand, DFT pore

diameter mode did show some correlation with ethanol production of 0.47. Also, pH had some negative correlation of -0.36 with ethanol production (higher fermentation with lower pH materials), which suggests that chemisorption or chemical reaction processes may be significant in the detoxification process.

3.5 Sugar composition and inhibitor removal from pyrolytic sugars with activated biochar filtration columns

Various filtration tests were performed in order evaluate the potential adsorption of pyrolytic sugars to the biochar filtration column (Figure 9). Two sugar solutions of 50 g/L and 200 g/L of pyrolytic sugars were prepared and repeatedly filtered over the same biochar column (100g/L of media) to evaluate whether there is an effective removal of sugars from the solution.

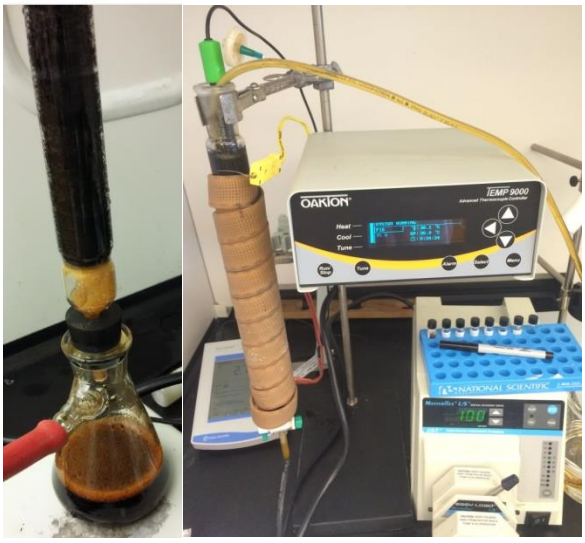

Figure 9. Temperature controlled activated carbon filtration column

Adsorption tests were made at 30°C and at a ratio of 10% w.t. of activated fast pyrolysis biochar to pyrolytic sugar solution. Eight consecutive filtrations were performed to evaluate the potential adsorption and removal of pyrolytic sugars from the solution (Figure 10). The lack adsorption presented by the biochar media is an important requirement for screening detoxification materials in order to ensure high levels of sugars left for fermentation.

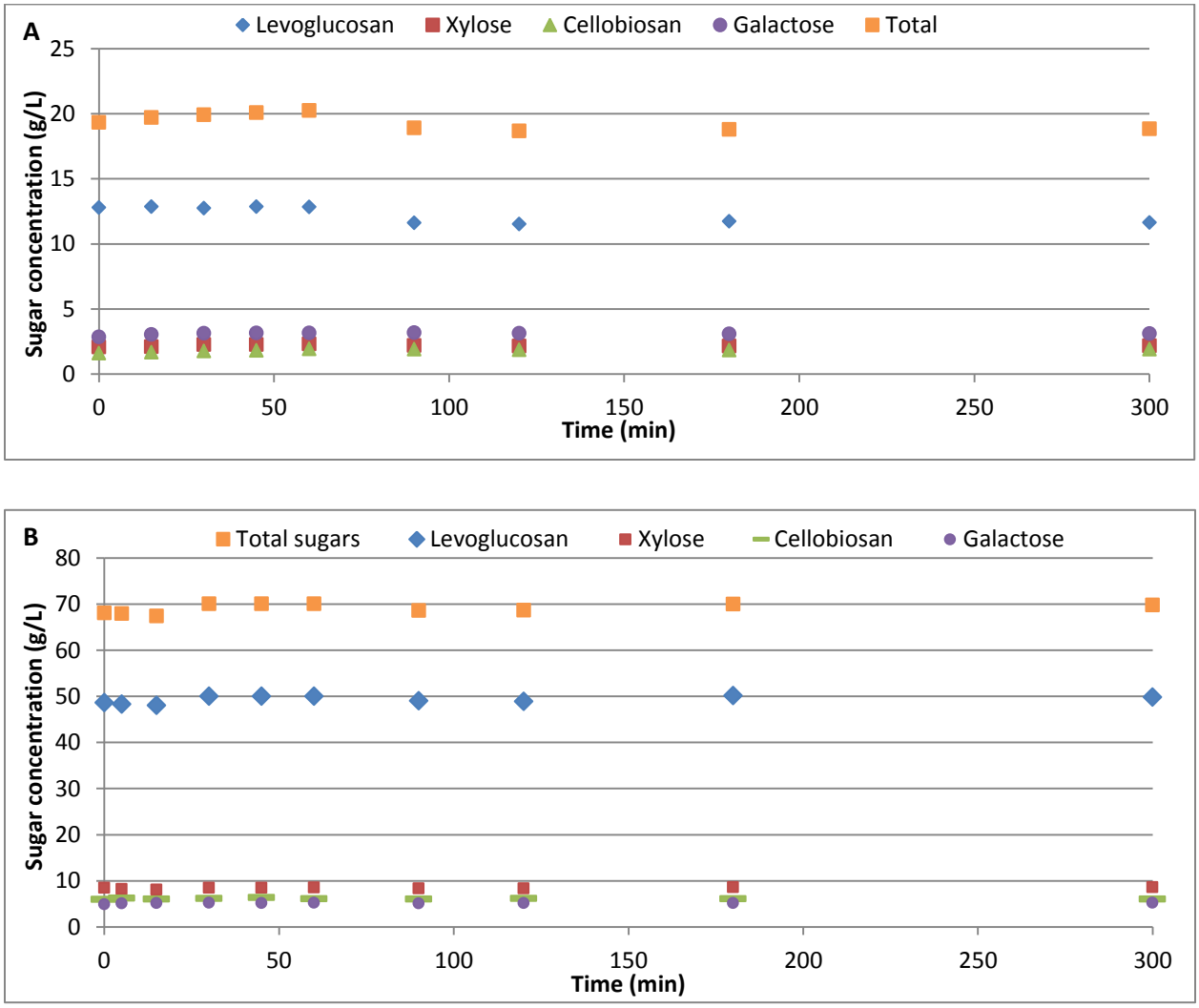

Figure 10. Sugar concentration of consecutive filtrations of 50 g/L (A) and 200 g/L (B) of pyrolytic sugars.

From the filtrations above the first important result to highlight is the lack of sugar removal from the two different solutions over consecutive filtrations. The initial concentration of sugars before being filtered (denoted at time 0) resulted in 24.6% w.t. levoglucosan, 6.2% w.t. galactose, 4.4% w.t. xylose and 3.6% w.t. of cellobiosan accounting for 38.8% of the total mass of the clean pyrolytic sugar fraction.

Other components identified in the pyrolytic sugar recovered from the bio-oil stage fraction 1 were moisture 9.6% w.t. (measured with Karl Fischer MKS-500 ® moisture titrator) and compounds other than sugars (Figure 11).

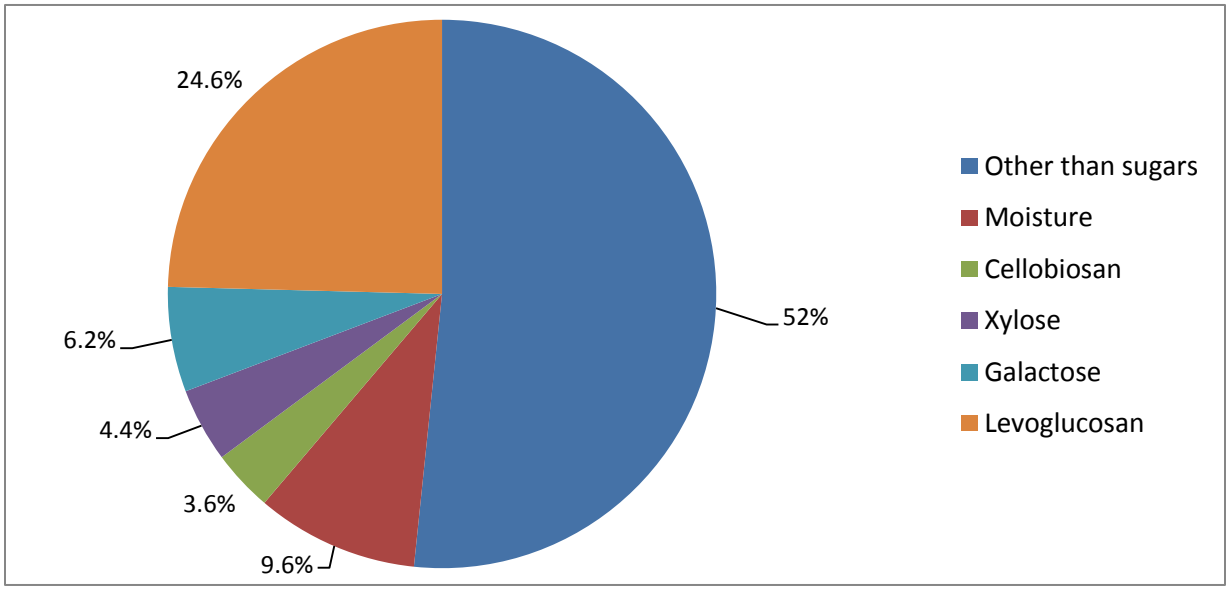

Figure 11. Pyrolytic sugars composition obtained from bio-oil stage fraction 1

Pyrolytic sugar samples were analyzed using a GC-FID in order to quantify components other than sugars that are present in this fraction. Identification and quantification of the chemicals present in the clean pyrolytic sugar fraction and whether they can be effectively removed is essential for later fermentation. Overall, these compounds accounted for 52% w.t of this fraction spread in many compounds at very small concentration, making them very challenging to identify and quantify. From previous analyses approximately 46 compounds were identified and calibrated for quantification in the GC-FID. These compounds were: 2,6-Dimethoxyphenol, 3,4-dimethoxytoluene, 3-methoxy-5-methylphenol, Styrene, Guaiacyl Acetone, 4-methyl-2,6-dimethoxyphenol, 3,5-dimethoxy-4-hydroxybenzaldehyde, 2-methoxy-4-vinylphenol, 1,2-benzenedimethanol, 3-methylanisole, m-tolualdehyde, 3',5'-dimethoxy-4'-hydroxyacetophenone, 1,2,4-trimethoxybenzene, 1,2,3-trimethoxybenzene, m,p-cresol, 3,5-dimethylphenol, 4'-Hydroxy-3'-methoxyacetophenone, Anisole, Vanillin, Naphthalene, 2,5-dimethoxybenzylalcohol, 3'4'-dimethoxyacetophenone, 3-ethylphenol, 4-ethoxystyrene, Phenol,

p-xylene, Indene, Ethylbenzene, 4-ethyl-2-methoxyphenol, 2,6-dimethylphenol, 3,4-dimethylphenol, 2-methoxy-4-methylphenol, 2-ethylphenol, Vinylanisole, 2-methylanisole, 2,3-dimethoxytoluene, 4-vinylphenol, m-xylene, 3-ethyl-5-methylphenol, Toluene, Coniferaldehyde, o-cresol, Methanol, o-xylene, 2',4'-dimethoxyacetophenone. From the 46 compounds previously identified only 20 were above the minimum concentration used for calibration (0.05% w.t.) and overall accounted for 10.3% w.t. of the original clean pyrolytic sugar fraction. The ten chemicals with highest concentration identified in the sugar fraction utilized in this study are presented below (Table 4). In addition, the removal rate of these compounds by activated red oak biochar from the filtration column is also shown below.

Table 4: Major compounds identified and quantified in the pyrolytic sugar fraction and the removal rate with activated red oak biochar

Chemical compounds name	**Concentration % w.t.**	**Activated Red Oak biochar removal rate**
2,6-Dimethoxyphenol	2.15	51%
3,4-dimethoxytoluene	1.08	17%
3-methoxy-5-methylphenol	0.85	25%
Styrene	0.83	100%
Guaiacyl Acetone	0.53	28%
4-methyl-2,6-dimethoxyphenol	0.44	36%
3,5-dimethoxy-4-hydroxybenzaldehyde	0.43	75%
2-methoxy-4-vinylphenol	0.39	55%
1,2-benzenedimethanol	0.33	36%
3-methylanisole	0.32	0%

Note that beside 2,6-Dimethoxyphenol and 3,4-dimethoxytoluene the concentration of the rest of the compounds are below 1% w.t. Moreover, for detoxification and fermentation the concentration of pyrolytic sugars (and associated compounds) are also diluted, making it more challenging to quantify.

4. Conclusions

Biochars, activated biochars and commercial activated carbon were able to remove fermentation inhibitors and significantly increase bacterial growth and ethanol production from pyrolytic sugars. Preliminary fermentation trials on bioreactors with activated carbon and activated red oak activated biochar produce 2.1 and 1.0 g/L ethanol, from the original 20 g/L of pyrolytic sugars, in 72 hours. Fermentation in microplates with various types of biochar and activated chars suggests that some of these materials could be effective at detoxifying pyrolytic sugars to produce ethanol. BET, micropore, and external surface area, positively correlated with bacterial growth but did not have a high correlation with the ethanol production in microplates fermentation. Only DFT pore mode and pH had some correlation with ethanol produced. These preliminary results of biochar and activated biochar detoxification are quite promising to enhance pyrolytic sugars fermentation and ethanol production. Further investigation is necessary to better assess and enhance their performance.

5. Acknowledgements

The research reported in this publication was supported by Iowa State University, the Iowa Energy Center (12-06) and the NSF Energy for Sustainability (CBET-1133319). The author, Bernardo del Campo of this publication has equity ownership in Advanced Renewable Technology International, Inc. (ARTi) which is developing products related to the research being reported. The terms of this arrangement have been reviewed and approved by Iowa State University in accordance with its Conflicts of Interest and Commitment Policy

6. Appendix

The figure below depicts 6 different materials analyzed with FTIR with higher absorbance in specific regions after they were used for detoxification. Most material presented higher absorbance around 3000-3300 cm^{-1} suggesting adsorption of OH groups. In addition some materials presented high absorbance of other bands such as 2850-2922 cm^{-1} for C-H (aliphatic groups) and around 1600 cm^{-1} for C=O carbonyl groups.

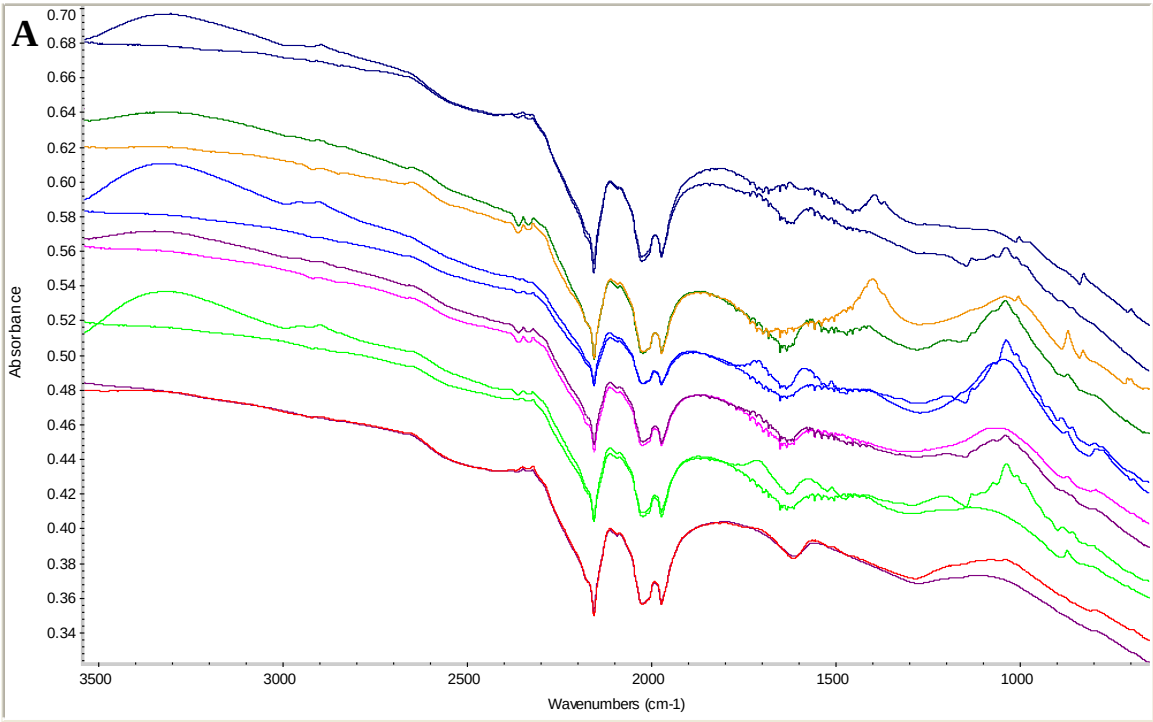

Summary of 6 different adsorbent before and after detoxification showing various peaks being identified through FTIR after the detoxification step from top to bottom.

1. Corn Cob Activated biochar
2. Corn stover pellets activated biochar
3. Corn stover powder activated biochar
4. Switchgrass pellets activated biochar
5. Red Oak Activated biochar
6. Darco Activated carbon

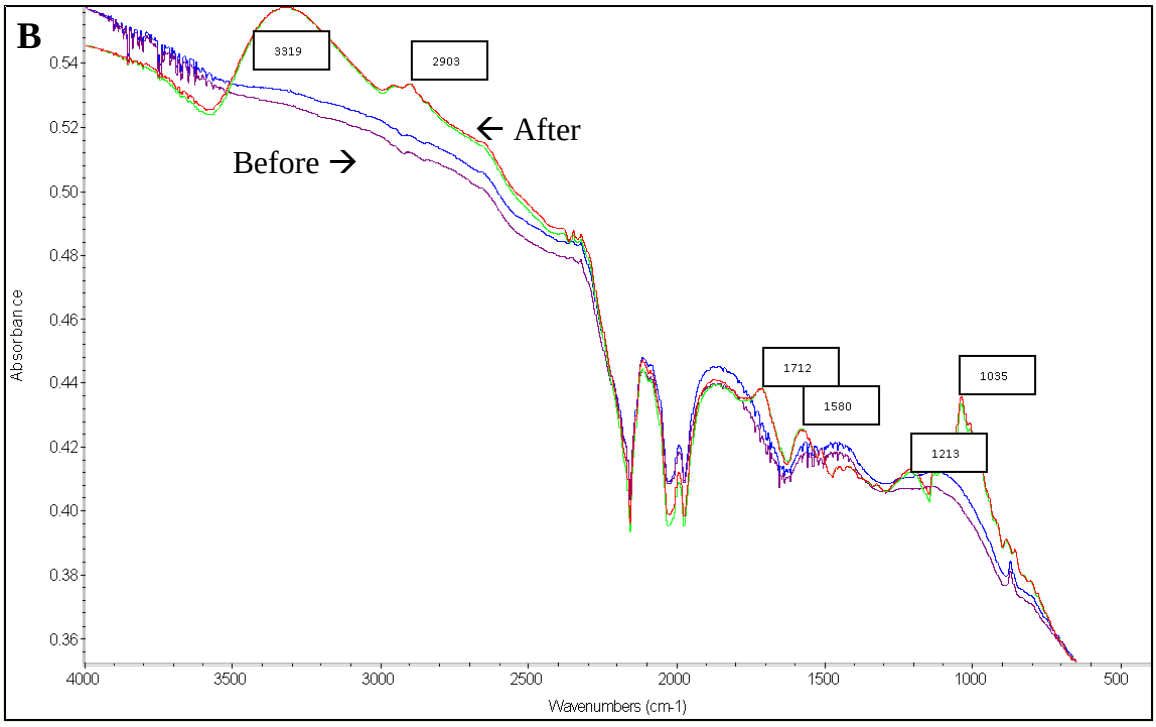
B
3319
2903
← After
Before →
1712
1580
1035
1213
Absorbance
Wavenumbers (cm-1)

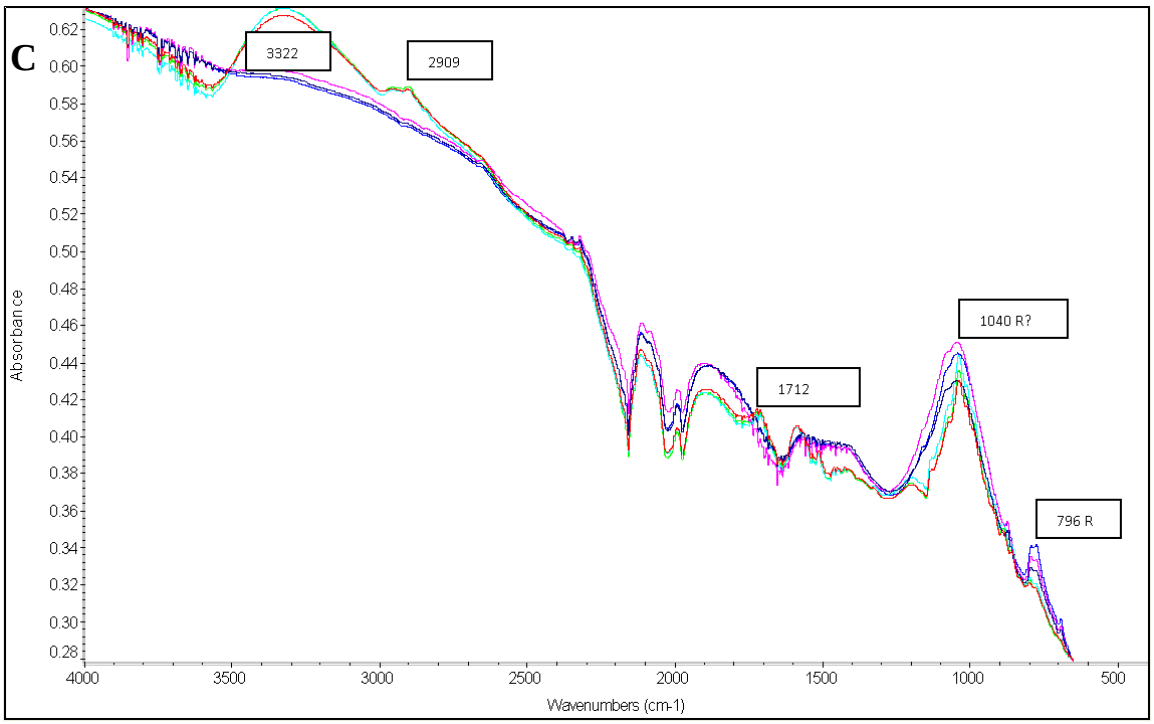
C
3322
2909
1040 R?
1712
796 R
Absorbance
Wavenumbers (cm-1)

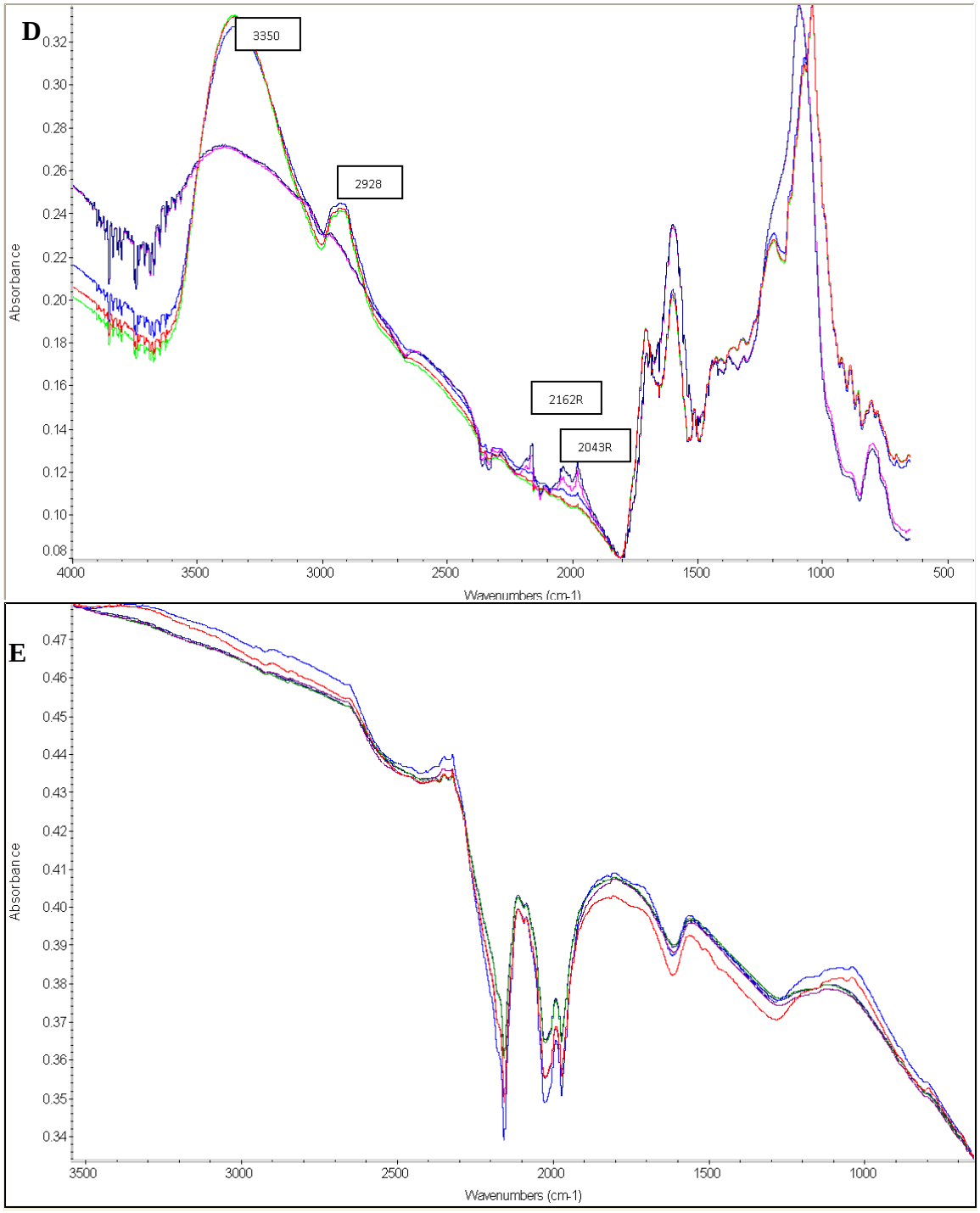

Figure 12. FTIR spectra with the appearance of various functional groups for different media before and after detoxification. A) summary of 6 different adsorbent before and after adsorption to denote new peaks, B) Corn cob activated biochar, C) corn stover activated biochar, D) Switchgrass biochar E) Darco activated carbon.

Pictures of biomass, biochar and activated biochar

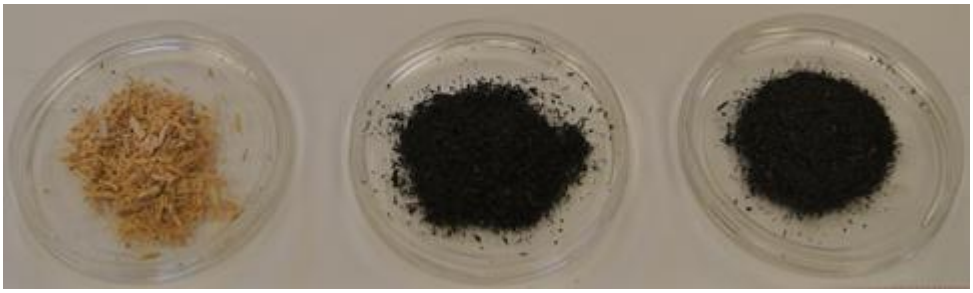

Figure 13. Red oak biomass (left), biochar (center) and activated biochar (right)

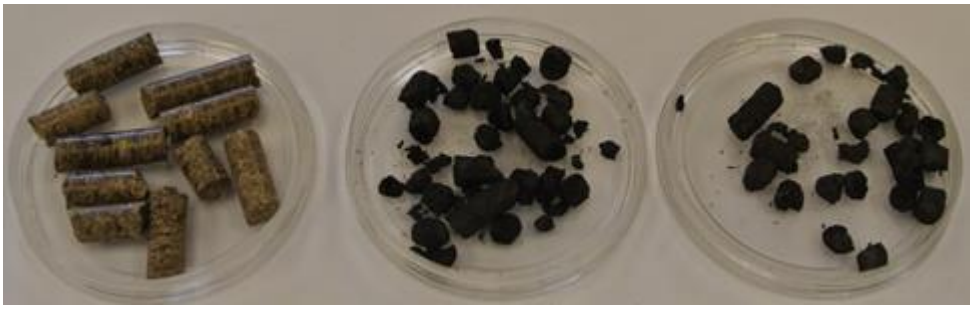

Figure 14. Switchgrass pellets biomass (left), biochar (center) and activated biochar (right)

Figure 15. Switchgrass activated biochar pellets after bio-oil detoxification

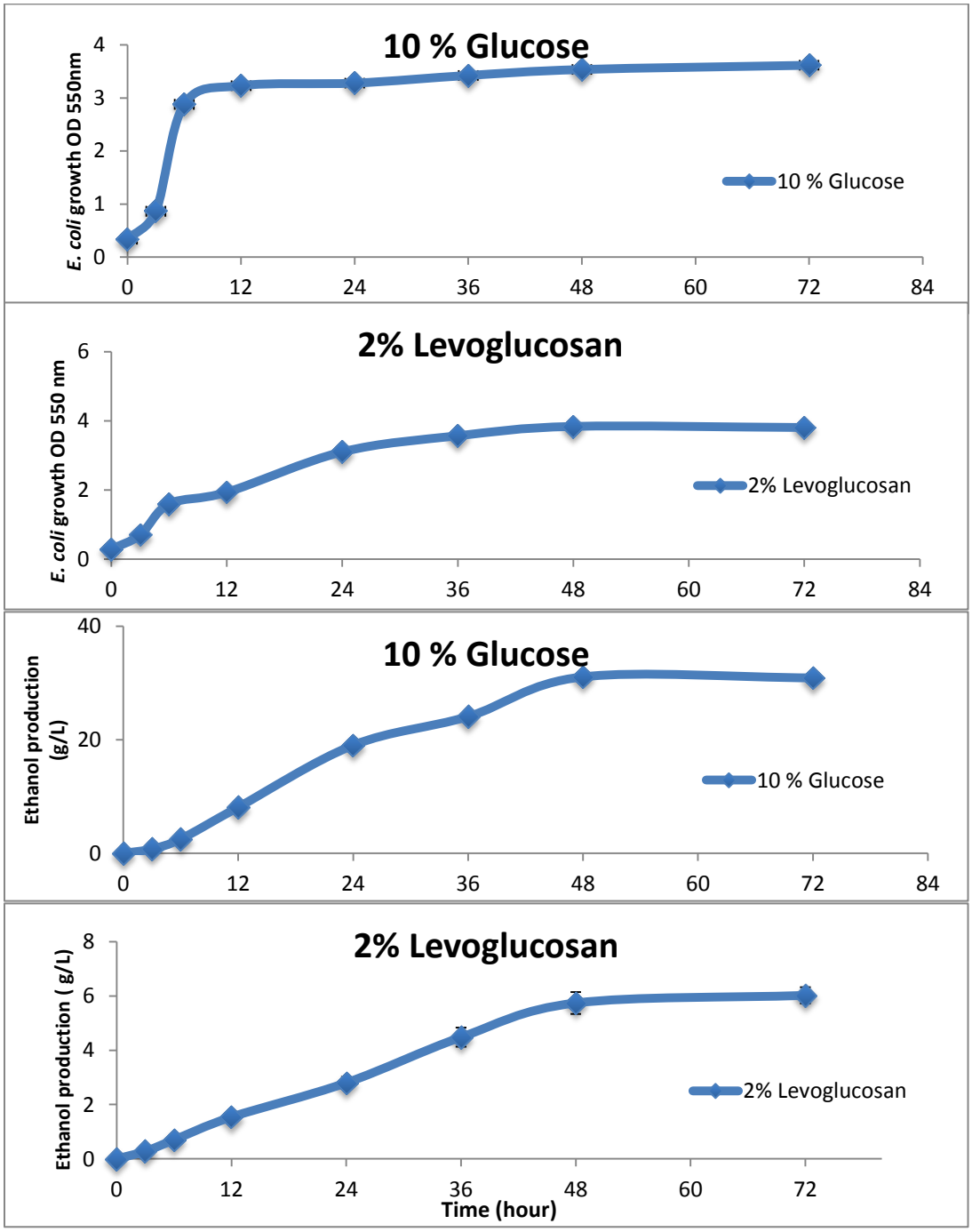

Figure 16. Ethanol and OD550nm of Glucose and levoglucosan fermentation in a 200 mL bioreactor

These trials were made to test the bioreactor efficiency and validate the fermentation process with known substrates and fermentation conditions. After the fermentation process was validated pyrolytic sugars were tested.

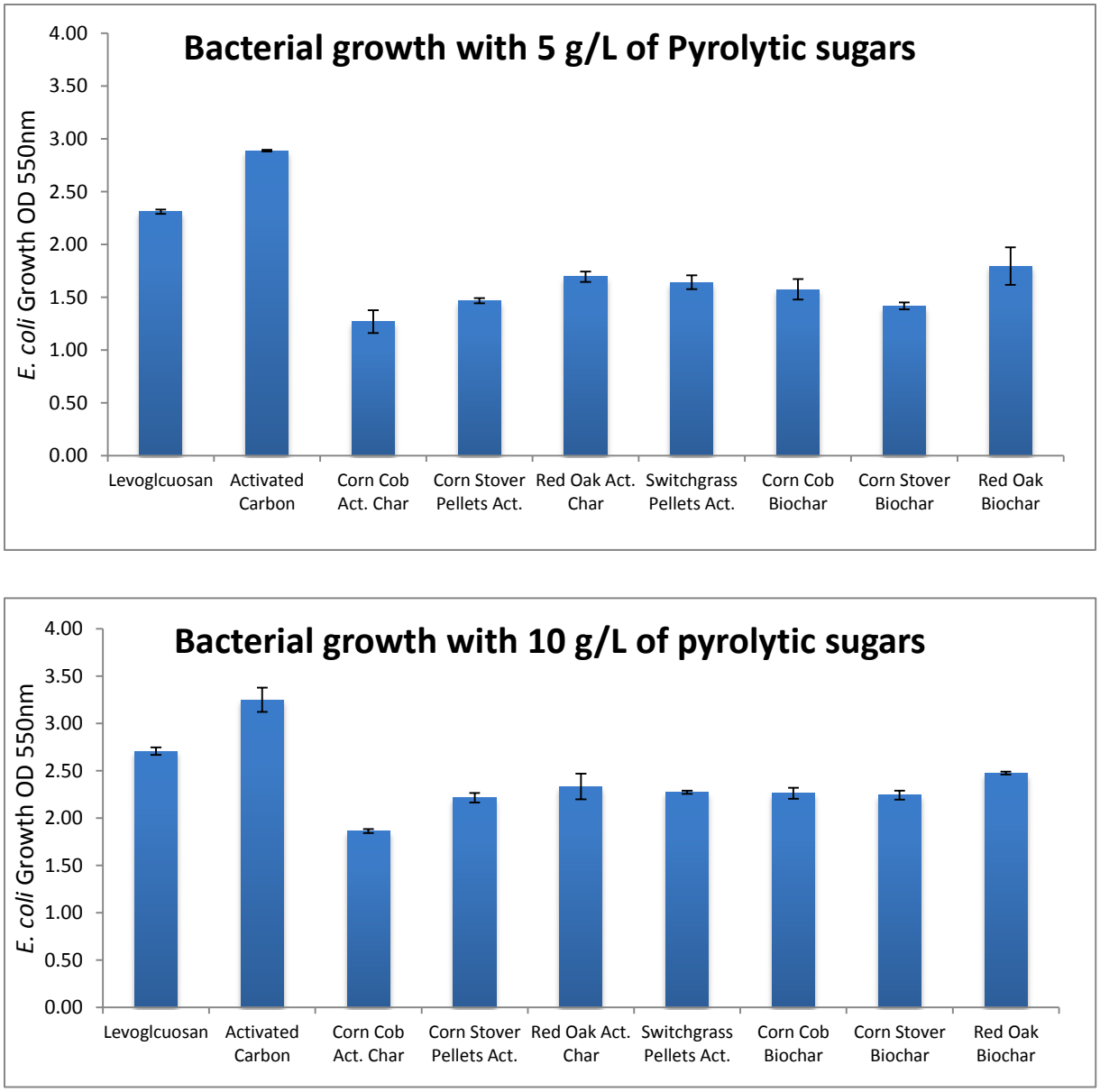

Figure 17. Bacterial growth at 5 and 10 g/L of pyrolytic sugars

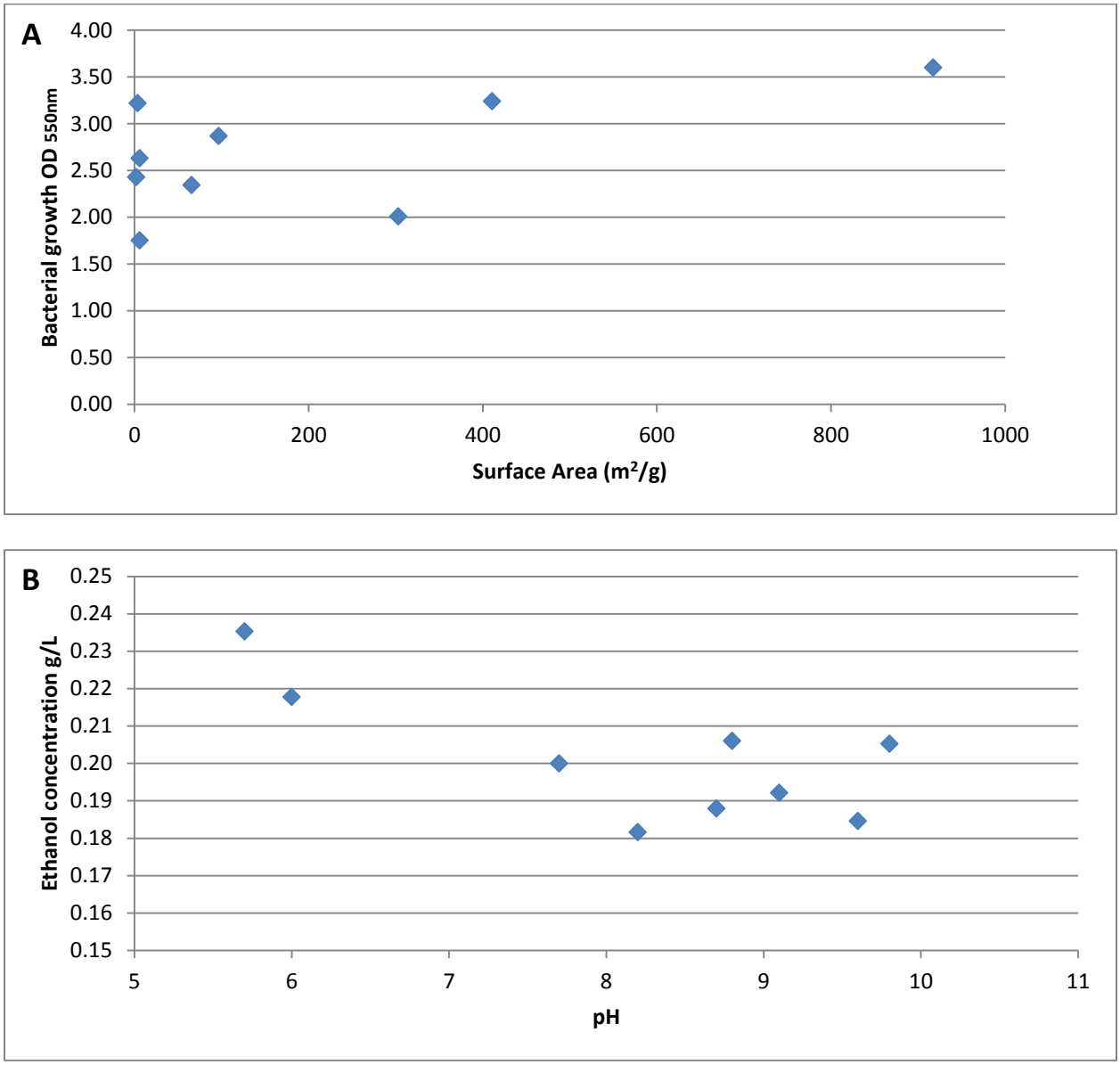

Figure 18. Relationship of bacterial growth and BET surface area (A) and relationship of ethanol concentration with pH of the adsorbent (B).

CHAPTER 4 TECHNO-ECONOMIC ANALYSIS OF AN INTEGRATED THERMOCHEMICAL BIOREFINERY PRODUCING ETHANOL FROM PYROLYTIC SUGARS AND ACTIVATED CARBON FROM CORN STOVER BIOCHAR

Bernardo G. Del Campo[a], Longwen Ou[a], Matthew M. Kieffer[a], Mark M. Wright[a] and Robert C. Brown[a,b*]

To be Submitted to *Biofuels, Bioproducts, and Biorefining*
[a] Mechanical Engineering, Iowa State University, Ames, Iowa 50010
[b] Bioeconomy Institute, Iowa State University, Ames, Iowa 50010

Abstract

This study evaluated the internal rate of return (IRR) for renewable fuels and chemical production from a thermochemical biorefinery, based on a fast pyrolysis facility that processes 2000 dry metric tons of corn stover per day. Products from bio-oil and biochar include gasoline, diesel, ethanol, hydrogen, and activated carbon (AC). This study demonstrated an IRR of 16% from a total project investment of $414 million, assuming a 20-year operation. Annual output includes 31 million gallons of transportation fuels, 8,700 tons of hydrogen, and 66,600 tons of activated carbon providing $154 million of gross revenue.

Highlights

- Fermentation of pyrolytic sugars into ethanol significantly improves the IRR of the fast pyrolysis biorefinery.
- Activated carbon improves the overall economic feasibility by producing a high value product from the biochar stream.
- The biorefinery requires $414 million in investment, primarily driven by the cost of hydroprocessing and combustion equipment.
- The expected IRR of this biorefinery is 16% being the biomass cost and fixed capital investment the factors with higher impact on profitability.

Keywords

Biorefinery, fast pyrolysis, techno-economic analysis, ethanol, activated carbon

Introduction

Thermochemical processing of biomass has promise for producing a variety of renewable products and technologies. Fast pyrolysis, in particular, has attracted attention for its flexibility to produce a variety of biobased products from very different biomass feedstock. However, finding an economical and efficient pathway for every pyrolysis product that effectively competes with its petro-base counterpart is still a major challenge for the implementation of fast pyrolysis biorefineries.

Fast pyrolysis is designed to maximize the production of bio-oil at the expense of biochar and non-condensable gases. High yields of bio-oil from biomass are achieved using high heating rates (~100 °C/s), small particle sizes (less than 10 mm), fast reaction rates (measured in seconds) in a temperature range of 400-600°C, and in the absence of oxygen. Depending upon operating conditions, type of reactor, and feedstock used in the process (Figure 1), approximately 50-70 wt% of the biomass is converted into bio-oil, 15-30 wt% into non-condensable gases, and 15-30 wt% into biochar[73-75].

Previous analyses of pyrolysis-based biorefineries[4-9] explored a variety of product portfolios, including the production of transportation fuels by hydrotreating the bio-oil; electricity generation, heat, and power through direct combustion; and the purification and commercialization of specialty chemicals[76,87,100,101]. From an economic prospective, however, large capital investment has hindered development of commercial-scale operations.

We explore recent technologies to improve the profitability of products from the pyrolysis-based biorefinery. These include enhancement of sugar production, sugar detoxification, fermentation of anhydrosugars, and activation of biochar.

Sugar production during pyrolysis of lignocellulosic biomass can be enhanced by pretreating biomass with sulfuric or phosphoric acid to passivate alkali and earth alkaline metals in biomass that otherwise catalyze unfavorable cellulose deconstruction reactions.[82] In principle, cellulose can be converted to the anhydrosugar levoglucosan in yields as high as 60 wt%,[13] although these have been limited to 30 wt% of cellulose in continuous pyrolysis trials using woody and herbaceous biomass[6]. Polysaccharides not depolymerized to anhydrosugars are

converted to a variety of less desirable "light oxygenates," including hydroxyacetaldehyde, acetol, and formic acid, 5-hydroxymethylfurfural, 2-furaldehyde, etc.[78,92].

Anhydrohexoses can be hydrolyzed to monosaccharides and fermented with *Saccharomyces cerevisiae*. Alternatively, they can be directly fermented to ethanol with engineered bacteria.[8] The theoretical fermentation of levoglucosan yields up to 57% by weight of ethanol and 43% of CO_2.

Fast pyrolysis also produces a carbon-rich, solid, co-product known as biochar, currently considered a relatively low-value product. Although previous studies have proposed utilizing biochar in heat and energy production (burned in the process)[101] or as a soil amendment for agricultural lands[53,102], our study evaluated the activation and subsequent usage of this material as industrial adsorbents of various chemicals. Numerous studies have shown biochar can be readily upgraded through chemical or physical treatments to make "activated carbon"[45,49,103] effective in removing contaminants from various liquid and gaseous media such as pyrolytic sugars[77].

Pyrolytic sugars contain contaminants that dramatically reduce the fermentability, and final product (ethanol) yield and broth concentration. Reducing the fermentation performance of levoglucosan, results in overall lower product recovery rates and higher distillation costs. Some of these compounds were identified as phenols, furfural, formic acid, valeric acid, 5-methyl-furfural and butyric acid.[84,104]

Simply cleaning and later purifying the pyrolytic sugars with AC can be an effective and economical process to produce high-value products, such as ethanol. Activated carbon is traditionally manufactured by thermochemically transforming charcoal at high temperatures and using chemical or oxidizing gases to enhance porosity and surface functional groups of the raw carbonaceous material.[16,31,51]

The goal of this study was to quantify the economic internal rate of return of a fast pyrolysis, corn stover biorefinery by incorporating the detoxification and fermentation of pyrolytic sugars, and production of AC from biochar.

Methodology

This study was based on previous techno-economic analysis (TEA) models with process parameters obtained from experimentation. Energy costs were derived from historical prices available through the U.S. Energy Information Administration (EIA). A process model was developed using Aspen Plus 7.1 to evaluate mass and energy balances of six major process modules (Figure 1) to understand the system's performance. The economic viability of the system was estimated with a discounted cash flow rate of return (DCFROR) spreadsheet. Sensitivity analysis was conducted by varying different process, economic, and production parameters. The construction time was three years and the life-time for the biorefinery was 20 years.

Conventional fast pyrolysis platform and new modules integration

Similar to traditional fast pyrolysis systems, the first module is the pretreatment stage comprised of three stages: (1) hammer mill reduces the biomass particle size to 10 mm, (2) sulfuric acid is added, and (3) a rotary drier lowers the moisture to 10%wt (Figure 1).

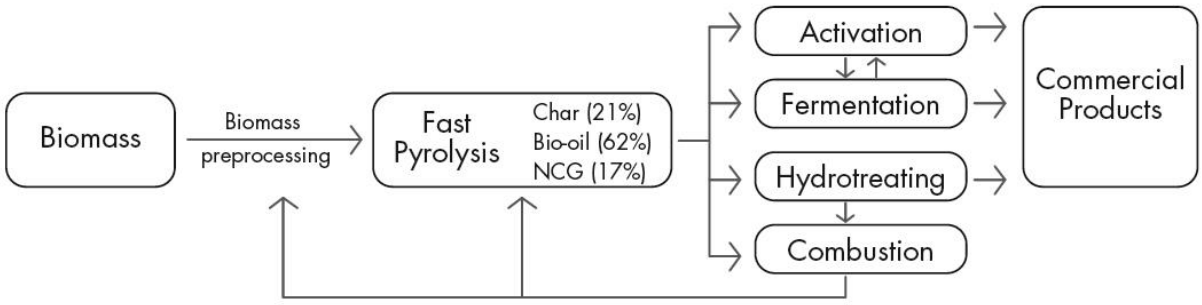

Figure 3. General outline of the biorefinery components: biomass pretreatment, fast pyrolysis, activation, fermentation, hydrotreating and combustion modules.
Note: NCG refers to non-condensable gases

A nitrogen gas fast pyrolysis fluidized bed reactor operating at 500°C processes the pretreated corn stover biomass producing 21% biochar, 62% bio-oil, and 17% non-condensable gases (Table 1). Initially, the biochar is removed from the hot vapor stream through a series of cyclonic filters before a heavy fraction of the bio-oil is condensed through a series of electrostatic precipitators set at different temperatures (<200°C), condensing phenolic oligomers and pyrolytic sugars. Lower temperature condensers later remove small molecular weight compounds, called light ends, from the non-condensable gas stream, such as organic acids and water.

Table 4: Fast pyrolysis output stream

Plant capacity (dry corn stover)	780934	ton/year	2000	ton/day
Pyrolysis co-products				
Bio-oil (62% wt)	481056	ton/year	1232	ton/day
Biochar (21% wt)	167120	ton/year	428	ton/day
NC-Gases (17% wt)	132759	ton/year	340	ton/day

From 2,000 dry tons of biomass processed per day, the bio-oil yields account for 1232 ton/day from a total of 34%wt water, 24% phenolic oligomers, 26% pyrolytic sugars, and 16% light ends of the biomass weight. The biochar accounts for 428 ton/day with a 39% fixed carbon 44% of vol and 21% of ash. The non-condensable gases are composed mainly of CO_2, N_2, $H_20_{(v)}$, CO, H_2O, CH_4, H_2, ethane, and light hydrocarbons, all but CO_2 and $H_20_{(v)}$ can be combusted to produce process heat and reduce natural gas consumption. The non-condensable gases (NCG)

have an estimated energy content of 10 MJ/kg when dried (HHV), approximately 18% of the energy content of natural gas.

Refining processes of fast pyrolysis intermediate streams

Biochar is activated with CO_2 derived from the fermentation of pyrolytic sugars (Figure 2a and Figure 2b). For every gallon of ethanol produced roughly 2.2 kg of CO_2 is also produced due to the fermentation process. For best activation conditions, a laboratory experiment was conducted to determine the optimal temperature, residence time for conditions that will maximize the surface area (quality parameter), and minimize the AC mass loss. This experimental approach to optimize activation output was similar to a previous study on steam activation of fast pyrolysis red oak biochar[15]. In addition to detoxifying pyrolytic sugar inhibitors, any remaining AC is commercialized to generate an additional revenue stream.

A pyrolytic sugar solution, containing 50 g/L of anhydrosugars, was purified by applying 1 %wt of AC to the solution. Fermentation of this sugar solution yielded 20 g/L of ethanol.

Phenolic oligomers and light ends are hydroprocessed into renewable gasoline, diesel, hydrogen, and fuel gas. Some of the fuel gas and all of the condensable gases produced during pyrolysis are combusted to produce heat for use in other modules of the biorefinery, such as the drier, pyrolysis reactor, and activation reactor (20, 62, and 40 MW, respectively). Natural gas is utilized to complete the energy requirements for the system with 59 ton/day (38 MW).

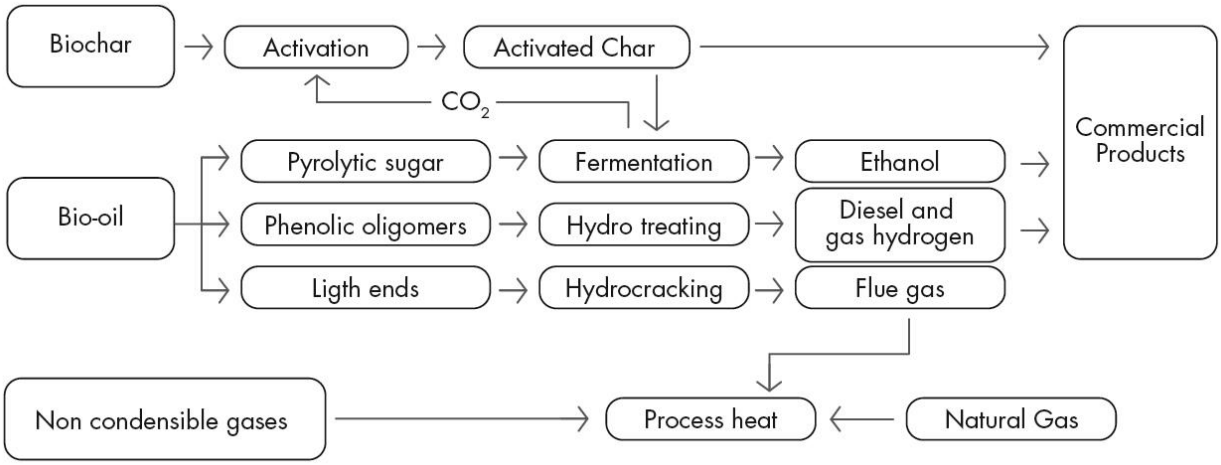

Figure 4a. Mass and energy flow from the fast pyrolysis streams and subsequent refining modules

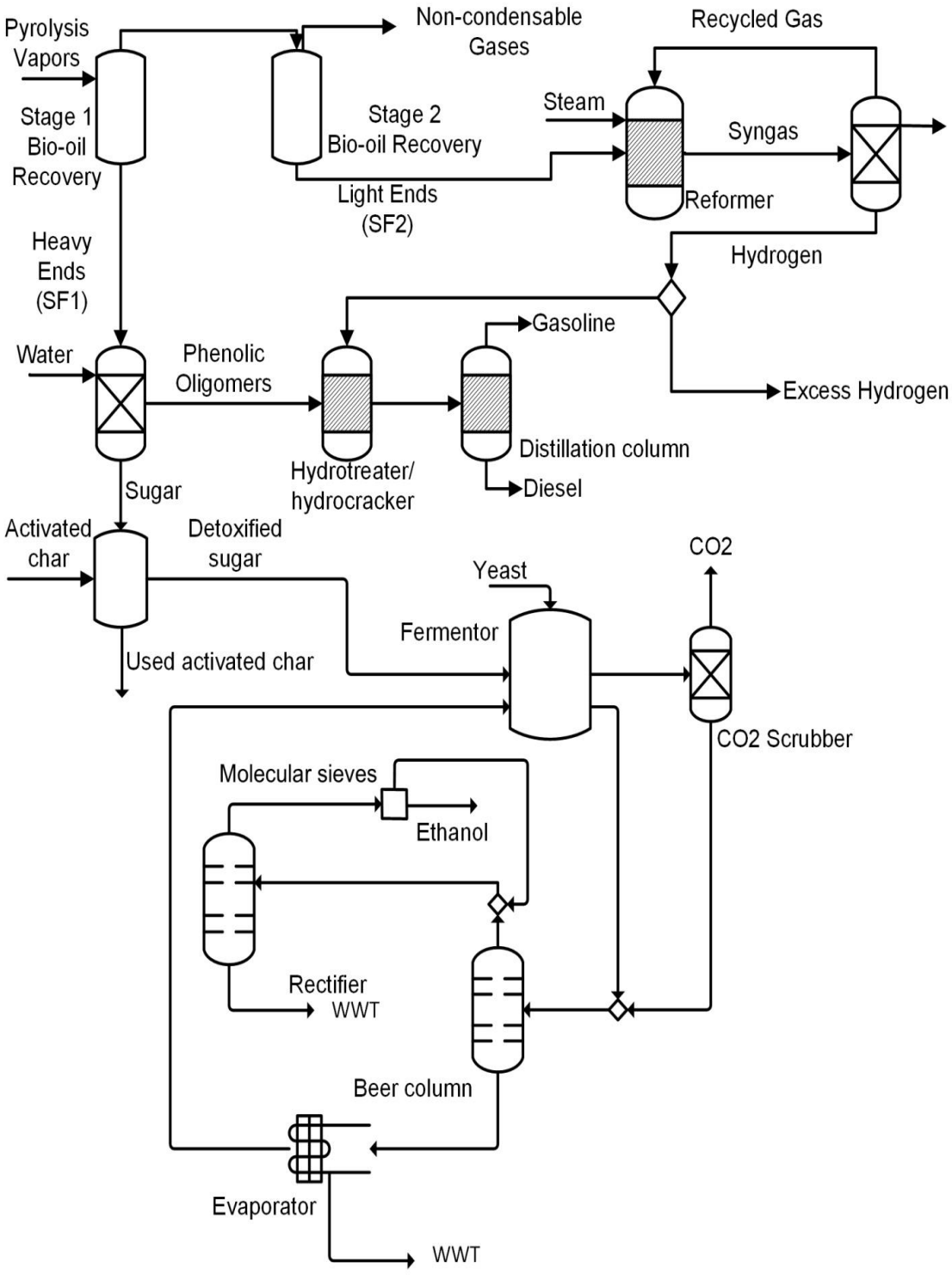

Figure 5b. ASPEN plus process design integrating the fuel production modules.

Process parameters and model outputs

From a feedstock acquisition perspective, the consumption of 780,934 tons of biomass per year would require 687 km^2 (269 mi^2) of corn crop to satisfy the processing need of the biorefinery. This area is the result of a typical corn yield of 180 bushel of grain and 10 tons of biomass per acre (with a 45% grain to biomass harvest index), assuming only 50% of the total stover is removed to prevent erosion and improving sustainability of the system, and considering 50% of the surrounding area is dedicated to crop production which is sold to the biorefinery. The feedstock acquisition will require an average radius of 21km (13 miles) around the plant to supply the biomass needed to operate every year. Table 2 describes the process parameters used for our model for certain product properties and energy contents.

Table 5: Process parameters used in this biorefinery model

Feedstock	Clean Corn Stover
Pyrolysis Temperature	500°C
Process heat needed (MW)	73
Feedstock:	Clean corn stover
Plant operation (days/year)	354
Feedstock ash (percent wet basis)	6%
Feedstock moisture (percent wet basis)	25%
NC-Gases energy content LHV (MJ/kg)	3.5
Ethanol LHV (Btu/gal)	76000
Gasoline LHV (Btu/gal)	115000
Activation yield (Biochar to AC)	68%
Levoglucosan yield from biomass	11%

Compared to red oak as feedstock[101], corn stover results in lower bio-oil yield (62 vs 65 wt%) and slightly higher biochar yield (21 vs 19 wt%). The process heat used in this plant is 435 MW, but most of the energy required comes from the fuel gas and non-condensable gases produced from pyrolysis.

To optimize the process parameters used in the biochar activation module, a full factorial design experiment was performed in a bench scale reactor to simulate larger scale activation conditions. The experiment consisted of three temperature levels (400, 600, and 800°C) and three residence times (5, 30, and 60 minutes), in similar conditions to a previous study.[105] From the

experimental results on mass yield and activation performance, a response surface model was constructed to optimize the economic benefits of the process by maximizing surface area and minimizing burn off (inverse of AC yield) for a specific quality appraisal (similar to previous steam activation study).[105]

The economic assumptions used in the model are detailed below and are consistent with previous studies[53,101].

Table 6: Economic parameters used in the model

Cost year for analysis (calendar year)		**2011**	**Reference**
Feedstock cost ($/dry ton)	$	50	[106]
Contingency (% of TFC)		17%	[107]
Electricity purchase ($/KWh)	$	0.061	[101]
Working Capital (% of FCI)		15%	[107]
Ethanol selling price ($/gal)	$	2.00	[108]
Activated carbon selling price ($/kg)	$	656	Prorated [44]
Hydrogen selling price ($/kg)	$	3.49	[101]
Gasoline and diesel selling price ($/gal)	$	3.00	[101]
Natural gas price ($/MM BTU)	$	5.24	[101]
Interest rate on borrowed funds (%)		7.5%	
Discount rate (%)		10%	[109]
Income Tax Rate (%)		39%	[109]
General Plant Depreciation Period (years)		7	[109]
Steam/Power Plant Depr. Period (years)		20	[109]
Equity Percent of Total Investment (%)		40%	
Type of Depreciation	Double declining balance		[109]

Results and Discussion

From the predicted models the optimum activation temperature and residence time resulted in 800°C and 60 min of residence time, resulting in 440 m^2/g of activated char, and an output yield of 68% wt. of the biochar mass. For the predicted AC quality and prorated for a third of the market price, due to the lower BET from the process, resulting in a final sale price of $656 per ton (see Appendix for more details). The BET surface area is here considered as a quality parameter indicating degree of activation defining the final price of the product. In terms of CO_2 needed for the activation of the biochar, for every gallon of ethanol produced, almost 2.2 kg of CO_2 is co-produced in the fermenters. Thus, this results in approximately 7 times more

CO_2 than needed for the activation process. In addition, the purity of the CO_2 from the fermenters is typically very high, which could be used directly for the activation with minor clean up and drying steps.

The prediction model for optimization in each AC yield and quality output (BET) resulted in:

$$S_{BET} = -128.51 + 0.593T_{\circ C} + 1.231R_{min} + [(T_{\circ C} - 600) \times (R_{min} - 31.67)] \times 0.00313 \quad (1)$$

$$\Delta_m = -0.117 + 0.00042T_{\circ C} = 0.00127R_{min} + [(T_{\circ C} - 600) \times (R_{min} - 31.67) \times 0.0000044 \quad (2)$$

where:
S_{BET}= Surface area (m2/g) measured by Brunauer, Emmett, and Teller,
Δ_m= fraction of mass loss during activation, burn off (%),
R_{min}= Residence time of activation (minutes), and
$T_{\circ C}$= Activation temperature (°C).

Total project investment (TPI) is $414 million for processing 2000 tpd of corn stover, which is higher than previous studies[53,101], due to the integration of two other modules—the fermenters of pyrolytic sugar and the AC reactor. The total project investment includes $63 million for contingency factors (unexpected expenses) accounting for 17% of the total project investment. In terms of processing capacity (tons of biomass), the total investment is about $530 per ton of biomass or $13 per gallon of liquid product. In comparison, the capital investment to construct a corn grain (dry mill) ethanol plant is $2-3 per gallon of annual production capacity[110], a cellulosic fermentation biorefinery costs $7-12 per gallon, depending upon the technology used,[111] but this advanced biorefinery is roughly $13 per gallon. However, the production of hydrogen and AC significantly contribute to the capital investment and not to the fuel production capacity. The selling price for hydrogen does not include compression and pipeline costs which will add higher capital investments.

Highlighting the most significant economic results from the model, the total installed equipment cost is $245 million, approximately three times the value of equipment itself, and the indirect cost associated with engineering, construction and legal fees accounted for $72 million.

In comparison to a similar model by Yanan et al. (2013), the incorporation of the ethanol fermenter and activator reactor increased the total investment cost by $29 million.

Table 4: Product sales and general revenue

Product stream	**Volume of product sales**				**MM$/yr**		**Percent Sales**
Gasoline & diesel sales	16.93	MM gal/year	47808	gal/day	$	51	33%
Ethanol sales	14.38	MM gal/year	40601	gal/day	$	29	19%
Hydrogen sales	8.68	MM Kg/year	24505	Kg/day	$	30	20%
Activated char sales	66.66	MM Kg/year	188212	Kg/day	$	44	28%
Total					*$*	*154*	*100%*

The total gross revenue from the commercialization of these four products is $154 million. The most important revenue stream is comprised of transportation fuels, totaling 52% of the total gross revenue, with 33% gasoline and diesel sales, and 19% for ethanol. Fuel gas and non-condensable gases are used to produce process heat, which reduced the energy consumption. Biochar is not used as a fuel source and none is burned. All is activated for use in the fermenters (approximately one-third of the total production) or is commercialized. Activated carbon sales accounted for about $44 million or 28% of the overall annual revenue. Considering the U.S. demand for AC is approximately 1.2 b tons per year, this fast pyrolysis biorefinery would be able to supply 66,600 tons of AC per year, addressing approximately 12% of the total US market demand.[112]

The AC module of this biorefinery is a significant economic improvement from earlier techno-economic analyses which used biochar to produce process heat (through combustion) or it is applied to agricultural land as a soil amendment, even including credits from carbon sequestration[53]. Still, there are few limitations and unknowns for large scale implementation AC from fast pyrolysis biochar. Firstly, the quality and adsorption capacity might not be the same to traditional materials due to the higher ash content and type of feedstock. Secondly, the production scale of this operation is much larger than any typical AC facility posing other major commercialization challenges. Thirdly, not one activated carbon fits every application, and a lot more research and development has to be implemented to engineer the AC for the various type of products and improve its performance and characteristics for very different applications.

Table 5: Energy inputs and outputs of the system

Energy in	**Quantity used**		**Energy distribution**			**MM$/yr**	
Biomass	2000	ton/day	398	MW	89%	$	39
Natural Gas	59	ton/day	38	MW	8%	$	6
electricity	14	MW	14	MW	3%	$	7
Total			*449*	*MW*	*100%*	*$*	*52*
Energy out	**Quantity produced**		**Energy distribution**			**MM$/yr**	
Gasoline & diesel sales	17	MM gal/year	65	MW	34%	$	51
Ethanol sales	14	MM gal/year	37	MW	19%	$	29
H2 sales	9	MM Kg/year	33	MW	17%	$	30
Activated char sales	67	MM Kg/year	58	MW	30%	$	44
Total			*193*	*MW*	*100%*	*$*	*154*

The overall energy efficiency (useful energy products over energy inputs) of the biorefinery is 34% after accounting for the energy inputs, natural gas, electricity and biomass, and the energy contained in the fuel products (gasoline, diesel, ethanol and hydrogen). The energy content contained in the char was subtracted from the initial biomass, as the activated char is not considered an energy product. This result is significantly lower than previous TEA analysis with similar fuels and co-products approach but focusing on monosaccharide production rather than activated char as co-product[101]. Among the energy inputs, 89% was derived from the biomass, 8% from the purchased natural gas, and 3% was electricity purchased from the grid. From an energy perspective, all sources of energy accounted for $52 million in inputs and value products were manufactured for a total value of $154 million and $110 million were energy products. When the remaining costs are included, such as depreciation, fixed, and other capital costs, a net profit around $52 million annually is achieved.

The installed (equipment) cost was $243 million. Two of the modules accounted for more than 50% of the installed equipment cost, and hydroprocessing and combustion with 29 and 24%, respectively. Note, pyrolysis and recovery represent 11% of the installed equipment cost (Figure 3)—the fourth installed equipment cost. The expenses incurred in the total installed equipment cost approximately generate $19 million dollars in capital depreciation annually.

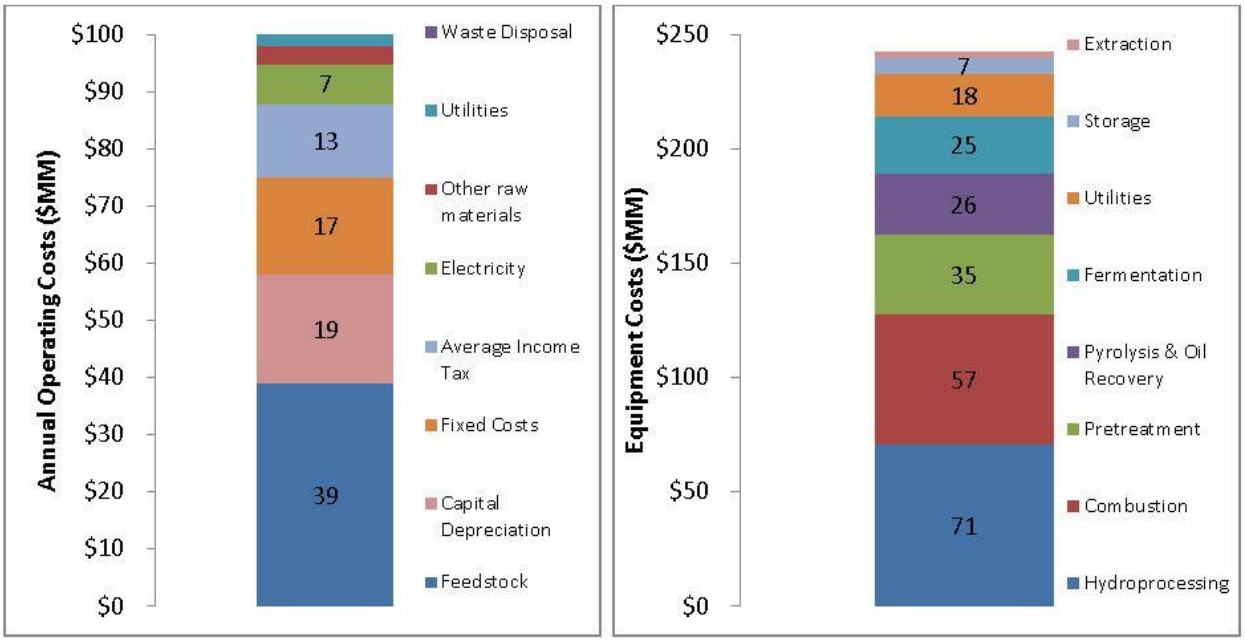

Figure 6. Annual operating costs and equipment costs for a 2000 tons per day biorefinery producing AC, gasoline and diesel, ethanol, and hydrogen.

Biomass feedstock acquisition at $50/ton is the most important operating cost, totaling $39 million annually, more than twice the following category (Figure 3). From a different perspective, the biomass feedstock cost represents about 75% of the average return on investment, highlighting the economic significance of the biomass use and pricing of the biorefinery economic performance. Due to the large TPI of $414 million, the resulting annual capital depreciation is $17 million. The third largest operational cost is salaries and wages (fixed operating costs), with an estimate of $16 million annually.

Sensitivity analysis

Varying the most critical production, economic, and financial parameters used in the model, a sensitivity analysis was performed to understand the uncertainty of the IRR output when varying different inputs (Figure 4).

Fixed capital cost had the greatest impact on the IRR in our model. The IRR rose from an estimated 16 to 24% when the fixed capital cost of the refinery fell 25%, from $381 to 266 million. Similarly, the IRR fell from 16 to 11% when fixed capital cost rose from $381 to 494

million. Following capital costs, the variability of the feedstock price (category that accounted for highest operational cost) had a major impact on the IRR. For example, if the acquisition cost was $25 per ton, then the IRR would result in 21% IRR; likewise, $75 per ton would result in 11% IRR. Note, in any case, the IRR was below zero. The next three categories were product appraisal in which a 25% variation of the selling price can have a 3-4% change in the final IRR for the refinery.

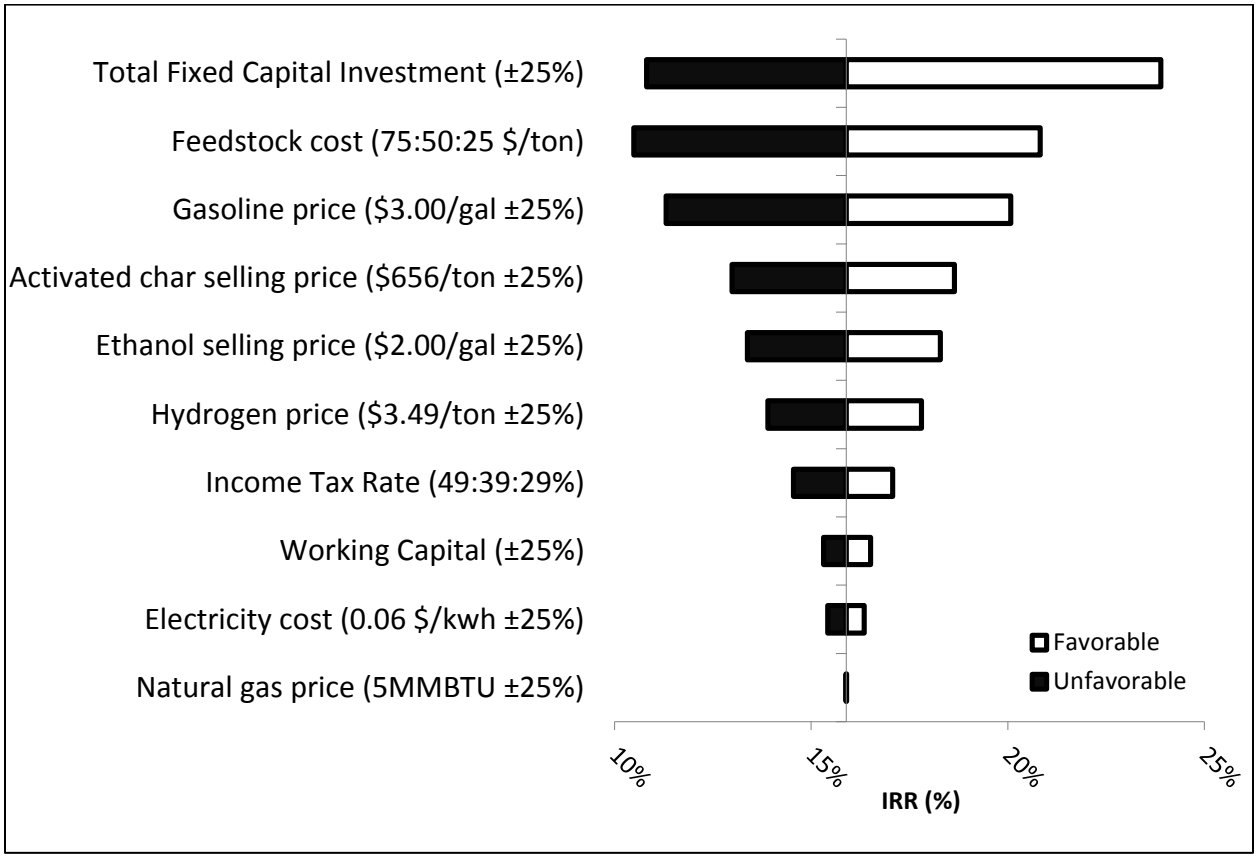

Figure 4. Sensitivity analysis for a 2000 ton per day fast pyrolysis biorefinery

Energy inputs, such as electricity and natural gas, were not important parameters to define the final IRR of the biorefinery. The process heat required for the drier, pyrolyzer, and activation is also provided from the combustion of pyrolysis and hydroprocessing co-product (non-condensable gases and fuel gas from hydrocracking light ends), substantially reducing the amount of external energy needed. In addition, both natural gas and electricity used is not as

significant as other industrial operations. Their overall cost is quite low in comparison to other processing inputs.

Due to the fact that two of the four commercial products sold by this biorefinery are not typically produced under these situations, Figure 5 displays the overall IRR and variations within their selling price. This figure shows the broader spectrum of selling prices (Figure 5).

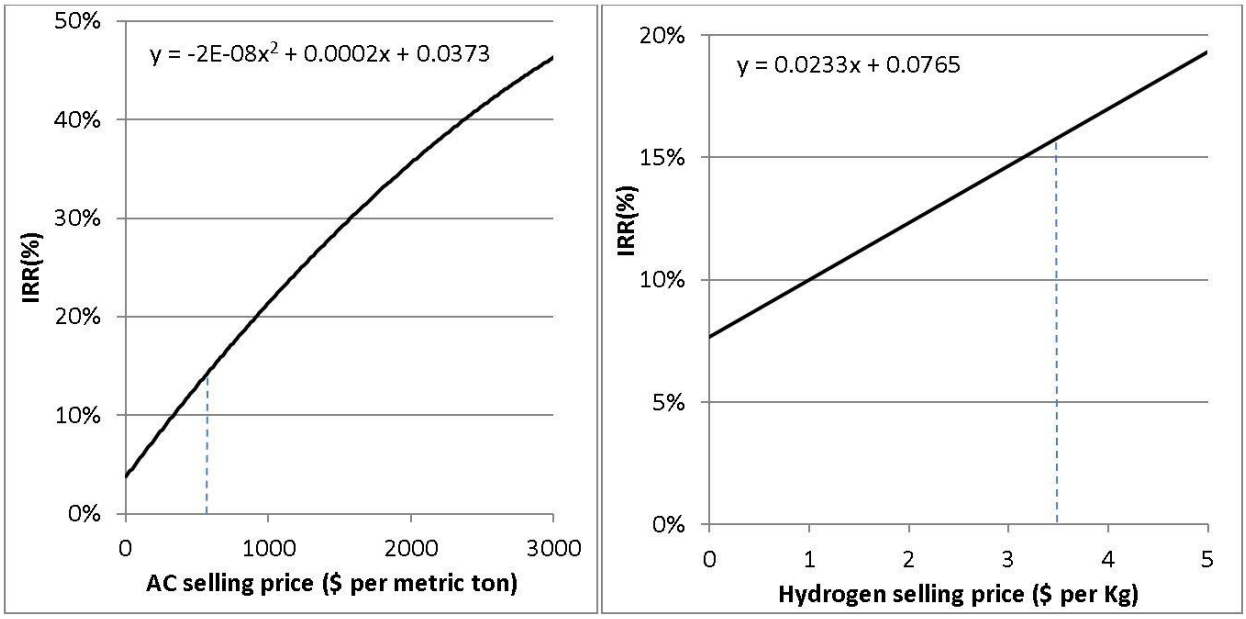

Figure 5. Internal rate of return with varying AC (left) and hydrogen (right) selling price.

Even if AC or hydrogen generated no revenue, due to no quantities sold or zero selling prices, still the IRR of the biorefinery was 4 or 7% (for no AC and hydrogen being sold, respectively). Currently, AC and hydrogen prices are not sold as commodity products. Therefore, their market prices and commercialization viability are one of the main assumptions of this biorefinery. However, there is potential for the biorefinery to have a positive IRR even without the sale of these co-products.

Conclusions

This study evaluated the economic feasibility of a thermochemical biorefinery producing transportation fuels and chemicals from fast pyrolysis of biomass. By incorporating ethanol, AC, and lower-cost sustainably harvested biomass in a 2000 ton/day biorefinery, our model saw a significant improvement in IRR of up to 16% compared to previous techno-economic analyses. The commercialization of 31 million gallons of transportation fuels (ethanol, gasoline and diesel) produced under a hybrid thermochemical and biological platform, accounted for most of the gross revenue produced by this biorefinery. Including activated carbon and hydrogen production, the biorefinery produced a gross revenue of $154 million per year for a total project investment of $414 million. Based on the sensitivity analysis, the two factors that have greatest influence on IRR were the feedstock price (corn stover) and fixed capital investments.

As demonstrated in our model, a biorefinery built upon these principles would be profitable. However, there are many technical and economic challenges associated with a large scale biorefinery that needs to be addressed. The scale of the facility that has to be implemented to make the overall system profitable is significant and requires a large capital investment. Certainly, there are major risks associated with this and other technologies that are not technically mature, which require several years to optimize the process and develop value added products from each stream. However, this study provides positive preliminary results from the integration of a thermochemical and biological biorefinery.

Acknowledgements

The research reported in this publication was supported by Iowa State University, the Iowa Energy Center (12-06), and the NSF Energy for Sustainability (CBET-1133319). The authors would like to acknowledge the technical support of the Bioeconomy Institute laboratory personnel and students, Eric Debner and Joseph Kopacz. The author of this publication, Bernardo del Campo, has equity ownership in Advanced Renewable Technology International, Inc. (ARTi), which is developing products related to the research reported. The terms of this

arrangement have been reviewed and approved by Iowa State University in accordance with its Conflicts of Interest and Commitment Policy.

Appendix

Table 7: Experimental BET surface area results (left) and standard deviation (right) from the activation of corn stover biochar with different temperatures and times

Temp\R.Time	5	30	60	Row Av.
400	106	187	155	149
600	249	249	292	263
800	301	439	419	386
Column Av.	219	292	289	266

Temp\R.Time	5	30	60	Row Av.
400	19	31	33	43
600	41	36	23	37
800	48	84	49	85
Column Av.	93	124	119	114

Table 8: Predicted model for surface area based on experimental results $R^2 = 0.825$

Temp\R.Time	5	30	60	Row Av.
400	132	147	165	148
600	233	264	301	266
800	335	382	438	385
Column Av.	233	264	301	266

Both models predictions models for BET and burn off are significant with alfa less (0.001)

Table 9: Experimental burn off results (left) and standard deviation (right) from the activation of corn stover biochar with different temperatures and times

Temp\R.Time	5	30	60	Row Av.
400	6%	13%	10%	10%
600	13%	16%	19%	16%
800	21%	25%	33%	26%
Column Av.	13%	18%	20%	17%

Temp\R.Time	5	30	60	Row Av.
400	3%	2%	3%	4%
600	1%	0%	2%	3%
800	5%	4%	13%	9%
Column Av.	7%	6%	12%	9%

Table 10: Predicted model for burn off (%) $R^2 = 0.732$

Temp\R.Time	5	30	60	Row Av.
400	8%	9%	10%	9%
600	14%	17%	21%	17%
800	20%	25%	32%	26%
Column Av.	14%	17%	21%	17%

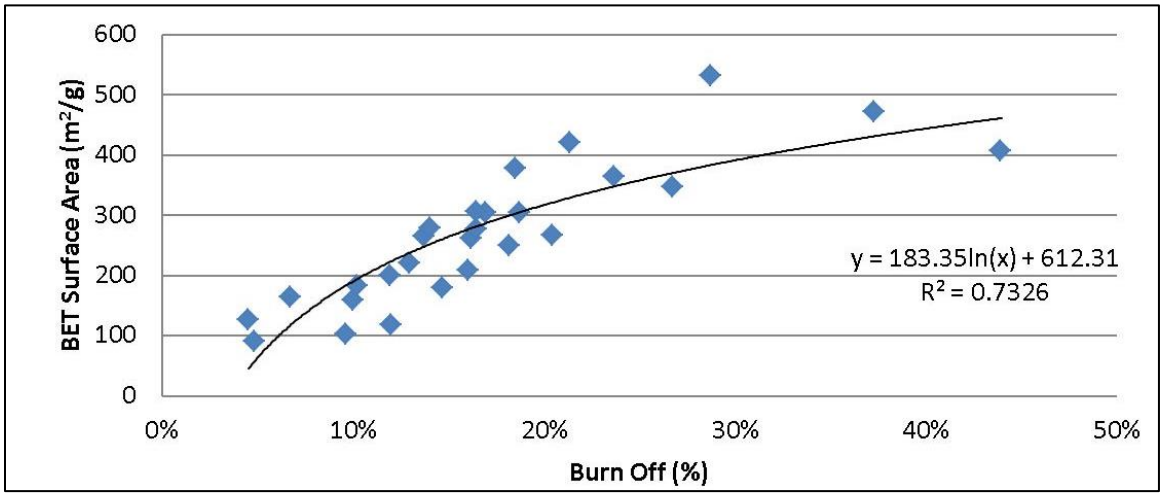

Figure 6. Relationship of surface area and burn off (%) of corn stover activated with CO_2

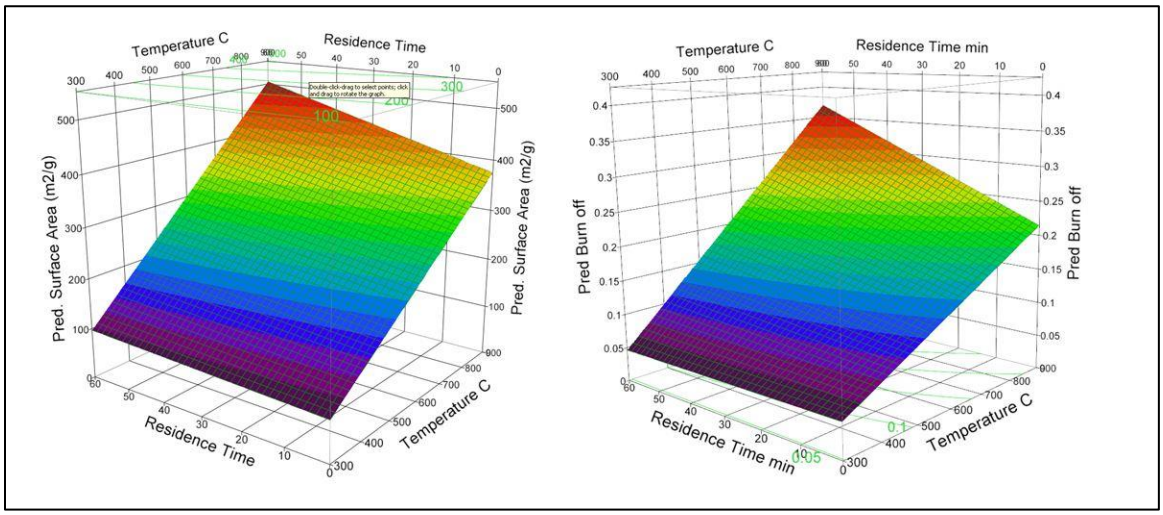

Figure 7. Surface response model for BET and burn off (%)

The surface response model for the predicted BET surface area and burn off (%) of activated biochar with CO_2 showed very small curvature and the quadratic term was not significant, neither the interaction effect within the two independent variables, therefore the proportional increments were closer planar

CHAPTER 5 GENERAL CONCLUSIONS

This study found that fast pyrolysis biochar can be readily activated with steam and different operating conditions greatly vary the final characteristic of the adsorbent material. Typical fast pyrolysis biochar has very low porosity and surface area. However, with one-step physical activation, this characteristic can be dramatically improved.

The use of response surface models made more efficient the experimental work, and more importantly, easier to understand the relationship between surface area and operating conditions. For the specific scenario in our study with this type of reactor, this specific type of biochar, and these ranges of operating conditions, the best economic scenario was determined at 800°C and a residence time of 5 minutes. Under this condition, the activated biochar resulted in 543 m^2/g of BET surface area with a burn off of 28% and $907 of net revenue.

Biochars, activated biochars, and commercially activated carbon were all able to detoxify and ferment to some extent pyrolytic sugar. The physicochemical characteristics of the adsorbent, such as BET, micropores, and external surface area, positively correlated with bacterial growth (on microplate studies), but did not correlate well with ethanol production. The DFT pore mode and pH of the adsorbent material resulted in some correlation with the ethanol produced (in microplate trials).

Preliminary results from fermentation tests in 200 mL bioreactors with activated carbon and activated red oak biochar produced 2.1 and 1.0 g/L ethanol, respectively, from the original 20 g/L of pyrolytic sugars in a 72-hour study. However, fermentation in microplates with various types of biochar and activated chars suggested that some of these materials could be effective at detoxifying pyrolytic sugars to produce ethanol. Therefore, further investigation is necessary to better assess the internal characteristics of the wide range of carbon adsorbent, as well as the different pretreatments and activation that will enhance their detoxification performance.

A technoeconomic study of a 2000 ton per day biorefinery that produced pyrolytic sugars and activated biochar indicated that the system would be profitable. This model predicted a significant improvement in internal rate of return up to 16% compared with similar techno-economic analyses with the newly added modules. The biorefinery would produce 31 million gallons of transportation fuels and co-products with gross revenue of $154 million for a total project investment of $414 million.

References

(1) Vitousek, P. M.; Mooney, H. A.; Lubchenco, J.; Melillo, J. M. Human domination of Earth's ecosystems. *Science* **1997**, *277*, 494-499.

(2) Hayhoe, K.; Cayan, D.; Field, C. B.; Frumhoff, P. C.; Maurer, E. P.; Miller, N. L.; Moser, S. C.; Schneider, S. H.; Cahill, K. N.; Cleland, E. E. Emissions pathways, climate change, and impacts on California. *Proceedings of the National Academy of Sciences of the United States of America* **2004**, *101*, 12422-12427.

(3) Pachauri, R. K.; Allen, M.; Barros, V.; Broome, J.; Cramer, W.; Christ, R.; Church, J.; Clarke, L.; Dahe, Q.; Dasgupta, P. Climate Change 2014: Synthesis Report. Contribution of Working Groups I, II and III to the Fifth Assessment Report of the Intergovernmental Panel on Climate Change. **2014**.

(4) Cantrell, K.; Martin, J. In *Tilte*2010; IEEE.

(5) Zhao, L.; Cao, X.; Mašek, O.; Zimmerman, A. Heterogeneity of biochar properties as a function of feedstock sources and production temperatures. *Journal of hazardous materials* **2013**, *256*, 1-9.

(6) Dalluge, D. L.; Daugaard, T.; Johnston, P.; Kuzhiyil, N.; Wright, M. M.; Brown, R. C. Continuous production of sugars from pyrolysis of acid-infused lignocellulosic biomass. *Green Chemistry* **2014**, *16*, 4144-4155.

(7) McKendry, P. Energy production from biomass (part 1): overview of biomass. *Bioresource technology* **2002**, *83*, 37-46.

(8) Jarboe, L. R.; Wen, Z.; Choi, D.; Brown, R. C. Hybrid thermochemical processing: fermentation of pyrolysis-derived bio-oil. *Applied microbiology and biotechnology* **2011**, *91*, 1519-1523.

(9) Joseph, S.; Downie, A.; Munroe, P.; Crosky, A.; Lehmann, J. In *Tilte*2007.

(10) Galinato, S. P.; Yoder, J. K.; Granatstein, D. The economic value of biochar in crop production and carbon sequestration. *Energy Policy* **2011**, *39*, 6344-6350.

(11) Roberts, K. G.; Gloy, B. A.; Joseph, S.; Scott, N. R.; Lehmann, J. Life cycle assessment of biochar systems: Estimating the energetic, economic, and climate change potential. *Environmental science & technology* **2009**, *44*, 827-833.

(12) Chen, X.; Chen, G.; Chen, L.; Chen, Y.; Lehmann, J.; McBride, M. B.; Hay, A. G. Adsorption of copper and zinc by biochars produced from pyrolysis of hardwood and corn straw in aqueous solution. *Bioresource technology* **2011**, *102*, 8877-8884.

(13) Harvey, O. R.; Herbert, B. E.; Rhue, R. D.; Kuo, L.-J. Metal interactions at the biochar-water interface: Energetics and structure-sorption relationships elucidated by flow adsorption microcalorimetry. *Environmental science & technology* **2011**, *45*, 5550-5556.

(14) Kizito, S.; Wu, S.; Kirui, W. K.; Lei, M.; Lu, Q.; Bah, H.; Dong, R. Evaluation of slow pyrolyzed wood and rice husks biochar for adsorption of ammonium nitrogen from piggery manure anaerobic digestate slurry. *Science of The Total Environment* **2015**, *505*, 102-112.

(15) del-Campo, B. G.; Morris, M. D.; Laird, D. A.; Kieffer, M. M.; Brown, R. C. Optimizing the production of activated carbon from fast pyrolysis char. *Technology* **2015**, *0*, 1-10.

(16) Lima, I. M.; McAloon, A.; Boateng, A. A. Activated carbon from broiler litter: Process description and cost of production. *Biomass and Bioenergy* **2008**, *32*, 568-572.

(17) Tam, M. S.; Antal, M. J. Preparation of activated carbons from macadamia nut shell and coconut shell by air activation. *Industrial & engineering chemistry research* **1999**, *38*, 4268-4276.

(18) Ahmedna, M.; Johns, M.; Clarke, S.; Marshall, W.; Rao, R. Potential of agricultural by-product-based activated carbons for use in raw sugar decolourisation. *Journal of the Science of Food and Agriculture* **1997**, *75*, 117-124.

(19) Daguerre, E.; Guillot, A.; Stoeckli, F. Activated carbons prepared from thermally and chemically treated petroleum and coal tar pitches. *Carbon* **2001**, *39*, 1279-1285.

(20) Kirubakaran, C. J.; Krishnaiah, K.; Seshadri, S. Experimental study of the production of activated carbon from coconut shells in a fluidized bed reactor. *Industrial & engineering chemistry research* **1991**, *30*, 2411-2416.

(21) Ioannidou, O.; Zabaniotou, A. Agricultural residues as precursors for activated carbon production—a review. *Renewable and Sustainable Energy Reviews* **2007**, *11*, 1966-2005.

(22) Nieto-Delgado, C.; Terrones, M.; Rangel-Mendez, J. R. Development of highly microporous activated carbon from the alcoholic beverage industry organic by-products. *Biomass and Bioenergy* **2011**, *35*, 103-112.

(23) Karanfil, T.; Kilduff, J. E. Role of granular activated carbon surface chemistry on the adsorption of organic compounds. 1. Priority pollutants. *Environmental science & technology* **1999**, *33*, 3217-3224.

(24) Klasson, K. T.; Boihem Jr, L. L.; Lima, I. M.; Marshall, W. E. In *Tilte*2007.

(25) Pendyal, B.; Johns, M. M.; Marshall, W. E.; Ahmedna, M.; Rao, R. M. Removal of sugar colorants by granular activated carbons made from binders and agricultural by-products. *Bioresource Technology* **1999**, *69*, 45-51.

(26) Hertzog, E.; Broderick, S. Activated carbon for sugar decolorization. *Industrial & Engineering Chemistry* **1941**, *33*, 1192-1198.

(27) Bagreev, A.; Rahman, H.; Bandosz, T. J. Study of H2S adsorption and water regeneration of spent coconut-based activated carbon. *Environmental science & technology* **2000**, *34*, 4587-4592.

(28) Azargohar, R.; Dalai, A. In *Tilte*2006; Springer.

(29) Lehmann, J.; Joseph, S.: *Biochar for environmental management: science and technology*; Routledge, 2012.

(30) Azargohar, R.; Dalai, A. Steam and KOH activation of biochar: Experimental and modeling studies. *Microporous and Mesoporous Materials* **2008**, *110*, 413-421.

(31) Boehm, H. Some aspects of the surface chemistry of carbon blacks and other carbons. *Carbon* **1994**, *32*, 759-769.

(32) Käldström, M.; Kumar, N.; Salmi, T.; Yu Murzin, D. Levoglucosan transformation over aluminosilicates. *Cellulose Chemistry & Technology* **2010**, *44*, 203.

(33) Li, L.; Quinlivan, P. A.; Knappe, D. R. Effects of activated carbon surface chemistry and pore structure on the adsorption of organic contaminants from aqueous solution. *Carbon* **2002**, *40*, 2085-2100.

(34) Dehkhoda, A. M.; Ellis, N.; Gyenge, E. Electrosorption on activated biochar: effect of thermo-chemical activation treatment on the electric double layer capacitance. *Journal of Applied Electrochemistry* **2014**, *44*, 141-157.

(35) Ho, M.; Khiew, P.; Isa, D.; Tan, T.; Chiu, W.; Chia, C. In *Tilte*2014; Trans Tech Publ.

(36) Brachet, M.; Brousse, T.; Le Bideau, J. In *Tilte*2014; The Electrochemical Society.

(37) Roosta, M.; Ghaedi, M.; Daneshfar, A.; Sahraei, R.; Asghari, A. Optimization of the ultrasonic assisted removal of methylene blue by gold nanoparticles loaded on activated carbon using experimental design methodology. *Ultrasonics sonochemistry* **2014**, *21*, 242-252.

(38) Rambabu, N.; Azargohar, R.; Dalai, A.; Adjaye, J. Evaluation and comparison of enrichment efficiency of physical/chemical activations and functionalized activated carbons

derived from fluid petroleum coke for environmental applications. *Fuel Processing Technology* **2012**.

(39) Mubarak, N.; Alicia, R.; Abdullah, E.; Sahu, J.; Haslija, A. A.; Tan, J. Statistical optimization and kinetic studies on removal of Zn 2+ using functionalized carbon nanotubes and magnetic biochar. *Journal of Environmental Chemical Engineering* **2013**, *1*, 486-495.

(40) Zhang, W.; Mao, S.; Chen, H.; Huang, L.; Qiu, R. Pb(II) and Cr(VI) sorption by biochars pyrolyzed from the municipal wastewater sludge under different heating conditions. *Bioresource Technology* **2013**, *147*, 545-552.

(41) Choi, G.-G.; Oh, S.-J.; Lee, S.-J.; Kim, J.-S. Production of bio-based phenolic resin and activated carbon from bio-oil and biochar derived from fast pyrolysis of palm kernel shells. *Bioresource technology* **2015**, *178*, 99-107.

(42) Jiang, J.; Zhang, L.; Wang, X.; Holm, N.; Rajagopalan, K.; Chen, F.; Ma, S. Highly ordered macroporous woody biochar with ultra-high carbon content as supercapacitor electrodes. *Electrochimica Acta* **2013**.

(43) Gong, J.; Liu, J.; Chen, X.; Jiang, Z.; Wen, X.; Mijowska, E.; Tang, T. Converting real-world mixed waste plastics into porous carbon nanosheets with excellent performance in the adsorption of an organic dye from wastewater. *Journal of Materials Chemistry A* **2015**, *3*, 341-351.

(44) Torrik, E.; Nejati, E.; Soleimani, M. Economic pre-feasibility study for physical conversion of polyethylene terephthalate wastes to activated carbon. *Asia-Pacific Journal of Chemical Engineering* **2014**, *9*, 759-767.

(45) Girgis, B. S.; Yunis, S. S.; Soliman, A. M. Characteristics of activated carbon from peanut hulls in relation to conditions of preparation. *Materials Letters* **2002**, *57*, 164-172.

(46) Ismadji, S.; Sudaryanto, Y.; Hartono, S.; Setiawan, L.; Ayucitra, A. Activated carbon from char obtained from vacuum pyrolysis of teak sawdust: pore structure development and characterization. *Bioresource technology* **2005**, *96*, 1364-1369.

(47) Cal, M.; Strickler, B.; Lizzio, A. High temperature hydrogen sulfide adsorption on activated carbon: I. Effects of gas composition and metal addition. *Carbon* **2000**, *38*, 1757-1765.

(48) Gergova, K.; Petrov, N.; Eser, S. Adsorption properties and microstructure of activated carbons produced from agricultural by-products by steam pyrolysis. *Carbon* **1994**, *32*, 693-702.

(49) Karagöz, S.; Tay, T.; Ucar, S.; Erdem, M. Activated carbons from waste biomass by sulfuric acid activation and their use on methylene blue adsorption. *Bioresource Technology* **2008**, *99*, 6214-6222.

(50) Tay, T.; Ucar, S.; Karagöz, S. Preparation and characterization of activated carbon from waste biomass. *Journal of Hazardous Materials* **2009**, *165*, 481-485.

(51) Lima, I. M.; Boateng, A. A.; Klasson, K. T. Physicochemical and adsorptive properties of fast-pyrolysis bio-chars and their steam activated counterparts. *Journal of Chemical Technology and Biotechnology* **2010**, *85*, 1515-1521.

(52) Schaeffer, K. Activated Carbon 2013 Market Update or, the Carbon Convolution. *Water Conditioning & Purification* [Online early access]2013 (accessed 09/16/2013).

(53) Brown, T. R.; Wright, M. M.; Brown, R. C. Estimating profitability of two biochar production scenarios: slow pyrolysis vs fast pyrolysis. *Biofuels, Bioproducts and Biorefining* **2011**, *5*, 54-68.

(54) Spokas, K. A.; Cantrell, K. B.; Novak, J. M.; Archer, D. W.; Ippolito, J. A.; Collins, H. P.; Boateng, A. A.; Lima, I. M.; Lamb, M. C.; McAloon, A. J. Biochar: a synthesis of its agronomic impact beyond carbon sequestration. *Journal of Environmental Quality* **2012**, *41*, 973-989.

(55) Lehmann, J.; Joseph, S.: *Biochar for Environmental Management: Science and Technology*; Earthscan, 2009.

(56) Otowa, T.; Nojima, Y.; Miyazaki, T. Development of KOH activated high surface area carbon and its application to drinking water purification. *Carbon* **1997**, *35*, 1315-1319.

(57) Hu, Z.; Lei, L.; Li, Y.; Ni, Y. Chromium adsorption on high-performance activated carbons from aqueous solution. *Separation and Purification Technology* **2003**, *31*, 13-18.

(58) Peterson, S. C.; Appell, M.; Jackson, M. A.; Boateng, A. A. Comparing corn stover and switchgrass biochar: characterization and sorption properties. *Journal of Agricultural Science* **2012**, *5*, p1.

(59) Peterson, S. C.; Jackson, M. A.; Kim, S.; Palmquist, D. E. Increasing biochar surface area: Optimization of ball milling parameters. *Powder Technology* **2012**, *228*, 115-120.

(60) Yang, S.; Hu, H.; Chen, G. Preparation of carbon adsorbents with high surface area and a model for calculating surface area. *Carbon* **2002**, *40*, 277-284.

(61) Vicente, G.; Coteron, A.; Martinez, M.; Aracil, J. Application of the factorial design of experiments and response surface methodology to optimize biodiesel production. *Industrial crops and products* **1998**, *8*, 29-35.

(62) Bezerra, M. A.; Santelli, R. E.; Oliveira, E. P.; Villar, L. S.; Escaleira, L. A. Response surface methodology (RSM) as a tool for optimization in analytical chemistry. *Talanta* **2008**, *76*, 965-977.

(63) Francis, F.; Sabu, A.; Nampoothiri, K. M.; Ramachandran, S.; Ghosh, S.; Szakacs, G.; Pandey, A. Use of response surface methodology for optimizing process parameters for the production of α-amylase by< i> Aspergillus oryzae</i>. *Biochemical Engineering Journal* **2003**, *15*, 107-115.

(64) Gangadharan, D.; Sivaramakrishnan, S.; Nampoothiri, K. M.; Sukumaran, R. K.; Pandey, A. Response surface methodology for the optimization of alpha amylase production by< i> Bacillus amyloliquefaciens</i>. *Bioresource Technology* **2008**, *99*, 4597-4602.

(65) Pollard, A.; Rover, M.; Brown, R. Characterization of bio-oil recovered as stage fractions with unique chemical and physical properties. *Journal of Analytical and Applied Pyrolysis* **2012**, *93*, 129-138.

(66) Brunauer, S.; Emmett, P. H.; Teller, E. Adsorption of gases in multimolecular layers. *Journal of the American Chemical Society* **1938**, *60*, 309-319.

(67) Mukherjee, A.; Zimmerman, A.; Harris, W. Surface chemistry variations among a series of laboratory-produced biochars. *Geoderma* **2011**, *163*, 247-255.

(68) Zimmerman, A. R. Abiotic and microbial oxidation of laboratory-produced black carbon (biochar). *Environmental science & technology* **2010**, *44*, 1295-1301.

(69) Mullen, C. A.; Boateng, A. A.; Goldberg, N. M.; Lima, I. M.; Laird, D. A.; Hicks, K. B. Bio-oil and bio-char production from corn cobs and stover by fast pyrolysis. *biomass and bioenergy* **2010**, *34*, 67-74.

(70) Liu, P.; Liu, W.-J.; Jiang, H.; Chen, J.-J.; Li, W.-W.; Yu, H.-Q. Modification of bio-char derived from fast pyrolysis of biomass and its application in removal of tetracycline from aqueous solution. *Bioresource Technology* **2012**.

(71) Figueiredo, J. L.; Pereira, M. F. R.; Freitas, M. M. A.; Órfão, J. J. M. Modification of the surface chemistry of activated carbons. *Carbon* **1999**, *37*, 1379-1389.

(72) Zabaniotou, A.; Stavropoulos, G.; Skoulou, V. Activated carbon from olive kernels in a two-stage process: Industrial improvement. *Bioresource technology* **2008**, *99*, 320-326.

(73) Mohan, D.; Pittman, C. U.; Steele, P. H. Pyrolysis of wood/biomass for bio-oil: a critical review. *Energy & Fuels* **2006**, *20*, 848-889.

(74) Brown, R. C. Hybrid thermochemical/biological processing. *Applied biochemistry and biotechnology* **2007**, *137*, 947-956.

(75) Sukhbaatar, B.; Li, Q.; Wan, C.; Yu, F.; Hassan, E.-B.; Steele, P. Inhibitors removal from bio-oil aqueous fraction for increased ethanol production. *Bioresource technology* **2014**, *161*, 379-384.

(76) Fatih Demirbas, M. Biorefineries for biofuel upgrading: a critical review. *Applied Energy* **2009**, *86*, S151-S161.

(77) Wang, H.; Livingston, D.; Srinivasan, R.; Li, Q.; Steele, P.; Yu, F. Detoxification and fermentation of pyrolytic sugar for ethanol production. *Applied biochemistry and biotechnology* **2012**, *168*, 1568-1583.

(78) Rover, M. R.; Johnston, P. A.; Jin, T.; Smith, R. G.; Brown, R. C.; Jarboe, L. Production of Clean Pyrolytic Sugars for Fermentation. *ChemSusChem* **2014**.

(79) Huber, G. W.; Iborra, S.; Corma, A. Synthesis of transportation fuels from biomass: chemistry, catalysts, and engineering. *Chemical reviews* **2006**, *106*, 4044-4098.

(80) Demirbas, A.; Pehlivan, E.; Altun, T. Potential evolution of Turkish agricultural residues as bio-gas, bio-char and bio-oil sources. *International Journal of Hydrogen Energy* **2006**, *31*, 613-620.

(81) Patwardhan, P. R.; Dalluge, D. L.; Shanks, B. H.; Brown, R. C. Distinguishing primary and secondary reactions of cellulose pyrolysis. *Bioresource technology* **2011**, *102*, 5265-5269.

(82) Kuzhiyil, N.; Dalluge, D.; Bai, X.; Kim, K. H.; Brown, R. C. Pyrolytic Sugars from Cellulosic Biomass. *ChemSusChem* **2012**, *5*, 2228-2236.

(83) Kim, K. H.; Bai, X.; Rover, M.; Brown, R. C. The effect of low-concentration oxygen in sweep gas during pyrolysis of red oak using a fluidized bed reactor. *Fuel* **2014**, *124*, 49-56.

(84) Zaldivar, J.; Martinez, A.; Ingram, L. O. Effect of alcohol compounds found in hemicellulose hydrolysate on the growth and fermentation of ethanologenic Escherichia coli. *Biotechnology and bioengineering* **2000**, *68*, 524-530.

(85) Prosen, E. M.; Radlein, D.; Piskorz, J.; Scott, D. S.; Legge, R. L. Microbial utilization of levoglucosan in wood pyrolysate as a carbon and energy source. *Biotechnology and bioengineering* **1993**, *42*, 538-541.

(86) Lian, J.; Chen, S.; Zhou, S.; Wang, Z.; O'Fallon, J.; Li, C.-Z.; Garcia-Perez, M. Separation, hydrolysis and fermentation of pyrolytic sugars to produce ethanol and lipids. *Bioresource technology* **2010**, *101*, 9688-9699.

(87) Lian, J.; Garcia-Perez, M.; Chen, S. Fermentation of levoglucosan with oleaginous yeasts for lipid production. *Bioresource technology* **2013**, *133*, 183-189.

(88) Zhang, T.; Walawender, W. P.; Fan, L.; Fan, M.; Daugaard, D.; Brown, R. Preparation of activated carbon from forest and agricultural residues through CO< sub> 2</sub> activation. *Chemical Engineering Journal* **2004**, *105*, 53-59.

(89) Alaya, M.; Girgis, B.; Mourad, W. Activated carbon from some agricultural wastes under action of one-step steam pyrolysis. *Journal of Porous Materials* **2000**, *7*, 509-517.

(90) Lillo-Ródenas, M.; Lozano-Castelló, D.; Cazorla-Amorós, D.; Linares-Solano, A. Preparation of activated carbons from Spanish anthracite: II. Activation by NaOH. *Carbon* **2001**, *39*, 751-759.

(91) Bharadwaj, A.; Wang, Y.; Sridhar, S.; Arunachalam, V. Pyrolysis of rice husk. *Current science* **2004**, *87*, 981-986.

(92) Chi, Z.; Rover, M.; Jun, E.; Deaton, M.; Johnston, P.; Brown, R. C.; Wen, Z.; Jarboe, L. R. Overliming detoxification of pyrolytic sugar syrup for direct fermentation of levoglucosan to ethanol. *Bioresource technology* **2013**, *150*, 220-227.

(93) Brunauer, S.; Deming, L.; Deming, W.; Teller, E. Multimolecular adsorption of gases on silica gel. *J. Am. Chem. Soc* **1940**, *62*, 1723-1728.

(94) Rover, M. R.; Johnston, P. A.; Jin, T.; Smith, R. G.; Brown, R. C.; Jarboe, L. Production of Clean Pyrolytic Sugars for Fermentation. *ChemSusChem* **2014**, *7*, 1662-1668.

(95) Liaw, S.-S.; Wang, Z.; Ndegwa, P.; Frear, C.; Ha, S.; Li, C.-Z.; Garcia-Perez, M. Effect of pyrolysis temperature on the yield and properties of bio-oils obtained from the auger pyrolysis of Douglas Fir wood. *Journal of Analytical and Applied Pyrolysis* **2012**, *93*, 52-62.

(96) Yu, Z.; Zhang, H. Pretreatments of cellulose pyrolysate for ethanol production by Saccharomyces cerevisiae, Pichia sp. YZ-1 and Zymomonas mobilis. *Biomass and Bioenergy* **2003**, *24*, 257-262.

(97) Zaldivar, J.; Martinez, A.; Ingram, L. O. Effect of selected aldehydes on the growth and fermentation of ethanologenic Escherichia coli. *Biotechnology and bioengineering* **1999**, *65*, 24-33.

(98) Zimmerman, J. R.; Werner, D.; Ghosh, U.; Millward, R. N.; Bridges, T. S.; Luthy, R. G. Effects of dose and particle size on activated carbon treatment to sequester polychlorinated

biphenyls and polycyclic aromatic hydrocarbons in marine sediments. *Environmental Toxicology and Chemistry* **2005**, *24*, 1594-1601.

(99) Silva, G. P. d.; Araújo, E. F. d.; Silva, D. O.; Guimarães, W. V. Ethanolic fermentation of sucrose, sugarcane juice and molasses by Escherichia coli strain KO11 and Klebsiella oxytoca strain P2. *Brazilian Journal of Microbiology* **2005**, *36*, 395-404.

(100) Anex, R. P.; Aden, A.; Kazi, F. K.; Fortman, J.; Swanson, R. M.; Wright, M. M.; Satrio, J. A.; Brown, R. C.; Daugaard, D. E.; Platon, A. Techno-economic comparison of biomass-to-transportation fuels via pyrolysis, gasification, and biochemical pathways. *Fuel* **2010**, *89*, S29-S35.

(101) Zhang, Y.; Brown, T. R.; Hu, G.; Brown, R. C. Techno-economic analysis of monosaccharide production via fast pyrolysis of lignocellulose. *Bioresource technology* **2013**, *127*, 358-365.

(102) Kauffman, N.; Hayes, D.; Brown, R. A life cycle assessment of advanced biofuel production from a hectare of corn. *Fuel* **2011**, *90*, 3306-3314.

(103) Zhang, T.; Walawender, W. P.; Fan, L.; Fan, M.; Daugaard, D.; Brown, R. Corrigendum to "Preparation of activated carbon from forest and agricultural residues through CO< sub> 2</sub> activation"[Chem. Eng. J. 105 (2004) 53–59]. *Chemical Engineering Journal* **2005**, *106*, 185.

(104) Zaldivar, J.; Ingram, L. O. Effect of organic acids on the growth and fermentation of ethanologenic Escherichia coli LY01. *Biotechnology and bioengineering* **1999**, *66*, 203-210.

(105) del Campo, B. G., M.D. Morris, D.A. Laird, M.M. Kieffer & R. C. Brown. OPTIMIZING THE PRODUCTION OF ACTIVATED CARBON FROM FAST PYROLYSIS CHAR *Technology for Bioenergy* **2015**, *to be published*, 18.

(106) Glassner, D.; Hettenhaus, J. R.; Schechinger, T. M. In *Tilte*1998.

(107) Van Wegen, R.; Ling, Y.; Middelberg, A. Industrial Production of Polyhydroxyalkanoates Using Escherichia Coll: An Economic Analysis. *Chemical Engineering Research and Design* **1998**, *76*, 417-426.

(108) Wang, K.; Ou, L.; Brown, T.; Brown, R. C. Beyond ethanol: a techno-economic analysis of an integrated corn biorefinery to produce hydrocarbon fuels and chemicals. *Pyrolysis and catalytic pyrolysis of protein-and lipid-rich feedstock* **2014**, 128.

(109) Ou, L.; Thilakaratne, R.; Brown, R. C.; Wright, M. M. Techno-economic analysis of transportation fuels from defatted microalgae via hydrothermal liquefaction and hydroprocessing. *Biomass and Bioenergy* **2015**, *72*, 45-54.

(110) Kocoloski, M.; Michael Griffin, W.; Scott Matthews, H. Impacts of facility size and location decisions on ethanol production cost. *Energy Policy* **2011**, *39*, 47-56.

(111) Kazi, F. K.; Fortman, J. A.; Anex, R. P.; Hsu, D. D.; Aden, A.; Dutta, A.; Kothandaraman, G. Techno-economic comparison of process technologies for biochemical ethanol production from corn stover. *Fuel* **2010**, *89, Supplement 1*, S20-S28.

(112) Freedonia. The Freedonia Group. *Inc. Cleveland, OH* **2014**, *161*.